TOPICS IN 2D INTEGRABLE FIELD THEORIES WITH BOUNDARY INTERACTIONS[1]

Sergei Skorik

Physics Department, University of Southern California, Los Angeles, CA 90089-0484

Abstract

We study different aspects of integrable boundary quantum field theories, focussing mostly on the "boundary sine-Gordon model" and its applications to condensed matter physics.

The first part of the review deals with formal problems. We analyze the classical limit and perform semi-classical quantization. We show that the non-relativistic limit corresponds to the Calogero-Moser model with a boundary potential. We construct a lattice regularization of the problem via the XXZ chain. We classify boundary bound states. We generalize the Destri de Vega method to compute the ground state energy of the theory on a finite interval.

The second part deals with some applications to condensed matter physics. We show how to compute analytically time and space dependent correlations in one-dimensional quantum integrable systems with an impurity. Our approach is based on a description of these systems in terms of massless scattering of quasiparticles. Correlators follow then from matrix elements of local operators between multiparticle states – the massless form-factors. Although, in general an infinite sum of these form-factors has to be considered, we find that for the current, spin and energy operators only a few (two or three) are necessary to obtain an accuracy of more than 1%. Our results hold for `arbitrary impurity strength`, in contrary to the perturbative expansions in the coupling constants. As an example, we compute the frequency dependent conductance, at zero temperature, in a Luttinger liquid with an impurity, and also discuss the succeptibility in the Kondo model and the time-dependent properties of the two-state problem with dissipation.

May 1996

[1]Pedagogical review based on the PhD dissertation

Acknowledgements

It is my pleasure to thank Hubert Saleur for his guidance, understanding and the financial support. I am indebted to Hubert for much of my new skills and acquisitions. I would like to thank also Nick Warner for sharing his enthusiasm towards theoretical physics, Itzhak Bars for teaching an excellent class on Quantum Field Theory and K. Pilch for teaching a remarkable class on Quantum Mechanics at USC.

I want to thank sincerely Anton Kapustin, Sergei Cherkis and Yuri Levin for an interesting collaboration and "live discussion" that sporadically took place in the kitchen around midnight. All three were graduate students at Caltech.

Finally, I want to thank those few friends, whose warm company, good jokes and optimism allowed me to survive four years and conduct this research in the Wild West. These are Sergei Cherkis, Jonathan Cohen, Yuri Levin, Alexei Shalopenok, Vyacheslav Solomatov, Jürgen Schulze, Naresh Talsania...

Contents

Chapter 0

Introduction

In one space dimension, a quantum field theory can be defined either on a circle, or on an open interval with certain boundary conditions. In Hamiltonian formulation, boundary conditions amount to the presence of additional interaction term on the boundary [1],

$$H = H_{bulk} + V(\{\phi_B\}),$$

where $\{\phi_B\}$ denotes the set of boundary degrees of freedom – fluctuating fields at the boundary. The reasons for studying the theories with boundary conditions seem natural since in practice one has to deal often with a bounded system having some interface with the external world, as in the problem of polymer adsorption [2]. [2] Also, the problems on the semi-infinite interval in 1D sometimes appear as the reductions of 3D problems to the s-wave dependence as e.g. in the case of the monopole-catalysed baryon decay [3].

One of the most appreciated and rich at the present applications of the boundary field theory is to the impurity problems of condensed matter physics [4, 77, 70, 76], provided that the scattering on impurity can be mapped onto the scattering off the boundary with some boundary potential. An incomplete list of examples includes the Kondo model [10], the dissipative quantum mechanics [85] and the quantum Hall liquids with constriction [79]. All of the mentioned above three models look alike from the point of view of the bulk part, which is a free massless boson, but differ by the boundary interaction. The role of integrability here is two-folded. First, it allows to find the static properties (e.g. via the Bethe ansatz) of the model from the bare Hamiltonian, including the mass spectrum, scattering matrices, or the free energy. Second, it allows to take advantage of working with the physical excitations in the formalism of the FS theory. Namely, integrability suggests a convenient basis of massless particle states which are particular combinations of plane waves that scatter diagonally off the boundary. [3] Working with these massless particles at first sight adds some complexity, but it is paid off by the final simple and manageable results. Let us stress that we deal only with such boundary interactions that preserve the integrability of the bulk part. Fortunately,

[2] E.g., for the Ising model such an interface can be modeled by a boundary magnetic field [53].

[3] Corresponding classical solutions are presented in [31].

there are quite a few of such models in the real world. [4]

Different integrable boundary theories have been introduced and solved throughout the history of integrable models. A noticable contribution in this field has been made by Cardy [6, 7], who studied the critical surface behavior withing the framework of conformal field theory. Another substantial advancement has been done by the work of Ghoshal and Zamolodchikov [1]. The authors have succeeded in formulating and (partially) solving the set of general constraints for the factorizable boundary field theory, thus generating a powerful method of obtaining the integrable boundary models from the integrable bulk field theories. The equations of [1] resolve the boundary integrability (boundary Yang-Baxter equation) together with the physical constarints of unitarity and crossing symmetry and possess the restrictive power to determine the scattering matrices up to "CDD ambiguity". In a more simple words, given a FS theory in the bulk with its two-particle scattering matrices, we can derive all possible integrable boundary models compatible with this bulk theory. Of course, what we get is merely the FS description, leaving the identification of the Hamiltonian structure to our intuition. But other methods, developed in [8] and [70], allow us to obtain the exact free energy and the correlation functions correspondingly. Thus, the FS approach turns out to be very productive.

The paper [1] in such a way sets basis for a more systematic study of the boundary integrable models, marking them out as a subfield of integrable models. We undertake in this dissertation a close study of some particularly interesting boundary models, such as the boundary sine-Gordon model (chapters 2,3,4,6), as well as develop some general techniques (chapters 5,7). We assume that all the properties of the bulk models of interest are known to us, so we can focuse on the peculiar boundary phenomena. One example of the boundary phenomena are the boundary bound states (chapter 4). The existence of such states, localized at the boundary of the crystal lattice, was first pointed out by I.E.Tamm. Finally, in chapter 7 we describe in some detail the physics behind the impurity and dissipative two-state models and set up the technique for calculating the physical observables (correlation functions) in these models by making heavy use of the boundary factorized scattering. Quite remarkable, such characteristics as the conductance can be expressed in terms of the boundary scattering matrices!

In chapter 1 we review the Bethe ansatz technology. We start with the traditional Hamiltonian approach and show how to extract physical observables (mass spectrum, scattering matrices etc) from a bare Hamiltonian. Although we do not present any new contributions with respect to the existing extensive literature on the subject, this material is necessary to understand further chapters. We focuse our discussion on the Thirring model, which is the fermionic analog of the sine-Gordon model.

In chapter 2 we consider the sine-Gordon model on a half-line, with an additional potential term of the form $-M\cos\frac{\beta}{2}(\varphi-\varphi_0)$ at the boundary. We construct the classical solutions by using the bulk sine-Gordon theory and the "generalized method of images." From the

[4] The term "integrable models" in our context amounts to the model having an infinite number of conserved charges in involution (i.e. mutually commuting), both on quantum and classical levels. The integrability results to the factorized scattering property by making use of the argument that S-matrix must commute with the infinite number of charges [5].

classical solutions in hand we extract the time delay (2.18). From the time delay we reconstruct the semi-classcial phase-shift using the method of Jackiw and Woo [22]. We establish the agreement with the semi-classical limit $\beta \to 0$ of the exact boundary reflection matrix, (2.34). The exact expressions for the boundary reflection matrices are known up to CDD ambiguities [1]. They were obtained as a "minimal" solution to the general set of constraints for the integrable boundary field theory.

The purpose of chapter 3 is to investigate the non-relativistic, $\theta \to 0$, limit of the boundary sine-Gordon model and to determine the quantum-mechanical potential induced by the presence of boundary. We show that the generalized Calogero-Moser model with boundary potential of the Pöschl-Teller type describes the non-relativistic limit in question.

In chapter 4 we address the *exact* quantum field theory solution of the boundary sine-Gordon model, which we obtain by means of the Bethe ansatz technique. Among other things, this solution allows to re-derive the boundary reflection matrices of [1], (3.1)-(3.3), and to relate them to the physical parameters in the Hamiltonian [39]. The present chapter includes a complete study of boundary bound states and related boundary S-matrices for the sine-Gordon model with Dirichlet boundary condition. Our analysis is based on the solution of the boundary bootstrap equations, representing the integrability constraints, together with the explicit Bethe ansatz solution of the inhomogeneous XXZ model in a boundary magnetic field – a lattice regularization of the boundary sine-Gordon model. We identify boundary bound states with new *boundary strings* in the Bethe ansatz.

The main purpose of chapter 5 is to study the ground state energy of 1+1 integrable relativistic quantum field theories with boundaries. This involves several questions. One is the energy associated with a boundary for an infinite system, the other is the way the energy of the theory on an interval varies with its length - the "genuine" Casimir effect. The elegant method of Destri and de Vega [54] for the periodic systems leads directly to the expression for the ground state energy from which the infinite size contribution and the finite size correction can be easily extracted. The heart of the DDV method is a non-linear integral equation (5.45) being derived from the Bethe equations. We generalize the Destri-de-Vega method to the systems with boundaries and apply it to compute the ground state energy for the boundary sine-Gordon model.

In chapter 6 We study an open XXZ chain in the regime $\Delta > 1$ with a boundary magnetic field h and discuss some of its peculiar features due to the presence of boundary. In the Bethe ansatz formalism, boundary bound states are represented by the "boundary strings" as described in chapter 4. We find that for certain values of h the ground state wave function contains boundary strings, and from this infer the existence of two "critical" fields in agreement with [49]. An expression for the vacuum surface energy in the thermodynamic limit is derived and found to be an analytic function of h. We argue that boundary excitations appear only in pairs with "bulk" excitations or with boundary excitations at the other end of the chain. The case where the magnetic fields at the left and the right boundaries are antiparallel has non-trivial differences with the case of the parallel fields. The Ising ($\Delta = \infty$) and isotropic ($\Delta = 1$) limits are discussed thoroughly and found helpful for the intuitive understanding of the behavior of the boundary XXZ chain at arbitrary Δ.

In chapter 7 we show how to compute analytically time and space dependent correlations

in one-dimensional quantum integrable systems with an impurity. Our approach is based on a description of these systems in terms of massless scattering of quasiparticles [69]. Correlators follow then from matrix elements of local operators between multiparticle states – the massless form-factors. Although, in general an infinite sum of these form-factors has to be considered, we find that for the current, spin and energy operators only a few (two or three) are necessary to obtain an accuracy of more than 1%. Our results hold for `arbitrary impurity strength`, in contrary to the perturbative expansions in the coupling constants. As an example, we compute the frequency dependent condunctance, at zero temperature, in a Luttinger liquid with an impurity, and also discuss the succeptibility in the Kondo model and the time-dependent properties of the two-state problem with dissipation.

This review is based mostly on the published papers [23], [32], [40], [56], [65], [70].

Chapter 1

Introduction to the Bethe Ansatz

One of the efficient approaches to quantization of interacting fields is based on the conformal field theory (CFT), while yet another on the factorized scattering theory (FST). In both cases the knowledge of the Hamiltonian is not required. Rather, the data is encoded into the particular representation of the Virasoro algebra on the space of fields and the dimension of the perturbing operator, or in the exact scattering matrices as in the case of FST. We start, however, with the traditional Hamiltonian approach and show in this chapter how to extract physical observables (mass spectrum, scattering matrices etc) from a bare Hamiltonian using the Bethe ansatz technology. Although we do not present any new contributions with respect to the existing extensive literature on the subject [9, 10], this material is necessary to understand further chapters.

This chapter is by no means the complete review of the Bethe ansatz. We focuse our discussion on the Thirring model, which is the fermionic analog of the sine-Gordon model. The relation between the two models becomes an exact mapping of one onto another due to the bosonization technique of Coleman and Mandelstam.

1.1 Hamiltonian formulation

The massive Thirring model is defined by the Hamiltonian

$$H_T = \int dx[-i(\psi_1^+\partial_x\psi_1 - \psi_2^+\partial_x\psi_2) + m_0(\psi_1^+\psi_2 + \psi_2^+\psi_1) + 2g\psi_1^+\psi_2^+\psi_2\psi_1]. \qquad (1.1)$$

It can be rewritten in terms of the creation and annihilation operators of the Fock fermionic space and diagonalized [11]. The vacuum of the Fock space $|0\rangle$ is a particular eigenstate annihilated by ψ_1 and ψ_2 and is called *bare* vacuum. The *physical* vacuum is the state with the Dirac sea filled which has an infinite negative energy. Thus, to perform calculations a high-energy cutoff is required. Physical excitations are obtained by removing pseudoparticles from the Dirac sea and placing them above it, allowing in general some complex combinations called bound states.

The model possesses the conserved charge $N = \int dx(\psi_1^+\psi_1 + \psi_2^+\psi_2)$ (total number of pseudoparticles), as well as an infinite family of other local commuting charges, and therefore it is integrable. The latter can be shown by passing to the discrete Thirring model [12],

which is known as lattice XYZ chain.[1] The presence of conserved charges puts tremendous constraints on the dynamics of the model and, in fact, makes it analagous to the free Dirac fermions. The non-trivial difference comes from the mutual pairwise interaction of pseudoparticles in the vacuum. Loosely speaking, the Dirac sea is sensitive to the removal of one of its pseudoparticles, i.e. a *polarization* of vacuum occurs. In yet another sense the properly regularized Thirring model is analogous to the quantum-mechanical N-body problem with the pairwise interaction potential $V \sim \delta(x-y)$.

N-particle bare wave-functions are constructed by glueing up free solutions to the Dirac equation at the boundaries of the domains $x_{i_1} < x_{i_2} < \ldots < x_{i_N}$, similar to the way one proceeds in the quantum-mechanical problem with the delta-function potential. The solution to the free Dirac equation in two dimensions can be written in the form

$$\vec{\Psi} = \vec{u}(\beta) e^{ipx - iEt}, \tag{1.2}$$

where

$$\vec{u} = \frac{1}{\sqrt{2}} \begin{pmatrix} e^{-\beta/2} \\ e^{\beta/2} \end{pmatrix}, \qquad E^2 - p^2 = m_0^2.$$

it is convenient to parametrize the energy and momentum in terms of rapidity β:

$$E = m_0 \cosh\beta, \qquad p = m_0 \sinh\beta. \tag{1.3}$$

Matching solutions (1.2) leads to the pairwise phase shifts in the wave-function

$$\Phi(\beta) = -i \log \frac{\sinh \frac{1}{2}(2i\mu - \beta)}{\sinh \frac{1}{2}(2i\mu + \beta)}, \qquad \cot\mu = -\frac{1}{2}g, \tag{1.4}$$

arising at the hyperplanes $x_i = x_j$, with the *bare* S-matrix being

$$S = e^{i\Phi}, \qquad S(0) = 1. \tag{1.5}$$

The domain $\mu < \pi/2$ is called a *repulsive regime*, while the domain $\mu > \pi/2$ is called an *attractive regime*. The value $\mu = \pi/2$ is the *free point*.

1.2 Bethe equations, thermodynamic limit and solution for the density of states

The above heuristic discussion can be made more rigorous. Let us consider first the model (1.1) compactified on the circle of length L and then take the limit $L \to \infty$. The wave-functions of the states[2]

$$|\beta_1, \beta_2, \ldots, \beta_N\rangle = \int \prod_{i=1}^{N} e^{ip(\beta_i)x_i} dx_i \prod_{i<j\le N} [1 - i\lambda(\beta_i - \beta_j)\theta(x_i - x_j)] \cdot \cdot A^+(\beta_1, x_1) \cdots A^+(\beta_N, x_N)|0\rangle, \tag{1.6}$$

[1] There exist many lattice models that have Thirring model as the continuum limit. XYZ chain is, however, the most studied one. See [13] for another example.

[2] Notice the peculiar to integrable models factorized structure of the N-particle states: the wave-function consists of the product of two-particle terms.

where $\theta(x)$ is the step function and

$$A^+(\beta,x)=(2\cos\beta)^{-1/2}[e^{\beta/2}\psi_1^+(x)+e^{-\beta/2}\psi_2^+(x)]$$

are subject to the periodic boundary conditions, called Bethe equations:

$$\prod_{j\neq i}[1+i\lambda(\beta_i-\beta_j)]=e^{ip(\beta_i)L}\prod_{j\neq i}[1-i\lambda(\beta_i-\beta_j)]. \tag{1.7}$$

Taking the logarithm of Eq.(1.7) we get

$$-p(\beta_i)L=\sum_j\Phi(\beta_i-\beta_j)+2\pi I_i. \tag{1.8}$$

Such equations should be written for each particle's index i and form together a complex set of coupled transcendental equations. Different solutions are obtained for different sets of integers I_i. For example, the Dirac sea corresponds to the dense set of integers from $-I$ to I, while excited states correspond to the sets with ν of I_j's missing. Such vacancies will be called *holes*. Thermodymanic limit is the limit $L\to\infty$, $N\to\infty$. Class of states for which ν is fixed and finite when $N\to\infty$ is called *scaling states* [14].

Besides the real solutions to (1.8) and the Dirac sea solutions with $\mathrm{Im}\beta=\pi$, there exist various other solutions with some of β_i complex. In the thermodynamic limit it is possible to show [16] that all permissible complex roots form strings. From the point of view of the wave function, strings are bound states. They contain the rapidities with common real part $\mathrm{Re}\beta$ and equally spaced imaginary parts and are located symmetrically with respect to $\mathrm{Im}\beta=0$ or $\mathrm{Im}\beta=\pi$ lines. (see Figure 1.1). The easiest way to determine the spacing along imaginary axis is to look at the poles of the bare S-matrix (1.5). The latter are given by $\Delta\beta=2\pi il-2i\mu$. Since by periodicity $-\pi<\mathrm{Im}\beta<\pi$, it is enough to consider $l=0,1$. We find that $\Delta\beta=-2i\mu$ in the repulsive regime, and $\Delta\beta=-2i\omega$ in the attractive regime, where

$$\omega\equiv\pi-\mu.$$

More rigorous classification of strings based on the analysis of Bethe equations is given in [16].

Denote by

$$\Phi_{m,n}=\sum_{p=0}^{m-1}\sum_{l=0}^{n-1}\Phi(\beta+i\mu(m-2p-n+2l)) \tag{1.9}$$

the scattering phase of m-string on n-string, and by

$$\Phi_{-1,n}=\sum_{p=0}^{n-1}\Phi(\beta+i\pi+i\mu(n-1-2p))=\Phi_{1,n}(\beta+i\pi) \tag{1.10}$$

the scattering phase of the Dirac sea pseudoparticle on the n-string. For technical simplicity we restrict μ and ω to certain "rational" values equal to π/t, where $t=2,3,\ldots$. Then

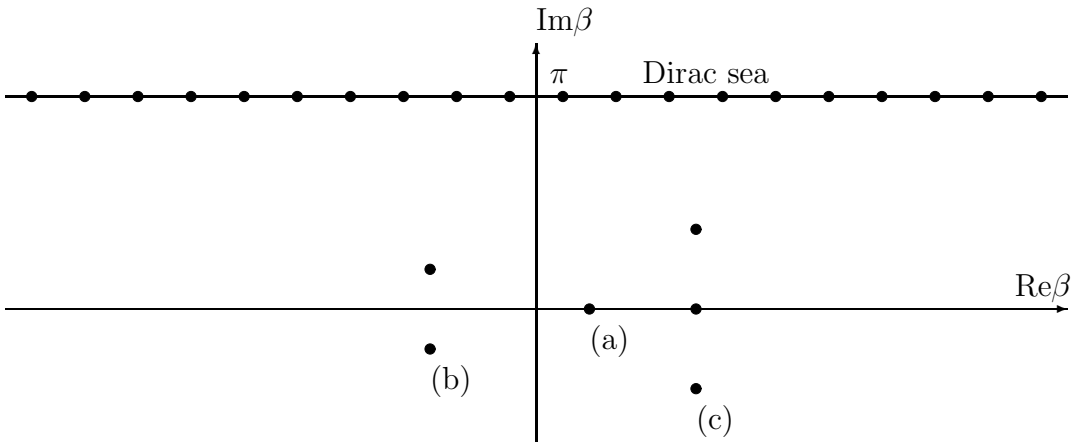

Figure 1.1: Various root configurations: (a) 1-string; (b) 2-string; (c) 3-string.

only the strings of the length $1, 2, \ldots, t-1$ exist. [3] Note that $(t-1)$-string is qualitatively different from all the shorter strings and is similar to a hole in the Dirac sea as far as the bare energy, momentum and scattering phase with other objects are concerned.

In the thermodynamic limit the distribution of roots of Bethe equations is described by continuous positive functions $\rho_j(\beta)$ and $\tilde{\rho}_j(\beta)$, where $\rho_j(\beta)$ is a density of j-strings, ρ_{-1} is a density of the Dirac sea pseudoparticles, and $\tilde{\rho}_j$ is a density of holes. Summing the Bethe equations and rearranging, we get the equations for strings:

$$p_s(\beta_i)L = -\sum_l \sum_j \Phi_{sl}(\beta_i - \beta_j) + 2\pi I_{si}, \tag{1.11}$$

where

$$p_s(\beta_i) = \sum_{a=0}^{s-1} p(\beta_i + i\mu(s-1-2a)),$$

$$p_{-1}(\beta) = p(\beta + i\pi),$$

and β_i are now the real numbers. Introduce σ_s =sign$(I_{i+1} - I_i)_s$. Since the density of roots must be positive, then

$$\frac{I_{i+1} - I_i}{L\Delta\beta} \sim \sigma_s(\rho + \tilde{\rho})_s. \tag{1.12}$$

[3] At first glance it seems that the t-string should be allowed, too. However, it is easy to check that it has vanishing energy, momentum and scattering phase. So, it is a "ghost."

Eq. (1.12) is the definition of the density functions. After the thermodynamic limit is taken, the Bethe equations assume the form:

$$p'_s(\beta) = -\sum_l \Phi'_{sl} * \rho_l + 2\pi\sigma_s(\rho_s + \tilde{\rho}_s). \tag{1.13}$$

Introducing

$$A_{sl} = -\frac{\Phi'_{sl}}{2\pi} + \sigma_s\delta_{sl}\delta(\beta), \tag{1.14}$$

we get

$$\frac{p'_s}{2\pi} = \sum_l A_{sl} * \rho_l + \sigma_s\tilde{\rho}_s, \tag{1.15}$$

where the involution operator $*$ is defined as:

$$A * \rho(x) \equiv \int A(x-y)\rho(y)dy.$$

The choice of sign of σ_s is determined by the behavior of the function

$$p_s(\beta) + L^{-1}\sum_{j,l}\Phi_{sl}(\beta-\beta_j) \equiv y_s(\beta),$$

namely, whether $y_s(\beta)$ increases or decreases. Thus, we are interested in the sign of $y'_s(\beta)$:

$$p'_s(\beta) + L^{-1}\sum_{j,l}\Phi'_{sl}(\beta-\beta_j) = y'_s(\beta).$$

Alas, we cannot compute the infinite sum of the terms whose values depend on unknown yet β_j. However, if $p'_s(\beta)$ and $\sum\Phi'$ have the same sign, then the conclusion regarding the sign of y'_s can be made without the evaluation of sum. For example, for the attractive regime $\mu > \pi/2$ we have

$$\begin{aligned} &p'_{-1} \sim -\cosh\beta < 0, \qquad \Phi'_{-1,-1}(\beta) < 0 \\ &p'_t(\beta) > 0, \qquad \Phi'_{-1,t}(\beta) > 0, \qquad t \geq 1. \end{aligned}$$

Hence,

$$\sigma_{-1} = -1, \qquad \sigma_1, \ldots, \sigma_{t-1} = 1.$$

Let us compute the density of roots in the ground state in the attractive regime. We should choose appropriate regularization of the momentum, since Eqs. (1.15) make no sense with $p \sim \sinh\beta$. In [18], for example, the sharp momentum cutoff is chosen, i.e. $p = 0$ for $|\beta| > \Lambda$ with some large Λ. Such a choice makes the function of momentum to be non-analytic, and disregards large momentum pseudoparticles at all. Although it works in the attractive regime fine, it gives some problems in the repulsive regime for $\mu < \pi/3$. We shall choose here a smooth cutoff, which comes naturally from the lattice regularization of the Thirring model (see Figure 1.2):

$$p(\beta) = -im_0\ln\left[\frac{\sinh\frac{1}{2}(\beta+f-i\omega)}{\sinh\frac{1}{2}(\beta+f+i\omega)}\right] - im_0\ln\left[\frac{\sinh\frac{1}{2}(\beta-f-i\omega)}{\sinh\frac{1}{2}(\beta-f+i\omega)}\right], \tag{1.16}$$

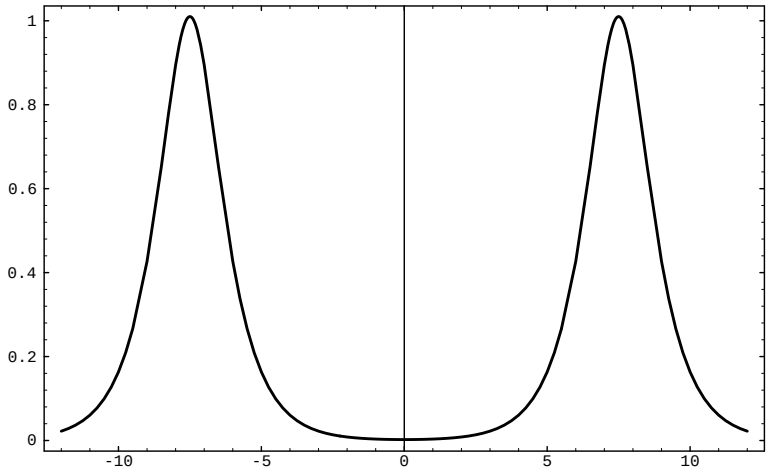

Figure 1.2: Smoothly regularized momentum $p'(\beta)$.

$$p'(\beta) = m_0 \sin\omega \left[\frac{1}{\cosh(\beta+f) - \cos\omega} + \frac{1}{\cosh(\beta-f) - \cos\omega} \right]. \tag{1.17}$$

We reproduce the usual relativistic expression in the limit $f \to \infty$:

$$p(\beta) \to 4m_0 \sin\omega e^{-f} \sinh\beta = m_1 \sinh\beta, \qquad f \to \infty.$$

Denote the first term in (1.16) by $f_+(\beta)$ and the second one by $f_-(\beta)$. Then the regularized energy is

$$h(\beta) = -f_+(\beta) + f_-(\beta) \tag{1.18}$$

As expected, $h(\beta) \to m_1 \cosh\beta$ as $f \to \infty$. The Fourier image of (1.17) is

$$\begin{aligned} \hat{p}'_{-1}(k) &= \int e^{ik\beta} p'_{-1}(\beta) d\beta = \int e^{ik\beta} p'(\beta + i\pi) d\beta \\ &= -4\pi m_0 \frac{\sinh\omega k \cos fk}{\sinh\pi k} \end{aligned} \tag{1.19}$$

We need to solve the Bethe equation for the ground state density ρ_{-1}:

$$\frac{p'_{-1}}{2\pi} = A_{-1,-1} * \rho_{-1}.$$

This can be easily done by passing to the Fourrier transformed equation:

$$\frac{\hat{p}'_{-1}}{2\pi} = \hat{A}_{-1,-1} \cdot \hat{\rho}_{-1},$$

where

$$\frac{\hat{\Phi}'}{2\pi} = -\frac{\sinh(\pi - 2\omega)k}{\sinh\pi k}, \qquad \hat{A}_{-1,-1} = -\left(\frac{\hat{\Phi}'}{2\pi} + 1 \right) = -\frac{2\sinh\omega k \cosh(\pi-\omega)k}{\sinh\pi k}.$$

Thus, we get

$$\hat{\rho}_{-1} = \frac{\hat{p}'_{-1}}{2\pi \hat{A}_{-1,-1}} = m_0 \frac{\cos fk}{\cosh(\pi-\omega)k}, \tag{1.20}$$

Eventually,

$$\begin{aligned} \rho_{-1}(\beta) &= \frac{1}{2\pi} \int e^{-ik\beta} \hat{\rho}_{-1}(k) dk = \\ &= \frac{m_0}{4\mu} \left[\frac{1}{\cosh\frac{\pi}{2\mu}(\beta+f)} + \frac{1}{\cosh\frac{\pi}{2\mu}(\beta-f)} \right]. \end{aligned} \tag{1.21}$$

Upon the cutoff removal, $f \to \infty$, the density (1.21) becomes

$$\rho_{-1}(\beta) \to \frac{m_0 e^{-f}}{\mu} \cosh\frac{\pi\beta}{2\mu}. \tag{1.22}$$

We see that what we got looks like the density of free pseudoparticles in the Dirac sea, with the bare mass and bare rapidity renormalized as a result of interactions. Note that mass renormalization depends upon the regularization procedure chosen.

1.3 Thermodynamic Bethe ansatz

The thermodynamic Bethe ansatz (TBA) method allows one to obtian the excitation energies and to compute the exact free energy. We employ it here for the Thirring model and discuss briefly its main concepts. The idea of TBA dates back to the work of C.N.Yang and C.P.Yang [15]. They introduced the temperature into the Bethe ansatz technique and used Eqs. (1.15) to realize the statistics of states at temperature T.

The basic equation of the TBA method can be written in the form:

$$\varepsilon(\beta) = h(\beta) - A + \frac{T}{2\pi}\Phi' * \ln(1 + e^{-\varepsilon/T}). \tag{1.23}$$

By virtue of its definition, the pseudoenergy of excitations $\varepsilon(\beta)$ is

$$e^{\varepsilon/T} \equiv \frac{\tilde{\rho}}{\rho}. \tag{1.24}$$

Eq. (1.23) is the result of minimization of the free energy $F = E - TS$ over ρ under the condition $\int \rho$ =const. Thus, the Lagrange multiplier A is just the chemical potential. The entropy of the system S is given in [15], and E is the total energy of all pseudoparticles. We note here that the expression for the entropy differs for the "fermionic" and "bosonic" cases. We work with the fermionic case where for each quantum number I_j corresponds only one pseudoparticle.

Eq. (1.23) is a non-linear integral equation that cannot be solved analyticaly in general. In the limit $T \to 0$ Eq. (1.23) reduces to

$$\varepsilon(\beta) = h(\beta) - A - \frac{1}{2\pi}\Phi' * \varepsilon. \tag{1.25}$$

Integration in the latter formula is over all rapidities where $\varepsilon(\beta)$ is negative. From (1.24) also follows that for such β we have $\tilde{\rho}(\beta) = 0$, and, respectively, for the values of β where $\varepsilon(\beta)$ is positive, $\rho(\beta) = 0$. Let us represent $\varepsilon(\beta)$ in the form

$$\varepsilon(\beta) = \varepsilon^+ + \varepsilon^- = \varepsilon H(\varepsilon) + \varepsilon H(-\varepsilon),$$

where $H(\varepsilon)$ is the Heaviside step function. Then from (1.25) follows:

$$\varepsilon^+(\beta) = h(\beta) - A - \left(\frac{\Phi'}{2\pi} + \delta\right) * \varepsilon^-. \tag{1.26}$$

In other words, $\varepsilon^+ > 0$ corresponds to the particle excitation energy, and $|\varepsilon^-|$ to the hole excitation energy. ε^- coincides with ε where ε is negative, i.e. in the Dirac sea. For example, if we take a pseudoparticle out of the Dirac sea and put it above the sea, the excitation energy would be

$$E_{ext} = \varepsilon(\beta_p) - \varepsilon(\beta_h) = \varepsilon^+(\beta_1) - \varepsilon^-(\beta_2) > 0.$$

The total energy

$$E = \int h\rho d\beta = \int \rho(\varepsilon + A + \frac{1}{2\pi}\Phi' * \varepsilon^-)d\beta = \tag{1.27}$$
$$= \int [\varepsilon\rho + A\rho + \frac{1}{2\pi}\varepsilon^- \cdot (\Phi' * \rho)] = \int (\varepsilon^+\rho - \varepsilon^-\tilde{\rho}) - \frac{1}{2\pi}\int p'_{-1}\varepsilon^- + A\int \rho,$$

where we used (1.25), (1.15) and the permutation property of the convolution operator. Eq. (1.27) has clear physical interpretation: the energy of an arbitrary state at $T = 0$ can be expanded as the sum $E = E_{vac} + E_{exc}$+const, where

$$E_{vac} = -\frac{1}{2\pi}\int p'_{-1}\varepsilon^- < 0$$

is vacuum energy, and

$$E_{exc} = \int (\varepsilon^+\rho - \varepsilon^-\tilde{\rho}) > 0$$

is excitation energy.

TBA equations for $T = 0$ can be obtained also directly from the variation of total energy [17]. Under small perturbations $\rho_j^{(0)} \to \rho_j^{(0)} + \delta\rho_j$ of the ground state densities $\rho_j^{(0)}$ the total energy changes by

$$\delta E = \sum_j \int h_j \delta\rho_j = \sum_j [\varepsilon_j^+ \delta\rho_j - \varepsilon_j^- \delta\tilde{\rho}_j].$$

Substituting $\delta\tilde{\rho}_j$ from the Bethe equations (1.15) we obtian the *basic spectral equations*

$$h_j = \varepsilon_j^+ + A_{jk} * \sigma_k \varepsilon_k^-. \tag{1.28}$$

Similarly, we deduce

$$p_j = \pi_j^+ + A_{jk} * \sigma_k \pi_k^-. \tag{1.29}$$

From (1.28) it follows for the Thirring model

$$\hat{\varepsilon}_{-1}^- = -\hat{h}_{-1}/\hat{A}_{-1,-1}, \tag{1.30}$$

with

$$\hat{h}'_{-1}(k) = -4\pi i m_0 \frac{\sinh\omega k \sin fk}{\sinh \pi k}. \tag{1.31}$$

We obtain

$$\hat{\varepsilon}_{-1}^- = \frac{2\pi m_0}{k}\frac{\sin fk}{\cosh \mu k}.$$

In the limit $f \to \infty$ we get for the energy of hole in the Thirring model:

$$\varepsilon_{-1}^- \to -4m_0 e^{-\pi f/2\mu}\cosh\frac{\pi\beta}{2\mu}. \tag{1.32}$$

The hole of the Thirring model corresponds to a soliton of the sine-Gordon model. For the rest of the excitations we have

$$\hat{\varepsilon}_j^+ = \hat{h}_j + \hat{A}_{j,-1}\hat{\varepsilon}_{-1}^- = \hat{h}_j - \frac{\hat{A}_{j,-1}}{\hat{A}_{-1,-1}}\hat{h}_{-1}, \tag{1.33}$$

where we have substituted (1.30) to get the latter. Using the Fourier transforms $\hat{A}_{jk}$ together with

$$\hat{h}'_j(k) = 4\pi i m_0 \frac{\sinh(\pi - j\omega)k \sin fk}{\sinh \pi k},$$

we obtain

$$\varepsilon_j^+(\beta) \to 8m_0 e^{-\pi f/2\mu} \sin\left[\frac{(\pi-\mu)\pi j}{2\mu}\right] \cosh\frac{\pi\beta}{2\mu}, \qquad j < t-1$$

and

$$\varepsilon_{t-1}^+(\beta) = -\varepsilon_{-1}^-(\beta).$$

$t-1$ string in the Thirring model correspond to antisoliton of the sine-Gordon model, while the other j-strings correspond to the breathers.

1.4 Scattering matrices

The method to compute elastic S-matrices from the Bethe ansatz equations was developed in [18]. We describe the basic idea briefly, taking as an example scattering of holes (solitons in the sine-Gordon model).

By definition, the phase shift for scattering of two holes is given by

$$\delta_h(\beta_1 - \beta_2) \equiv \frac{1}{i}\log S = \varphi_1 - \varphi_2, \tag{1.34}$$

where φ_1 is the phase gained by a hole when going around the system and φ_2 the same phase but in the presence of another hole. The $\varphi_{1,2}$ are composed of a sum of two-particle bare phase shifts; for example

$$\varphi_2 = Lp_{-1}(\beta_1) + \sum_j \Phi_{1,1}(\beta_1 - \beta_j)$$

Here the sum is taken over all the solutions β_j of the Bethe equations (1.8) with two holes at positions β_1 and β_2. The result of subtraction $\varphi_1 - \varphi_2$ is proportional to the *backflow function* of vacuum: $\delta_h = 2\pi F(\beta_2|\beta_1)$. The latter is defined using the difference of the two solutions of the Bethe equations obtained with and without the hole at β_0,

$$F(\beta_0|\beta) \equiv (\beta - \tilde{\beta})L\rho(\beta).$$

One can show using (1.8) that F satisfies the following integral equation:

$$\Phi(\beta - \beta_0) = \dot{\Phi} * F + 2\pi F \tag{1.35}$$

Equation (1.35) describes the backflow caused by a hole at $\beta = \beta_0$ on $\mathrm{Im}\beta = \pi$ axis. Taking a derivative with respect to β and applying the Fourier transform to both sides of (1.35) we arrive at the following solution (in Fourier space):

$$\hat{F}'(k) = \frac{\sinh(\pi - 2\mu)k}{2\cosh\mu k \sinh(\pi-\mu)k} \tag{1.36}$$

From (1.34) we obtain:

$$\frac{1}{i}\frac{d}{d\theta}\log S(\theta) = \int_{-\infty}^{+\infty} e^{-ik\theta}\frac{\sinh(\pi-2\mu)k}{2\cosh\mu k\sinh(\pi-\mu)k}dk, \tag{1.37}$$

where $\theta \equiv \beta_1 - \beta_2$. Note that this method does not fix the constant normalization factor in the matrix element, which should be fixed by other constraints (e.g. unitarity). Expression (1.37) is in agreement with the results of [5], which enables us to identify coupling constants in the Thirring model with those of the SG model: $\mu = \pi - \beta_{SG}^2/8$.

The conserved charge equals to the total number of pseudoparticles $Q = \int \rho d\beta$. The physical (renormalized) charge is obtained after the subtraction of the charge of vacuum. It can be easily calculated from the Bethe equations using the backflow functions. E.g., for a hole $Q_{hole} = -1 + \hat{F}'(0)$, while for n-string $Q_n = n + \hat{F}_n'(0)$. Thus, we obtain the following values: $Q_{hole} = -\pi/2\omega$ for the hole, $Q_{t-1} = \pi/2\omega$ for the $t-1$ string, and $Q_n = 0$ for the other strings.

1.5 Remarks

There are many interesting issues of the Bethe ansatz technology left beyond the scope of this chapter. We want merely to mention some of them here.

Somewhat more accurate analysis of the permissible solutions of the Bethe equations for the XXZ chain, based on the counting arguments, shows that there are certain constraints on the space of physical states. For example, the holes can exists only in pairs in this model [14]. Another interesting example is so-called imaginary mass Thirring model discussed in [19], where the pseudoparticles are paired in the Dirac sea.

The important questions are the norm of the Bethe states [20], and their completeness [21]. The latter issue for the XXZ chain is equivalent to showing that the number of the physical states obtained from the Bethe ansatz equations equals to 2^N, where N is the number of sites on the chain.

Finally, it is worth to mention that the thermodynamic Bethe ansatz technique can be applied also to the *physical* excitations, and in this context it allows to find the exact free energy as a function of scaling parameter mL, as well as the central charges of the fixed point theories [8].

Chapter 2

Classical and semi-classical analysis of the boundary sine-Gordon model

We consider the sine-Gordon model on a half-line, with an additional potential term of the form $-M\cos\frac{\beta}{2}(\varphi-\varphi_0)$ at the boundary. We construct the classical solutions in the next section by using the bulk sine-Gordon theory and the "generalized method of images." From the classical solutions in hand we extract the time delay (2.18) as follows. We send a soliton (anti-soliton) which lives in the semi-infinite world governed by the boundary sine-Gordon model from some large position x_0 at time t_0 and measure the time t_1 it takes to bounce off the boundary and come back to x_0. At the same time t_0 in some other, infinite, world governed by the bulk sine-Gordon model we send a soliton with the same speed but in the opposite direction from the position $-x_0$ and measure the time t_2 it takes to arrive at x_0. Now, $\Delta t = t_1 - t_2$ is our time delay. From the time delay one can reconstruct the semi-classcial phase-shift using the method of Jackiw and Woo [22]. We establish the agreement with the semi-classical limit $\beta \to 0$ of the exact boundary reflection matrix, (2.34). The exact expressions for the boundary reflection matrices are known up to CDD ambiguities [1]. They were obtained as a "minimal" solution to the general set of constraints for the integrable boundary field theory. This chapter is based on [23].

2.1 The boundary sine-Gordon model

The Lagrangian of the boundary sine-Gordon model is given by:

$$\mathcal{L}_{SG} = \frac{1}{2}\int_0^{+\infty}\left[(\partial_t\varphi)^2-(\partial_x\varphi)^2+\frac{m_0^2}{\beta^2}\cos\beta\varphi\right]dx \;+\; M\cos\frac{\beta}{2}(\varphi(x=0)-\varphi_0) \tag{2.1}$$

Vanishing of the variation of Lagrangian (2.1) under a small perturbation $\varphi \to \varphi+\delta\varphi$ is equivalent to two conditions for the field φ. One is the sine-Gordon equation on the interval $[0,\infty)$

$$\phi_{tt}-\phi_{xx} = -\sin(\phi), \tag{2.2}$$

where $\beta\varphi \equiv \phi$, whereas another is the boundary condition

$$\partial_x \phi|_{x=0} \;=\; M \sin \frac{1}{2} \left(\phi - \phi_0\right)|_{x=0} \; . \tag{2.3}$$

The condition (2.3) is the most generic boundary condition preserving the integrability of the bulk problem [1]. It has two arbitrary paramenters, boundary mass M and a phase ϕ_0.

2.2 The classical solutions

The initial-boundary value problems compatible with integrability for the classical non-linear equations is a field itself withing the non-linear science. Such problems were studied extensively by mathematicians. One of the first results on the initial-boundary value problem for the classical sine-Gordon equation were obtained by Sklyanin [24]. In [24] the particular form of the most generic boundary condition was reported, $\partial_x \phi = M \sin(\phi/2)$ at $x = 0$. Later, this condition was widened in [25] to include the Dirichlet $\phi(x = 0) = const$ and $\partial_x \phi = M \cos(\phi/2)$ cases. Some solutions to the posed boundary value problems were obtained using the inverse scattering method and the Backlund transformations [26, 27]. Still, the most generic boundary condition was missed in [25]. The condition (2.3) first appeared in the physics litearure in the seminal work of Ghoshal and Zamolodchikov [1].

In this section we construct explicitly the solution to (2.1)-(2.3) that replicates the soliton (antisoliton) scattering from a boundary, as well as the solution localized at the boundary, called *boundary breather*. The idea that we use to construct such solutions is a remniscent of the method of images (and therefore we refer to it as the "generalized method of images.") We employ the known solutions on the full line – kinks and anti-kinks. To provide the reflection of the kink from a boundary (and thus the correct assymptotic behavior at infinity), we send another kink of the same kind towards it – the "mirror image". Such a solution automatically satisfies (2.1). Besides, in order to satisfy also (2.3), we place the third, stationary kink at the origin. We check by a direct calculation that condition (2.3) is satisfied. To obtain the three-kink solution, we need the knowledge of the τ-function for sine-Gordon equation.

2.2.1 The τ-functions

On the infinite interval, $(-\infty, \infty)$, the classical multi-soliton solution to the sine-Gordon equation is well known [28]. It is usually expressed as:

$$\phi(x,t) \;=\; 4 \, \arg(\tau) \;\equiv\; 4 \, \mathrm{artan}\Big(\frac{\mathcal{I}m(\tau)}{\mathcal{R}e(\tau)}\Big) \; , \tag{2.4}$$

where the τ-function for the N-soliton solution is:

$$\begin{aligned} \tau \;&=\; \sum_{\mu_j = 0,1} e^{\frac{i\pi}{2}\left(\sum_{j=1}^{N} \epsilon_j \mu_j\right)} \; \exp\Big[- \sum_{j=1}^{N} \frac{1}{2} \mu_j \Big[\Big(k_j + \frac{1}{k_j}\Big) x + \Big(k_j - \frac{1}{k_j}\Big) t \;-\; a_j \Big] \\ &+\; 2 \sum_{1 \le i < j \le N} \mu_i \mu_j \; \log\Big(\frac{k_i - k_j}{k_i + k_j}\Big)\Big] \; . \end{aligned} \tag{2.5}$$

The parameters k_j, a_j and ϵ_j have the following interpretations. The velocity of the $j^{\rm th}$ soliton is given by:

$$v_j \;=\; \left(\frac{k_j^2-1}{k_j^2+1}\right) . \tag{2.6}$$

(Note that v_j is positive for a left-moving soliton.) The a_j represent the initial positions of each of the solitons, and $\epsilon_j = +1$ if the $j^{\rm th}$ soliton is a kink, while $\epsilon_j = -1$ if it is an anti-kink. The rapidity, θ, of the soliton is defined by $k = e^\theta$, and we have normalized the soliton masses to unity (in further discussion, the words "soliton" and "kink" will be used synonymously).

It is fairly obvious how to get a single soliton solution on $[0,\infty)$ with either $\phi|_{x=0} = 0$ or $\partial_x\phi|_{x=0} = 0$. One exploits the symmetry of (2.2) under $\phi \to -\phi$ and $x \to -x$, and simply takes a two soliton solution on $(-\infty,\infty)$ where one soliton is a mirror image of the other through $x = 0$ [29]. If one does this with a double-kink solution then it satifies the foregoing Dirichlet condition, while the kink-anti-kink solution satisfies the Neumann condition. It is also not hard to guess how one can go beyond this solution: For $M = \infty$, the boundary condition (2.3) reduces to $\phi|_{x=0} = \phi_0$. The only way that this can be obtained from a multi-soliton solution on $(-\infty,\infty)$ is to put a third, *stationary* soliton at the origin.

We therefore consider the three soliton solution with $k_1 = k$, $k_2 = 1/k$ and $k_3 = 1$. That is, we consider:

$$\begin{aligned}\tau \;&=\; 1 \;-\; \epsilon v^2 e^{-\frac{1}{k}(k^2+1)x-a} \;-\; \epsilon_0\left(\frac{k-1}{k+1}\right)^2 e^{-\frac{1}{2k}(k+1)^2x-b}\; F(t) \\ &+\; i\Big\{\; e^{-\frac{1}{2k}(k^2+1)x}\; F(t) \;+\; \epsilon_0 e^{-x-b} \;-\; \epsilon\epsilon_0 v^2\left(\frac{k-1}{k+1}\right)^4 e^{-\frac{1}{k}(k^2+k+1)x-a-b}\;\Big\} ,\end{aligned} \tag{2.7}$$

where we have introduced the shorthand:

$$\epsilon = \epsilon_1\epsilon_2 , \qquad \epsilon_0 = \epsilon_3 , \qquad a = a_1 + a_2 , \qquad b = a_3 . \tag{2.8}$$

The function $F(t)$ is defined by:

$$F(t) \;\equiv\; \epsilon_1 e^{-\frac{1}{2k}(k^2-1)t-a_1} \;+\; \epsilon_2 e^{\frac{1}{2k}(k^2-1)t-a_2} . \tag{2.9}$$

This solution has $\phi = 0$ at $x = \infty$, and for $k > 1$ it describes a left-moving soliton moving from $x = \infty$ with a right-moving "image" starting at $x = -\infty$. There is a stationary soliton with center located at $x = -b$. Viewing this as scattering off a boundary at $x = 0$ one can easily see that a is the phase delay of the returned soliton. To make this more explicit, observe that τ has the following asymptotic behaviour:

$$\begin{aligned}\tau(x,t) \;&\sim\; 1 \;+\; i\epsilon\; e^{-\frac{1}{2k}[(k^2+1)x+(k^2-1)t]-a_1} \qquad x,-t\to\infty \;\text{ with }\; \frac{x}{t} = -\frac{k^2-1}{k^2+1} ; \\ \tau(x,t) \;&\sim\; 1 \;+\; i\epsilon\; e^{-\frac{1}{2k}[(k^2+1)x-(k^2-1)t]-a_2} \qquad x,t\to\infty, \;\text{ with }\; \frac{x}{t} = +\frac{k^2-1}{k^2+1} .\end{aligned}$$

The problem now is to first show that the τ-function given by (2.7) provides a solution to the boundary value problem on $[0,\infty)$ defined by (2.2) and (2.3). Our second purpose is to relate the parameters a and b of (2.7) to the parameters M and ϕ_0 of (2.3), thereby obtaining the classical phase delay, a, in terms of M and ϕ_0.

2.2.2 The classical phase delay for $M = \infty$ case

In the center of mass reference frame the solution to (2.2) obtained by means of the τ-function method reads:

$$\phi = \mp 4 \arctan \frac{2e^{x\mathrm{ch}\theta - a_1}\mathrm{ch}(t\mathrm{sh}\theta) \pm e^{x-a_3} \mp e^{x(1+2\mathrm{ch}\theta)-2a_1-a_3+2\log(u^2v)}}{2e^{x(1+\mathrm{ch}\theta)-a_1-a_3+2\log(u)}\mathrm{ch}(t\mathrm{sh}\theta) \pm e^{2x\mathrm{ch}\theta-2a_1+2\log(v)} \mp 1}, \tag{2.10}$$

where $u = \tanh(\frac{\theta}{2})$, $v = \tanh(\theta)$, and we have set $a_1 = a_2$, which means that the solution is invariant under the transformation $t \to -t$. The upper (resp. lower) sign corresponds to the situation when a stationary soliton (resp. anti-soliton) is used to adjust the value of field at the boundary. Solution (2.10) refers to the case when the incoming and outgoing particle is the soliton with asymptotic value $\phi = 2\pi$ at $x = +\infty$.

Let us represent (2.10) in the form of rational function of variable $\mathrm{ch}(t\mathrm{sh}\theta)$:

$$\phi(x,t) = 4 \arctan \frac{r_2 + s_2\mathrm{ch}(t\mathrm{sh}\theta)}{r_1 + s_1\mathrm{ch}(t\mathrm{sh}\theta)}.$$

The condition $\phi(x=0,t) = \phi_0$ implies that

$$\frac{r_2}{r_1} = \frac{s_2}{s_1} = \tan\left(\frac{\phi_0}{4}\right), \tag{2.11}$$

from which follows immediately

$$a_3 = \log\left(\mp u^2 \tan\frac{\phi_0}{4}\right).$$

For the argument of logarithm to be positive one should take $\phi_0 > 0$ with the stationary anti-soliton and $\phi_0 < 0$ with the stationary soliton. This is illustrated in figure 2.1. Further, we obtain from (2.11)

$$2a_1 = \log\left[u^2v^2\frac{u^2 + \tan^2(\frac{\phi_0}{4})}{1 + u^2\tan^2(\frac{\phi_0}{4})}\right]. \tag{2.12}$$

Note that the time delay, obtained by (2.12), is in fact always a time *advance* in both the attractive and repulsive cases. For the same value of ϕ_0 the time delay for the soliton that lives on the left half-line $x < 0$ is not the same as that of the right half-line soliton (except for $\phi_0 = \pm\pi$). The position of the "left" soliton is not the exact mirror image of the "right" soliton for generic ϕ_0.

2.2.3 The classical phase delay for generic case

To summarize the computation briefly, one substitutes (2.7) into (2.3), and obtains the constraint:

$$\begin{aligned} & [\mathcal{R}e(\tau)\partial_x\mathcal{I}m(\tau) - \mathcal{R}e(\tau)\partial_x\mathcal{I}m(\tau)]_{x=0} = \\ = \; & M \; \left[2\cos(\frac{1}{2}\phi_0)\; \mathcal{R}e(\tau)\mathcal{I}m(\tau) \; - \; \sin(\frac{1}{2}\phi_0)\; \left(\mathcal{R}e(\tau)^2 - \mathcal{I}m(\tau)^2\right)\right]_{x=0} \; . \end{aligned} \tag{2.13}$$

One can solve this by brute force substitution for the real and imaginary parts of τ, but it is somewhat simpler to find constants α, β, γ and δ such that:

$$\begin{aligned} \partial_x\mathcal{R}e(\tau)\,|_{x=0} \; &= \; [\alpha\; \mathcal{R}e(\tau) \; + \; \beta\; \mathcal{I}m(\tau)]\,|_{x=0} \; , \\ \partial_x\mathcal{I}m(\tau)\,|_{x=0} \; &= \; [\gamma\; \mathcal{R}e(\tau) \; + \; \delta\; \mathcal{I}m(\tau)]\,|_{x=0} \; . \end{aligned} \tag{2.14}$$

One then finds that (2.13) can be satisfied if and only if one has $\alpha = \delta$, which indeed turns out to be true. Using this one arrives at:

$$\begin{aligned} M\; \cos(\frac{1}{2}\phi_0) \; &= \\ -\frac{(k^2+1)}{k\Delta} \qquad & \left\{\left(1 \; + \; \epsilon\; v^2 e^{-a}\right) \; - \; e^{-2b}\left(\frac{k-1}{k+1}\right)^2\left[1 \; + \; \epsilon\; v^2 \; \left(\frac{k-1}{k+1}\right)^4 \; e^{-a}\right]\right\} \\ M\; \sin(\frac{1}{2}\phi_0) \; &= \; -2\; \epsilon_0\; \frac{(k-1)^2}{k}\; e^{-b}\; \frac{1}{\Delta}\left\{1 \; + \; \epsilon\; v^2 \; \left(\frac{k-1}{k+1}\right)^2 \; e^{-a}\right\}, \end{aligned} \tag{2.15}$$

where

$$\Delta \; \equiv \; \left(1 \; - \; \epsilon\; v^2\; e^{-a}\right) \; + \; e^{-2b}\left(\frac{k-1}{k+1}\right)^2\left[1 \; - \; \epsilon\; v^2 \; \left(\frac{k-1}{k+1}\right)^4 \; e^{-a}\right] \; . \tag{2.16}$$

It is algebraically very tedious to invert this relationship. One proceeds by eliminating e^{-b}, and then solving for a. It is very convenient to introduce a new parametrization of M and ϕ_0:

$$\begin{aligned} \mu \; \equiv \; M\; \cos(\frac{1}{2}\phi_0) \; &\equiv \; 2\; \cosh(\zeta)\cos(\eta) \\ \nu \; \equiv \; M\; \sin(\frac{1}{2}\phi_0) \; &\equiv \; 2\; \sinh(\zeta)\sin(\eta) \; , \end{aligned} \tag{2.17}$$

where $0 \leq \zeta < \infty$ and $-\pi < \eta \leq \pi$. (In the (μ, ν)-plane the curves of constant ζ are ellipses, while the curves of constant η are hyperbolae whose asymptotes make an angle of $\frac{1}{2}\phi_0$ with the μ-axis.)

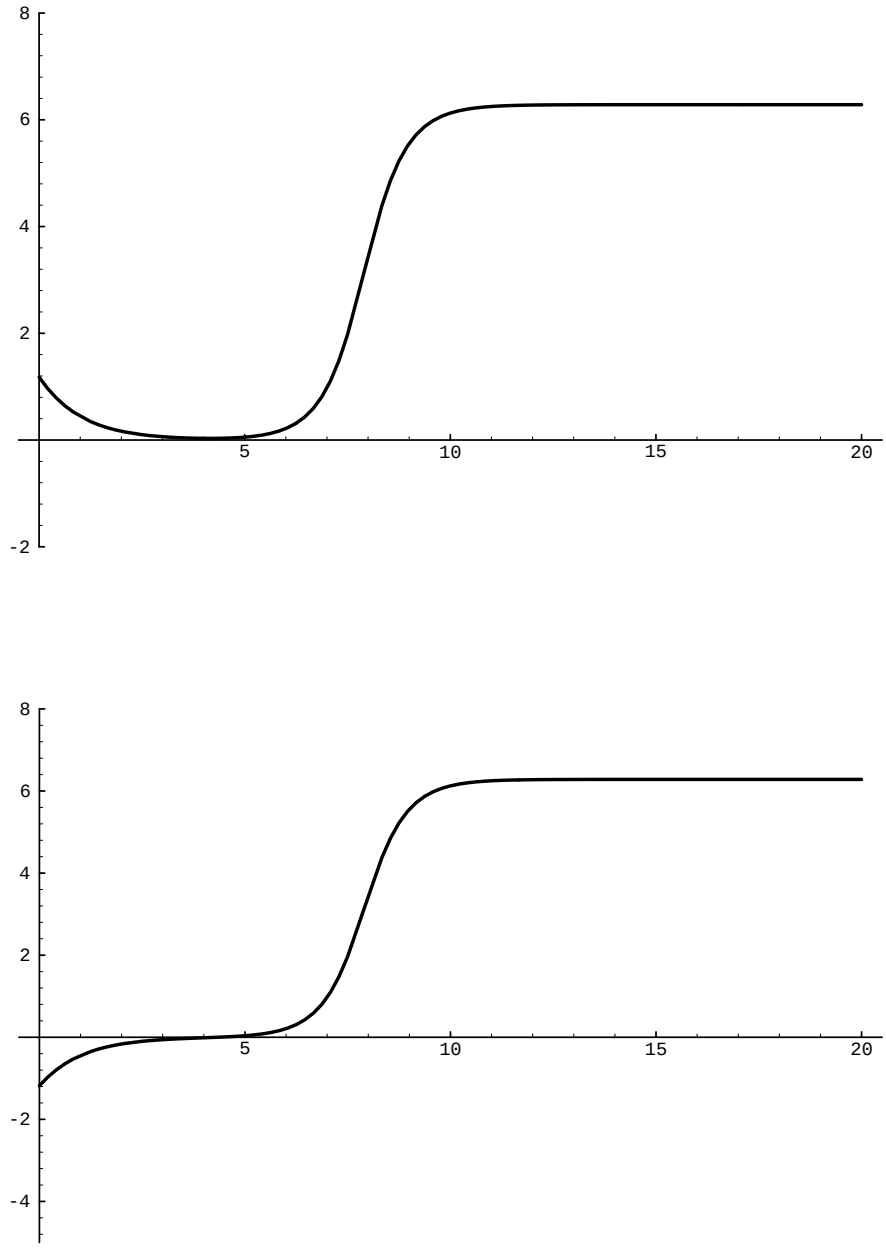

Figure 2.1: a solution of the classical Sine-Gordon equation with the fixed boundary conditions. For $\phi|_{x=0} = \phi_0 = \frac{3\pi}{8}$ solution is constructed out of a left-moving soliton, its right-moving image at $x < 0$ and the stationary antisoliton in the middle (upper graph). For $\phi|_{x=0} = \phi_0 = -\frac{3\pi}{8}$ the solution is built out of three solitons (lower graph).

We then find that the phase delay is given by:

$$a \;=\; \log\left\{-\epsilon\;\tanh^2(\theta/2)\tanh^2\theta\left[\frac{\tanh\frac{1}{2}(\theta+i\eta)\;\;\tanh\frac{1}{2}(\theta-i\eta)}{\tanh\frac{1}{2}(\theta+\zeta)\;\;\tanh\frac{1}{2}(\theta-\zeta)}\right]^{\pm 1}\right\}\;. \tag{2.18}$$

There are several things to note about this formula.

(i) The ambiguity of the ± 1 power comes from solving a quadratic equation, and is a direct reflection of the fact that (2.3) is not invariant under $\phi \to \phi + 2\pi$ (whereas (2.2) *is* invariant under this shift). Equivalently, one can flip between the + and − powers by sending $\phi_0 \to \phi_0 + 2\pi$.

(ii) The argument of the log is *always* real and positive. The discrete parameter, $\epsilon = \epsilon_1\epsilon_2$, must be chosen to arrange this. Hence:

$$\epsilon = +1 \;\;\text{for}\;\; -\zeta < \theta < \zeta \qquad\qquad \epsilon = -1 \;\;\text{for}\;\; |\theta| > \zeta\;. \tag{2.19}$$

This means that a kink reflects into kink for $-\zeta < \theta < \zeta$, and reflects into an anti-kink for $|\theta| > \zeta$. This is consistent with the fact that Dirichlet boundary conditions ($M = \infty$) cause a kink to reflect as a kink, whereas Neumann boundary conditions ($M = 0$) cause a kink to reflect as an anti-kink. Note that these two domains of parameter space (in which a kink reflects differently) are separated from one another by a logarithmic singularity in the classical phase delay.

(iii) The choice of the power ± 1 in (2.18) is correlated with the parameter η and whether there is a kink, or anti-kink at the origin. Specifically, we have:

$$\epsilon_0 \;=\; \pm\; sign(\tan(\frac{\eta}{2}))\;, \tag{2.20}$$

where the $\pm$ is the same as that of (2.18).

(iv) In the $M \to \infty$, or Dirichlet, limit we see that:

$$\zeta \;\sim\; \log(M)\;, \qquad \eta \;\sim\; \frac{1}{2}\phi_0 \qquad \text{and} \qquad \epsilon \;=\; -1\;, \tag{2.21}$$

and the phase delay collapses to (2.12):

$$a \;=\; \log\left\{\tanh^2\left(\frac{\theta}{2}\right)\tanh^2(\theta)\left[\tanh\frac{1}{2}(\theta+i\frac{\phi_0}{2})\;\;\tanh\frac{1}{2}(\theta-i\frac{\phi_0}{2})\right]^{\pm 1}\right\}\;. \tag{2.22}$$

In this limit (2.3) enforces Dirichlet boundary conditions. It is, however, important to note that there are *two* possible distinct boundary values: $\phi|_{x=0} = \phi_0$ and $\phi|_{x=0} = \phi_0 + 2\pi$. Since the boundary potential is $-M\cos(\frac{1}{2}(\phi - \phi_0))$, one sees that $\phi|_{x=0} = \phi_0$ is stable, while $\phi|_{x=0} = \phi_0 + 2\pi$ is unstable.

From now on we consider only the stable boundary value that corresponds to the positive sign in (2.22). Then one has from (2.20)

$$\epsilon_0 \;=\; -\; sign(\tan(\frac{1}{4}\phi|_{x=0}))\;. \tag{2.23}$$

It is essential to observe that we have taken $\phi_{x=\infty}=0$, *ab initio*. For different boundary conditions at $x=\infty$, one should replace ϕ_0 by $\phi|_{x=0}-\phi|_{x=\infty}$. This physical parameter is defined mod 4π.

2.2.4 Boundary breather solutions

To fully understand the semi-classical scattering computation one also needs another class of classical solutions, which we call here *boundary breathers*. It is well-known that breathers represent bound states in the soliton-anti-soliton channel in the bulk sine-Gordon theory. In the same way that the classical bulk breathers can be obtained from the appropriate solution by analytic continuation of θ to imaginary axis, one might expect that the same procedure would give boundary breathers on the half-line. To see this, we set $\theta=i\vartheta$ $(0<\vartheta<\frac{\pi}{2})$ in the formula (2.10). Next, we impose the following conditions for a solution to be boundary breather:

a) it should be a real function,

b) it should have finite energy and

c) the asymptotic value at $x=+\infty$ must be fixed and equal to $2\pi n$ (n – integer number).

The three-soliton (resp. soliton-anti-soliton-soliton) configuration satisfies the first condition provided that $\vartheta<-\frac{\phi_0}{2}$ (resp. $\vartheta<\frac{\phi_0}{2}$). However, the other conditions are satisfied by the soliton-anti-soliton-soliton configuration only, which one could have foreseen from the analogy with the bulk theory. The boundary breather solution has the form (see figure 2.2):

$$\begin{aligned}\phi_b \;&= 2\pi - \\ &-4\arctan\frac{2\cot\vartheta\cot\frac{\vartheta}{2}\sqrt{K}\cot\frac{\phi_0}{4}e^{x+x\cos\vartheta}\cos(t\sin\vartheta)+e^{2x\cos\vartheta}K\cot^2\frac{\vartheta}{2}+1}{2\cot\vartheta\cot\frac{\vartheta}{2}\sqrt{K}e^{x\cos\vartheta}\cos(t\sin\vartheta)+e^{x}\cot\frac{\phi_0}{4}(e^{2x\cos\vartheta}K+\cot^2\frac{\vartheta}{2})},\end{aligned} \tag{2.24}$$

where

$$K=\cot(\frac{\phi_0}{4}-\frac{\vartheta}{2})\cot(\frac{\phi_0}{4}+\frac{\vartheta}{2}).$$

So, we have a continuum of classical boundary bound states when $0<\vartheta<\frac{\phi_0}{2}<\frac{\pi}{2}$ and for other ϕ_0 according to the 2π-periodicity. In the quantum theory this continuum shrinks into a discrete set of bound states (see next section). Note that in the limit $\vartheta\to\frac{\phi_0}{2}$ the boundary breather (2.24) reduces to the ground state, figure 2.3, and the phase delay has singularities at $\theta=\pm\frac{1}{2}i\phi_0$. An analogous picture of bound states occurs for the anti-soliton scattering with fixed boundary conditions.

2.2.5 General solutions, integrability and Bäcklund transformations

Thus far we have only applied the method of images to obtain certain special classical solutions of the boundary sine-Gordon problem (2.1). It is natural to suggest that general solutions of (2.1) can be obtained by similar methods. This in turn would establish the classical integrability the boundary problem (2.1). It is, in fact, rather straightforward to show that both of these conclusions are true, at least for the problem (2.1) with $\phi_0 = 0$. The method we will employ [23] can almost certainly be generalized to problems with $\phi_0 \neq 0$, and also has the virtue that it can be used to construct the integrable boundary potentials for the more general Toda models. A related approach has been followed in [27, 30]. The basic idea is to use the fact that any integrable hierarchy has Bäcklund transformations: that is, solutions can be mapped into one another by non-trivial gauge transformations constructed from the affine Lie algebra action on the corresponding LAX system. For the sine-Gordon equation, the requisite Bäcklund transformation can be cast in the following form:

$$\begin{aligned} \partial_u(\phi + \psi) &= e^{\zeta} \sin\left(\frac{\phi - \psi}{2}\right) ; \\ \partial_v(\phi - \psi) &= e^{-\zeta} \sin\left(\frac{\phi + \psi}{2}\right) , \end{aligned} \tag{2.25}$$

where $u = x - t$, $v = x + t$, and ζ is an arbitrary constant parameter. The point is that ϕ satisfies the sine-Gordon equation (2.2) if and only if ψ does so as well. Suppose that ψ is a solution to sine-Gordon on $[0, \infty)$ satisfying a Dirichlet boundary condition: $\psi|_{x=0} = 2\eta$, where η is a constant. It follows immediately from (2.25) that ϕ is a solution to sine-Gordon satisfying (2.3), where M and ϕ_0 are given in terms of ζ and η by (2.17). Thus, if one can solve the Dirichlet problem, one can solve the more general problem by a Bäcklund transformation.

Observe that if $\eta = 0$, or equivalently $\phi_0 = 0$, then the Dirichlet problem can be solved trivially by method of images: one gets the solution on the half-line by extending it as an odd function on the full line. Thus, the Bäcklund transformation essentially defines the generalized method of images. It is also by no means an accident that the parameters entering into the Bäcklund transformation (η and ζ) are precisely the rapidity parameters that turn up in the phase delay (2.18). One should also note that the form of the integrable boundary potential is given directly by the Bäcklund transformation. This fact should easily generalize to Toda systems.

Bäcklund transformations, in general, are invertible transformations on the solution space of an integrable hierarchy. The simplest forms of them modify the constants of the motion of solution, and possibily add or subtract a soliton. One can certainly find a Bäcklund transformation that will introduce a stationary soliton into the soliton-soliton solution of sine-Gordon. As a result, the general three soliton solution employed above can be obtained from the two soliton solution that is appropriate for the "trivial" Dirichlet problem with $\phi_0 = 0$. We therefore expect that any solution of the trivial Dirichlet problem can be mapped onto the generic problem (2.1), thus establishing the classical integrability.

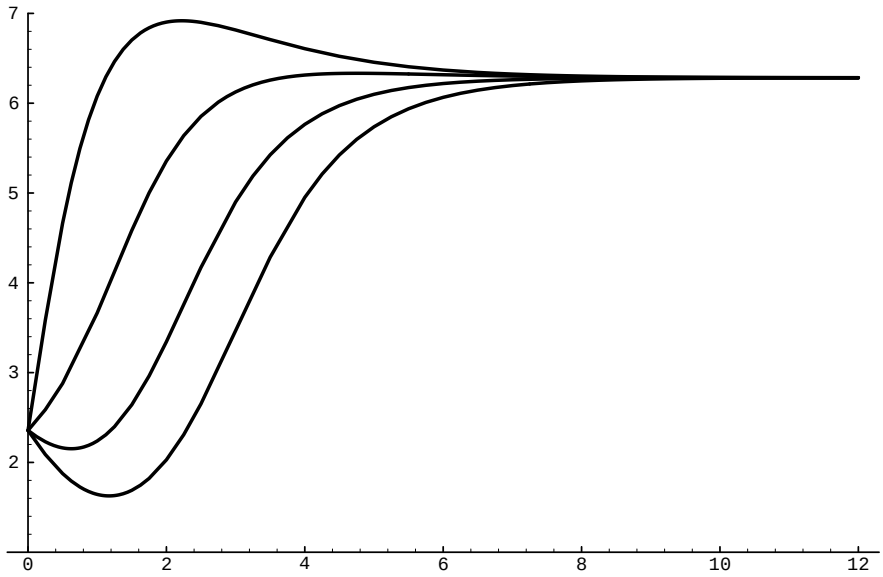

Figure 2.2: a boundary bound state (boundary breather) for the values $\theta = \frac{i\pi}{6}$, $\phi_0 = \frac{3\pi}{4}$ at four distinct instants of time.

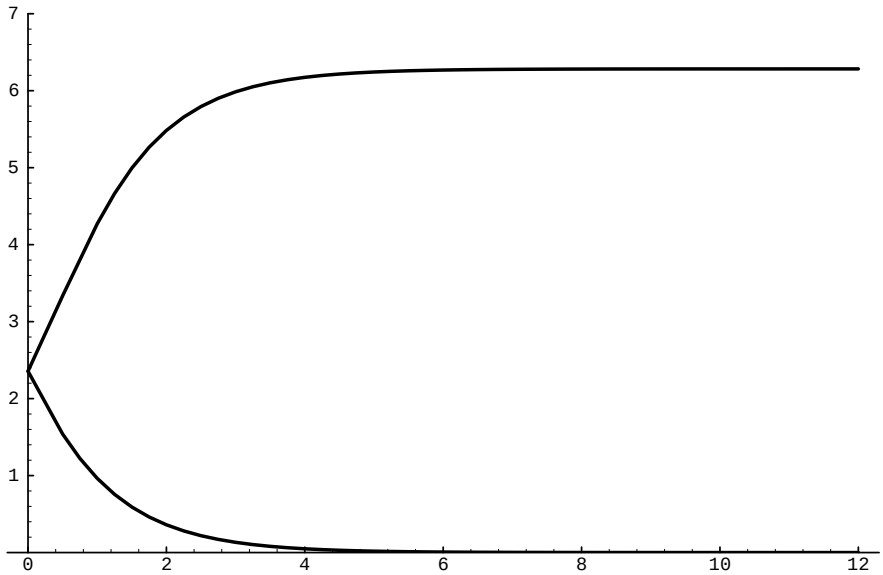

Figure 2.3: two possible ground state configurations for $\phi_0 = \frac{3\pi}{4}$. The configuration with asymptotic behaviour $\phi \to 0$ at infinity has lower energy than the other one.

2.3 The semi-classical analysis

2.3.1 The exact boundary reflection matrix

Let us recall some of the results of [1]. The *exact* (quantum) boundary S matrix elements are

$$\begin{aligned} S_+^+(\theta) \equiv P_+(\theta) &= \cos\left[\xi - (t-1)i\theta\right] R(\theta) \\ S_-^-(\theta) \equiv P_-(\theta) &= \cos\left[\xi + (t-1)i\theta\right] R(\theta), \end{aligned} \tag{2.26}$$

and

$$S_+^- \equiv Q_+(\theta) = S_-^+ = Q_-(\theta) = \frac{k}{2}\sin\left[2(t-1)i\theta\right] R(\theta)\ , \tag{2.27}$$

where θ is the rapidity of an incoming particle. The parameter t is defined by:

$$t \ = \ \frac{8\pi}{\beta^2}.$$

The function $R(\theta)$ decomposes as

$$R(\theta) = R_0(\theta)R_1(\theta), \tag{2.28}$$

where R_0 is a normalization factor ensuring unitarity and crossing symmetry that does not depend on the boundary conditions. The dependence upon boundary conditions appears in R_1, which reads

$$R_1(\theta) = \frac{1}{\cos\xi}\sigma(\eta,\theta)\sigma(i\Theta,\theta). \tag{2.29}$$

Two of the four parameters k, ξ, η, Θ are independent, and we have the relations

$$\cos\eta\cosh\Theta = \frac{1}{k}\cos\xi, \quad \cos^2\eta + \cosh^2\Theta = 1 + \frac{1}{k^2}. \tag{2.30}$$

These parameters are related with M and φ_0 in an unknown way. An expression for the functions R_0 and σ involving infinite products of Γ-functions is given below (see next chapter). There are also simple integral representations:

$$\sigma(\xi,\theta) = \frac{\cos\xi}{\cos[\xi - i(t-1)\theta]}\exp\left\{\int_{-\infty}^{\infty} \frac{dx}{x} \ \frac{\sinh(t-1+\frac{2\xi}{\pi})x}{2\cosh(t-1)x\sinh x}\ e^{i\frac{2}{\pi}(t-1)\theta x}\right\}, \tag{2.31}$$

and

$$R_0(\theta) = \exp\left\{-\int_{-\infty}^{\infty} \frac{dx}{x} \ \frac{\sinh\frac{3}{2}(t-1)x\sinh(\frac{t}{2}-1)x}{\sinh\frac{x}{2}\sinh 2(t-1)x}\ e^{i\frac{2}{\pi}(t-1)\theta x}\right\}. \tag{2.32}$$

One has $\sigma(\xi,\theta) = \sigma(-\xi,\theta)$. The only difference between the scattering of solitons and anti-solitons arises therefore from the pre-factor $\cos[\xi \mp i(t-1)\theta]$ in (2.26).

For simplicity we consider only the limit in which $M \to \infty$. One can identify the corresponding values $k = 0$ and $\Theta = \infty$ easily since, at these values, the topological charge

$$Q = \frac{\beta}{2\pi} \int_0^\infty \partial_x \varphi dx$$

is conserved and therefore the amplitudes $Q_\pm$ must vanish. One has also $\eta = \xi$ so

$$R_1(\theta) = \frac{1}{\cos \xi} \sigma(\xi, \theta). \tag{2.33}$$

Consider now the quantum boundary S matrix at the leading order in $\frac{1}{\beta^2}$ as $\beta \to 0$. The computation is most easily done by using the integral representation given above, and evaluating the integrals explicitly by the residue theorem. This provides convergent expressions where the $\beta \to 0$ limit can be investigated term by term. To get non-trivial results one must scale ξ as

$$\frac{\beta^2}{8\pi} \xi \to \hat{\xi}$$

We find then

$$P_\pm(\theta) = \exp\left(\pm \frac{8i\pi \hat{\xi} \kappa}{\beta^2} + \frac{8i\pi |\hat{\xi}| \kappa}{\beta^2} \right) \frac{\mathcal{S}(\theta; 0) [\mathcal{S}(2\theta; 0)]^{1/2}}{[\mathcal{S}(\theta; \hat{\xi}) \mathcal{S}(\theta; -\hat{\xi})]^{1/2}}, \tag{2.34}$$

where

$$\mathcal{S}(\theta; y) = \exp\left(\frac{8i}{\beta^2} \int_0^\theta dv \ln \tanh^2 \frac{v + iy}{2} \right), \tag{2.35}$$

$\mathcal{S}(\theta; 0)$ being the semi-classical approximation to the bulk soliton-soliton S-matrix [22] (in the following we denote it also as $\mathcal{S}(\theta)$), and $\kappa = \text{sign}\theta$ (in the following we assume that $\theta > 0$).

Before discussing the relation between formula (2.34) and the classical computations of the preceding section, it is useful to comment on the bound states of the quantum theory. Poles of the R_0 term are associated with breathers and do not correspond to the boundary (new) bound states. The latter correspond rather to poles of the $\sigma(\xi, \theta)$ term which are located in the physical strip $\text{Im}\theta \in [0, \pi/2]$. By inspection of the Γ-product expression [1] one finds two families of poles of σ:

$$\begin{aligned} \theta_{n,l}^{(1)} &= -i \frac{\pi}{t-1} \left(n + \frac{1}{2} \right) \pm i \frac{\xi}{t-1} - 2il\pi \\ \theta_{n,l}^{(2)} &= i \frac{\pi}{t-1} \left(n + \frac{1}{2} \right) \pm i \frac{\xi}{t-1} + (2l+1) i\pi, \end{aligned} \tag{2.36}$$

where n, l are integers. Let us restrict to $\xi > 0$. Then the only physical poles are those that correspond to $+$ sign in $\theta^{(1)}$ and $-$ sign in $\theta^{(2)}$. The first pole that enters the physical strip (from the bottom) is $\theta_{0,0}^{(1)}$ for $\xi \geq \frac{\pi}{2}$. The number of poles of σ in the physical strip increases monotonically with ξ for ξ small enough, and as t gets large it becomes simply of the form ξ/π. These poles are cancelled by the cosine term in P_- and therefore appear only in the P_+

amplitude. As ξ reaches the value $\xi = \frac{4\pi^2}{\beta^2}$ the poles densely fill the interval $0 < \mathrm{Im}\theta < \frac{\pi}{2}$ and a pole at $\theta = i\pi/2$ appears corresponding to the emission of a zero momentum soliton. As argued in [1] this corresponds to a change in the ground state of the system. For $0 < \varphi_0 < \frac{\pi}{\beta}$ the ground state is $\varphi \to 0$ at infinity but for $\frac{\pi}{\beta} < \varphi_0 < 3\frac{\pi}{\beta}$ it is $\varphi \to \frac{2\pi}{\beta}$ at infinity (see figure 2.3). Therefore the value $\xi = \frac{4\pi^2}{\beta^2}$ corresponds to $\varphi_0 = \frac{\pi}{\beta}$ and it is the upper physical value for ξ: as φ_0 varies arbitrarily, ξ never gets larger than $\frac{4\pi^2}{\beta^2}$ and the set of poles $\theta^{(2)}_{n,l}$ never enters the physical strip. Observe that there are bound states in the quantum theory when in the classical case the kink sitting in the middle and the incoming one are of opposite topological charges in complete agreement with the discussion of boundary breathers in section 2.1.4.

2.3.2 Classical time delay and quantum phase shift

To establish the relation between (2.34) and (2.22), first recall [22] the general relation between the quasi-classical scattering phase shift, $\delta(\theta)$, and the classical phase shift, $a(\theta)$:

$$\delta(\theta) = \text{constant} + \frac{m}{2}\int_0^\theta a(\eta)d\eta, \tag{2.37}$$

Here, m is the classical mass of the particles involved in the scattering. Using the "semi-classical Levinson theorem" to determine the constant in this formula we deduce, using (2.22), the relation

$$P_+(\theta) \equiv e^{2i\delta(\theta)}, \tag{2.38}$$

where

$$2\delta(\theta) = 2n_B\pi + \frac{8}{\beta^2}\int_0^\theta d\eta \log\frac{\tanh^2\eta\tanh^2\frac{\eta}{2}}{\tanh\frac{1}{2}(\eta + i\frac{\beta\varphi_0}{2})\tanh\frac{1}{2}(\eta - i\frac{\beta\varphi_0}{2})}, \tag{2.39}$$

and n_B is the number of bound states. Since according to the preceeding discussion $n_B = \frac{\xi}{\pi} = \frac{8\hat{\xi}}{\beta^2}$ for $0 < \xi < \frac{4\pi^2}{\beta^2}$ as $\beta \to 0$ we see that formula (2.34) is in complete agreement with the classical phase shift (2.22) and that ξ is proportional to ϕ_0. In the region $-\frac{4\pi^2}{\beta^2} < \xi < 0$ there are no physical poles for P_+ and $n_B = 0$. A similar discussion can be carried out for $\xi < 0$ and P_-. As $\beta \to 0$ the number of physical poles of P_- varies as $n_B = -\frac{\xi}{\pi} = -\frac{8\hat{\xi}}{\beta^2}$ and again we have agreement with the semi-classical Levinson theorem.

From comparison of (2.34) and the classical phase shift we see that ξ and φ_0 are related linearly as $\xi = \frac{4\pi}{\beta}\varphi_0$. This leads correctly to the emission of a zero momentum soliton with the ground state degeneracy as discussed in [1]. This linear relation can hold only for $|\xi| < \frac{4\pi^2}{\beta^2}$. Beyond that value the ground state changes. To compare the quantum result with the classical phase shift we must then correlate appropriately the value of ϕ at infinity in the latter. The net effect is to replace ϕ_0 by $\phi_0 - 2\pi$. Eventually, the variation of ξ with φ_0 is therefore

$$\xi = \frac{4\pi}{\beta}\left(\varphi_0 - \frac{2\pi}{\beta}\mathrm{Int}\left[\frac{\beta\varphi_0}{2\pi} + \frac{1}{2}\right]\right), \tag{2.40}$$

as illustrated in figure 2.4. It is very likely that (2.40) is exactly true for finite β as well.

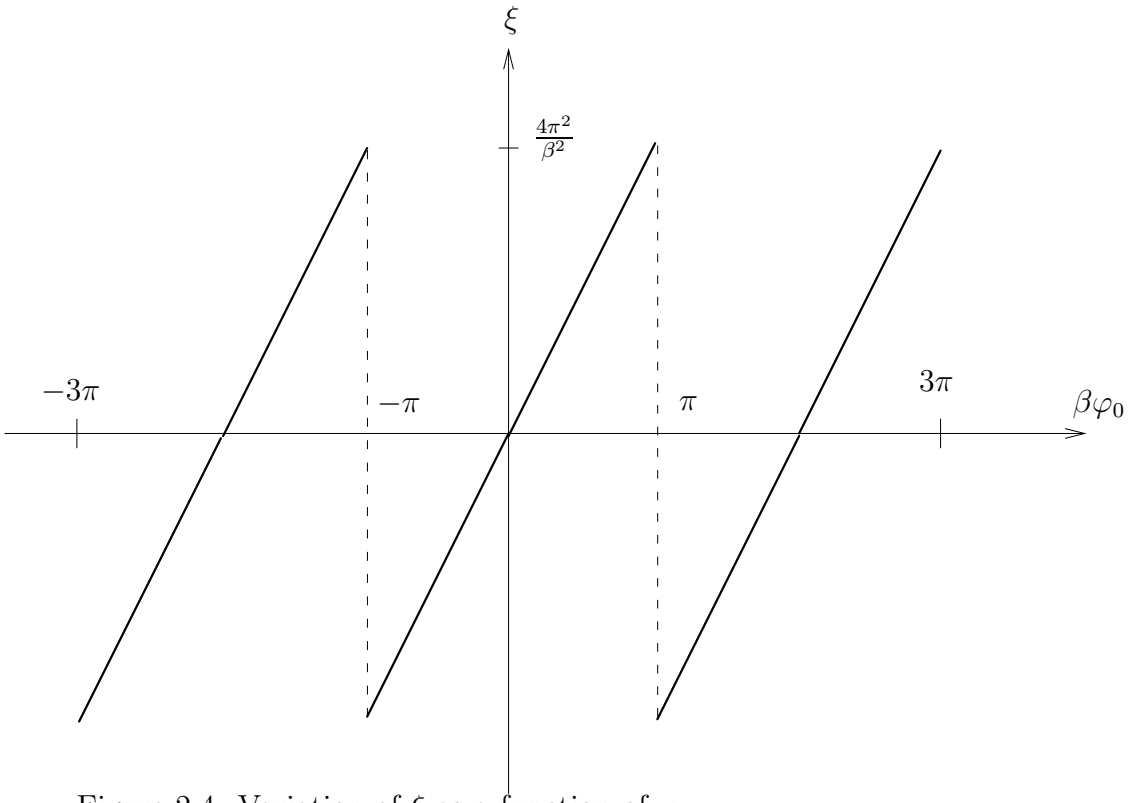

Figure 2.4: Variation of ξ as a function of φ_0.

We can finally recover (2.34) without appealing to our knowledge of quantum boundary bound states. For this one has to evaluate the action for the classical configuration. Following the discussion in [22] we have,

$$2\delta(\theta) = C(\varphi_0) + \frac{8}{\beta^2}\int_0^\theta d\eta \log \frac{\tanh^2\eta \tanh^2\frac{\eta}{2}}{\tanh\frac{1}{2}(\eta + i\frac{\beta\varphi_0}{2})\tanh\frac{1}{2}(\eta - i\frac{\beta\varphi_0}{2})}, \quad \text{if} \quad |\beta\varphi_0| < \pi, \quad (2.41)$$

where we used the soliton mass $m = \frac{8}{\beta^2}$, and δ satisfies the differential equation

$$\delta(\theta) \; - \; \tanh\theta \; \delta'(\theta) \; = \; \int_0^{+\infty} dt \left(\int_0^{+\infty} dx \dot{\varphi}^2 - 8\sinh\theta\tanh\theta \right). \quad (2.42)$$

We restrict to the situation where we send in a kink, and φ_0 is positive and so there is an anti-kink at the origin (see figure 4). In this case there are quantum boundary bound states. It is difficult to perform the double integral for the three-soliton solution explicitly because of the cumbersome expression for the integrand (2.10). One might hope that in order to find the θ-independent piece of the phase shift it is sufficient to evaluate both sides of (2.42) in the limit as $\theta \to +\infty$ or $\theta \to 0$. However both of these limits do not seem to be helpful, because due to the non-uniform convergence of the right hand side of (2.42) it is not allowed to interchange such a limit with the integration. We evaluated the right hand side of (2.42) (with fixed θ) numerically for several different values of ϕ_0 using Mathematica. Combining (2.41) and (2.42), we obtain an estimate for $C(\varphi_0)$, in agreement with $C(\varphi_0) = \frac{8\pi}{\beta}\varphi_0$ with accuracy 0.1%. This result was checked for different values of θ. We therefore obtain agreement with the semi-classical Levinson theorem.

2.4 Remarks

Although the method of images works nicely in the classical theory, it does not seem to extend to the quantum case: we have not been able to recast the boundary S matrix of [1] as a product of bulk S-matrix elements. A related phenomenon is the non-trivial structure of the boundary S-matrix with one-loop corrections (the semi-classical expressions being the tree approximation). Recall that in the bulk one has

$$\mathcal{S}_1(\theta; y) = \exp\left(\frac{8i}{\beta'^2}\int_0^\theta dv \ln\tanh^2\frac{v+iy}{2} \right),$$

where

$$\beta'^2 \equiv \beta^2 \frac{8\pi}{8\pi - \beta^2} = \frac{8\pi}{t-1}.$$

Scaling

$$\frac{\beta'^2}{8\pi}\xi \to \hat{\xi}_1,$$

one finds the following next-to-leading correction to the boundary S-matrix in the Dirichlet problem:

$$P_{\pm}(\theta) \approx \exp\left(\pm\kappa\frac{8i\pi\hat{\xi}_1}{\beta'^2} + \kappa\frac{8i\pi|\hat{\xi}_1|}{\beta'^2}\right)\frac{\mathcal{S}_1(\theta)[\mathcal{S}_1(2\theta)]^{1/2}}{[\mathcal{S}_1(\theta;-\hat{\xi}_1)\mathcal{S}_1(\theta;\hat{\xi}_1)]^{1/2}}\left[\tanh\left(\frac{\theta}{2}-i\frac{\pi}{4}\right)\right]^{1/2}.$$

In addition to the usual replacement of β^2 by β'^2 we see the appearance of an entirely new factor involving the square-root of a hyperbolic tangent.

The massless limit $m_0 = 0$ of the boundary sine-Gordon model (2.1) was studied in [31], where, in particular, the massless classical solutions were obtained.

Chapter 3

Non-relativistic limit of the quantum sine-Gordon model with Dirichlet boundary condition

In the previous chapter we studied the quantum sine-Gordon model on a half-line (2.1) in the semi-classical limit $\beta \to 0$. The purpose of this chapter is to investigate the non-relativistic, $\theta \to 0$, limit of this model and to determine the quantum-mechanical potential induced by the presence of boundary. We show that the generalized Calogero-Moser model with boundary potential of the Pöschl-Teller type describes the non-relativistic limit of (2.1). The discussion is based on [32].

3.1 Introduction

When $\theta \to 0$, the energy and momentum of relativistic particles – in our context solitons and anti-solitons – degenerates to

$$E = M_s \cosh\theta \to M_s - \frac{M_s\theta^2}{2},$$

$$p = M_s \sinh\theta \to M_s\theta.$$

So, θ is a speed of particles measured in the units of c (the speed of light).

Since such properties as integrability and factorized scattering survive in the above limit, we expect to get some quantum-mechanical *integrable* model on a half-line. Moreover, since a large class of such models based on the Lie-algrebraic classification is known [33], it is natural to look first for the appropriate candidate withing this class. Indeed, we show that the boundary Calogero-Moser model with boundary potential of the Pöschl-Teller type, whose integrability was established in [34, 35], describes the non-relativistic limit of (2.1).

Let us give an idea how one can come up with the boundary Calogero-Moser model by means of the heuristic arguments. It was known since long ago [5, 36] that the solitons and anti-solitons of the bulk sine-Gordon model interact via $\sinh^{-2}(x)$ (particles of the same

kind) and $\cosh^{-2}(x)$ (particles of different kinds) potentials in the non-relativistic limit. [1] Now, the question is to find out the form of the potential induced by the boundary. But from the semi-classical picture of the previous chapter we infer that the "boundary" can be represented by a stationary kink or an anti-kink and a moving "mirror image". So, we obtain the superposition of $\cosh^{-2}(x)$ and $\sinh^{-2}(x)$ potentials as a boundary potential, i.e. the Pöschl-Teller potential [37]. The $\sinh^{-2}(x)$ term is a hard-core reflecting potential, whereas the term $-\cosh^{-2}(x)$ is necessary to provide the existence of the boundary bound states.

3.2 The exact quantum field theory solution

In this chapter we consider the sine-Gordon model on a half-line (2.1), with the fixed value of field at the boundary: $\varphi(x=0,t)=\varphi_0$, or $M=\infty$ in (2.1). In [1], the quantum integrability and the exact S-matrix were conjectured for (2.1). The boundary scattering matrix is diagonal and, according to [1], the reflection amplitude of the soliton P_+ (resp. P_- for anti-soliton) reads:

$$P_\pm(\theta)=\cos(\xi\pm\lambda u)R(u,\xi)=\cos(\xi\pm\lambda u)R_0(u)R_1(u,\xi), \tag{3.1}$$

where $\theta=iu$ is the rapidity, $\xi=\frac{4\pi}{\beta}\varphi_0$ and $\lambda=\frac{8\pi}{\beta^2}-1$;

$$\begin{aligned} R_0(u) &= \frac{\Gamma\left(1-\frac{2\lambda u}{\pi}\right)\Gamma\left(\lambda+\frac{2\lambda u}{\pi}\right)}{\Gamma\left(1+\frac{2\lambda u}{\pi}\right)\Gamma\left(\lambda-\frac{2\lambda u}{\pi}\right)}\prod_{k=1}^{\infty}\frac{\Gamma\left(4\lambda k-\frac{2\lambda u}{\pi}\right)}{\Gamma\left(4\lambda k+\frac{2\lambda u}{\pi}\right)}\times \\ &\times \frac{\Gamma\left(1+4\lambda k-\frac{2\lambda u}{\pi}\right)\Gamma\left(\lambda(4k+1)+\frac{2\lambda u}{\pi}\right)\Gamma\left(1+\lambda(4k-1)+\frac{2\lambda u}{\pi}\right)}{\Gamma\left(1+4\lambda k+\frac{2\lambda u}{\pi}\right)\Gamma\left(\lambda(4k+1)-\frac{2\lambda u}{\pi}\right)\Gamma\left(1+\lambda(4k-1)-\frac{2\lambda u}{\pi}\right)} \end{aligned} \tag{3.2}$$

$$\begin{aligned} R_1(u,\xi) &= \frac{1}{\pi}\prod_{l=0}^{\infty}\frac{\Gamma\left(\frac{1}{2}+2l\lambda+\frac{-\xi+u\lambda}{\pi}\right)\Gamma\left(\frac{1}{2}+2l\lambda+\frac{\xi+u\lambda}{\pi}\right)}{\Gamma\left(\frac{1}{2}+2l\lambda+\lambda+\frac{-\xi+u\lambda}{\pi}\right)\Gamma\left(\frac{1}{2}+2l\lambda+\lambda+\frac{\xi+u\lambda}{\pi}\right)}\times \\ &\times \frac{\Gamma\left(\frac{1}{2}+2l\lambda+\lambda+\frac{\xi-u\lambda}{\pi}\right)\Gamma\left(\frac{1}{2}+2l\lambda+\lambda-\frac{\xi+u\lambda}{\pi}\right)}{\Gamma\left(\frac{1}{2}+2l\lambda+2\lambda+\frac{\xi-u\lambda}{\pi}\right)\Gamma\left(\frac{1}{2}+2l\lambda+2\lambda-\frac{\xi+u\lambda}{\pi}\right)} \end{aligned} \tag{3.3}$$

The poles of $P_\pm$ located in the physical domain $0<u<\pi/2$ at $u_n=\pm\frac{\xi}{\lambda}-\frac{2n+1}{2\lambda}\pi$ correspond to the "boundary" bound states of the theory. The latter exist in the soliton (resp. anti-soliton) scattering channel if $\xi>0$ (resp. $\xi<0$), and their energy is $E_n=M_s\cos u_n$. Note that the "physical" values of the parameter ξ are bounded: $|\xi|<4\pi^2/\beta^2$ (see previous chapter). In the semi-classical limit of the quantum field theory (2.1), $\beta\to 0$, the principal ("tree") approximation to the amplitudes (3.1) has the form (2.34).

[1] The quantum breathers correspond to the bound states in the $-\cosh^{-2}(x)$ potential.

3.3 The Calogero-Moser model on a half-line

Our purpose is to show that the non-relativistic dynamics of quantum sine-Gordon solitons in the presence of a boundary is described by the generalized Calogero-Moser Hamiltonian:

$$\begin{aligned}\hat{H} = &- \frac{1}{2M_s}\sum_{i=1}^{N}\frac{d^2}{dx_i^2} - \frac{1}{2M_s}\sum_{j=1}^{M}\frac{d^2}{dy_j^2} + \sum_{i<i'}^{N}\left(V_{AA}\left(x_i - x_{i'}\right) + V_{AA}\left(x_i + x_i'\right)\right) \\ &+ \sum_{j<j'}^{M}\left(V_{AA}\left(y_j - y_{j'}\right) + V_{AA}\left(y_j + y_{j'}\right)\right) + \sum_{i=1}^{N}\sum_{j=1}^{M}\left(V_{A\bar{A}}\left(x_i - y_j\right) + V_{A\bar{A}}\left(x_i + y_j\right)\right) \\ &+ \sum_{i=1}^{N}W_A\left(x_i\right) + \sum_{j=1}^{M}W_{\bar{A}}\left(y_j\right) \end{aligned} \tag{3.4}$$

Here V_{AA} and $V_{A\bar{A}}$ are bulk nonrelativistic potentials obtained long ago in [5, 36]:

$$V_{AA}\left(x\right) = \frac{\alpha_0^2}{M_s}\frac{\rho(\rho-1)}{\sinh^2\alpha_0 x}, \quad V_{A\bar{A}}\left(x\right) = -\frac{\alpha_0^2}{M_s}\frac{\rho(\rho-1)}{\cosh^2\alpha_0 x}, \tag{3.5}$$

with

$$\rho = \frac{8\pi}{\beta^2}, \tag{3.6}$$

$$\alpha_0 = \frac{m_0}{2}, \tag{3.7}$$

and W_A and $W_{\bar{A}}$ are boundary potentials of the Pöschl-Teller [37] type

$$\begin{aligned} W_A\left(x\right) &= \frac{\alpha_0^2}{2M_s}\left(\frac{\mu(\mu-1)}{\sinh^2\alpha_0 x} - \frac{\nu(\nu-1)}{\cosh^2\alpha_0 x}\right), \\ W_{\bar{A}}\left(x\right) &= \frac{\alpha_0^2}{2M_s}\left(\frac{\nu(\nu-1)}{\sinh^2\alpha_0 x} - \frac{\mu(\mu-1)}{\cosh^2\alpha_0 x}\right), \qquad \mu>1, \nu>1. \end{aligned} \tag{3.8}$$

Let us comment on the properties of the one-particle Schrödinger equation with the Pöschl-Teller potential $W_A(x)$. The energy of the bound states, which appear when $\nu > \mu+1$, is given by $E_n = -\frac{\alpha_0^2}{2M_s}(\nu-\mu-1-2n)^2$, where $n = 0, 1, 2...$ For a fixed value of $\nu-\mu$ there are in total $\left[\frac{\nu-\mu-1}{2}\right]$ bound states. The reflection coefficient, which is a pure phase, can be obtained to be equal to

$$S_A(k) = \frac{\Gamma\left(\frac{ik}{\alpha_0}\right)\Gamma\left(\frac{1}{2}+\frac{\mu-\nu}{2}-\frac{ik}{2\alpha_0}\right)\Gamma\left(\frac{\mu+\nu}{2}-\frac{ik}{2\alpha_0}\right)}{\Gamma\left(-\frac{ik}{\alpha_0}\right)\Gamma\left(\frac{1}{2}+\frac{\mu-\nu}{2}+\frac{ik}{2\alpha_0}\right)\Gamma\left(\frac{\mu+\nu}{2}+\frac{ik}{2\alpha_0}\right)} \tag{3.9}$$

This expression has "physical" poles on the upper imaginary half-axis in the complex momentum plane which correspond to the bound states. Besides, it has poles at the points $k_n = (1+n)\alpha_0$ that come from the first Γ-function in the numerator of (3.9). The latter set of poles is infinite and does not correspond to any bound states of the theory. The S-matrix

for the potential $W_{\bar{A}}$ can be obtained from (3.9) by the substitution $\mu \leftrightarrow \nu$. One can see that S_A and $S_{\bar{A}}$ satisfy the boundary Yang-Baxter equation of [1]:

$$S_A \cos\left(\frac{\pi}{2}(\nu-\mu)-\lambda u\right) = S_{\bar{A}} \cos\left(\frac{\pi}{2}(\nu-\mu)+\lambda u\right). \tag{3.10}$$

3.4 Relativistic vs non-relativistic integrable models

To establish the equivalence we will show in particular that the S-matrices of the quantum sine-Gordon theory and the model (3.4) coincide in the appropriate limit. The system (3.4) is integrable both at the classical and quantum levels [34, 35]. To see this one takes the hyperbolic-type Calogero-Moser Hamiltonian for $N+M$ particles based on the BC_{N+M} root system [33] and shifts the coordinates of the particles $N+1, ..., N+M$ by $i\pi/2$. The result is (3.4). Integrability means that the system admits a Lax representation and has $N+M$ integrals in involution. Moreover, since as $t \to \pm\infty$ these integrals reduce asymptotically to symmetric polynomials in particles' momenta, one can use the standard argument [38] to show that the S-matrix is factorized. A small modification arises due to the presence of the boundary; namely, one can consider the particles' collisions both very far from the boundary where the problem is reduced to the bulk one, and near the boundary where the colliding particles have enough time to reflect and go to $x = +\infty$. In the first case factorization gives the nonrelativistic Yang-Baxter equation for the bulk S-matrix [5], while in the second case we get exactly the boundary Yang-Baxter equation of [1], which in the Dirichlet case allows to express the boundary S-matrix of the anti-kink through that of the kink (3.10). The unitarity requires the latter to be a pure phase, but otherwise leaves it undetermined. So in both theories the S-matrix is factorized and fully determined by the bulk two-particle S-matrix and the boundary S-matrix. Thus to establish the equivalence it is sufficient to show that these S-matrices coincide when the nonrelativistic limit is taken.

Note that the translational invariance of the Hamiltonian (3.4) is broken not only by the boundary potentials, but also by the interaction of particles with their mirror images. This is very natural from the point of view of the underlying sine-Gordon theory, since, as was shown above, that the one soliton problem on a half-line is equivalent to the three-soliton bulk problem, with one of the particles staying at $x = 0$, and the other two being "generalized mirror images" of each other. The analogy becomes exact if we take $\varphi_0 = 0$. Then the ordinary method of images works, and it is obvious that the system of $N + M$ solitons on a half-line is equivalent to the system of $2(N + M)$ solitons on a line with symmetric initial conditions. Hence the corresponding nonrelativistic Hamiltonian can be obtained from the known [5, 36] nonrelativistic bulk Hamiltonian. One can easily see that the result is just (3.4) with $\mu = \nu$, $\mu(\mu-1) = \rho(\rho-1)/4$.

We will show below that μ and ν are related to the parameter ξ of the sine-Gordon model (2.1) as follows:

$$\frac{\nu-\mu}{2} = \frac{\xi}{\pi}. \tag{3.11}$$

3.5 Taking the non-relativistic limit

The nonrelativistic limit of (3.1) corresponds to the values $\theta \ll 1$. Simultaneously we must take the limit $\beta \ll 1$, so that $M_s = \frac{8m_0}{\beta^2} \gg m_0$ (otherwise the S-matrix becomes 1 and we do not get anything interesting.) In general, these two limits are to be taken without any further assumptions on the relative magnitude of θ with respect to β. However, it is worth to note that the region $\beta^2 \ll \theta \ll 1$ corresponds to the quasiclassical limit $\frac{k}{\alpha_0} \gg 1$, where

$$k \equiv M_s\theta \tag{3.12}$$

According to (3.7) $\frac{k}{\alpha_0} = \frac{16\theta}{\beta^2}$, which in general is not necessarily large. In what follows we assume that ξ is positive and $\beta\varphi_0 \sim 1$, so that ξ scales as $1/\beta^2$. Then P_+ has poles corresponding to the boundary bound states, and the energy of the bound states lying close to the edge of the continuous spectrum in the theory (2.1) becomes $E_n \simeq M_s - \frac{m_0\pi}{8\lambda}\left(\frac{2\xi}{\pi} - 1 - 2n\right)^2$. P_- does not have poles in the physical region. One can easily see then that (3.8),(3.9) describe correctly the spectrum of the boundary bound states provided that equations (3.7),(3.11) are fulfilled. To complete the identification of the boundary S-matrices we have to compare the phase shifts. Since ξ scales as $1/\beta^2$, by virtue of (3.11) the expression (3.9) can be rewritten as $S_{NR}(k, \nu - \mu)f(\theta)$, where

$$S_{NR}(k, \nu - \mu) = \frac{\Gamma\left(\frac{ik}{\alpha_0}\right)\Gamma\left(\frac{\mu-\nu}{2} - \frac{ik}{2\alpha_0}\right)}{\Gamma\left(-\frac{ik}{\alpha_0}\right)\Gamma\left(\frac{\mu-\nu}{2} + \frac{ik}{2\alpha_0}\right)} \tag{3.13}$$

is meromorphic and contains the poles located in the arbitrarily small neighbourhood of $\theta = 0$ as $\beta \to 0$, whereas the factor $f(\theta)$ can be expanded into the power series $f(\theta) = 1 + \sum_{l=1}^{\infty} a_l\theta^l$ with all the coefficients and a radius of convergence ~ 1 as $\beta \to 0$. In the same limit $P_\pm$ can be factorized analogously: $P_\pm = S_{NR}(k, \pm 2\xi/\pi)f_\pm(\theta)$ with $f_\pm$ admitting expansions of the form $f_\pm(\theta) = 1 + \sum_{l=1}^{\infty} a_l^\pm\theta^l$ with all the coefficients and the radius of convergence ~ 1 in the limit $\beta \to 0$. Therefore the boundary S-matrices agree when $\theta \ll 1$, and S_{NR} represents the nonrelativistic limit of the boundary S-matrix of the sine-Gordon theory. One can check that the same statements are true for the bulk two-particle sine-Gordon S-matrix of [5] and the S-matrix of the particles interacting via the potentials (3.5), provided that (3.6), (3.7) are satisfied (this result was first established in [36] in the quasiclassical approximation and later confirmed in [5]; note that our approach allows to give an exact sense to the statement that the nonrelativistic limit of the bulk sine-Gordon theory is the hyperbolic-type Calogero-Moser model.) Thus the equivalence of (3.4) and the nonrelativistic limit of (2.1) is established.

3.6 Remarks

It is instructive to compare also the combined nonrelativistic/quasiclassical limit of the S-matrix of (2.1) with the Pöschl-Teller S-matrix in the regime $\beta^2 \ll \theta \ll 1$ (i.e. $k \gg m_0$)

without appealing to the exact formula (3.1), similar to how it was first done in [36] for the bulk soliton scattering. This means that one should first take the limit $\beta \to 0$ and then, using (2.34), pass to the limit $\theta \to 0$. Expanding the integrals in (2.34) and using the asymptotic formulas for the Γ-functions in (3.9) we get for (2.34) and (3.9) in the principal order the following result:

$$P_+(k) = e^{2i\xi sign(k) + \frac{4ik}{m_0} \ln \frac{k\beta^2}{m_0}}, \qquad P_-(k) = e^{\frac{4ik}{m_0} \ln \frac{k\beta^2}{m_0}}, \tag{3.14}$$

once again confirming the equivalence of the two theories. Note that it is impossible to determine μ and ν separately, since in our limit the boundary S-matrices in both theories depend only on the difference $\mu - \nu$.

The identification of the nonrelativistic limit in the case of the most general integrable boundary condition (2.3) requires a nontrivial generalization of the Calogero-Moser Hamiltonians. Indeed, if in (2.1) $M < \infty$, then the boundary S-matrix does not conserve the topological charge, and we are not aware of any integrable nonrelativistic model which allows such a process.

Chapter 4

Boundary bound states and boundary bootstrap

In the previous chapters we discussed classical, semi-classical and non-relativistic limits of the boundary sine-Gordon model. Now we address the *exact* quantum field theory solution of this model, which we obtain by means of the Bethe ansatz technique. Among other things, this solution allows to re-derive the boundary reflection matrices of [1], (3.1)-(3.3), and to relate them to the physical parameters in the Hamiltonian [39]. The present chapter includes a complete study of boundary bound states and related boundary S-matrices for the sine-Gordon model with Dirichlet boundary condition. Our analysis is based on the solution of the boundary bootstrap equations, representing the integrability constraints, together with the explicit Bethe ansatz solution of the inhomogeneous XXZ model in a boundary magnetic field – a lattice regularization of the boundary sine-Gordon model. We identify boundary bound states with new *boundary strings* in the Bethe ansatz. This chapter is based on [40].

4.1 Introduction

In the seminal work [1] it appeared clearly that the boundary sine-Gordon model presents an extremely rich structure of boundary bound states, which was further explored in [41]. Our first purpose here is to study this structure thoroughly in the particular case of Dirichlet boundary conditions, that is the model

$$\mathcal{L}_{SG} = \frac{1}{2}\int_0^\infty \left[(\partial_t\varphi)^2 - (\partial_x\varphi)^2 + \frac{m_0^2}{\beta^2}\cos\beta\varphi\right] dx \tag{4.1}$$

with a fixed value of the field at the boundary: $\varphi(x=0,t)=\varphi_0$.

Also, the consideration of boundary problems poses interesting challenges from the point of view of lattice models, here lattice regularizations of (4.1). In [39] and also in [42] it was shown in particular how to derive the S-matrices of [1] from the Bethe ansatz. Our second purpose is to complete these studies by investigating which new types of strings correspond to boundary bound states, and by deriving as well the set of S-matrices necessary to close the bootstrap. Observe that lattice regularizations are useful to define what one means by

creating a bound state at the boundary. Indeed, some bound states (showing up as the pols of S-matrices) have no straightforward interpretation, and although they are easy to study formally using the Yang Baxter equation and the bootstrap, their meaning in the field theory is unclear.

In section 4.2 we consider the bootstrap problem directly in the continuum theory. We identify boundary bound states and we compute the related boundary S matrices. In section 4.3 we write the Bethe ansatz equations for the inhomogeneous six-vertex model with boundary magnetic field, which is believed [39] to be a regularization of (4.1). We show that these equations are also the bare equations for the Thirring model with $U(1)$-preserving boundary interaction, which is the fermionized version of (4.1). In section 4.4 we discuss in details new solutions ("boundary strings") to the Bethe ansatz equations made possible by the appearance of boundary terms. In section 4.5 we study the physical properties of the model, in particular the masses and S-matrices corresponding to these boundary strings, and we partially complete the identification with the bootstrap results of section 4.2. Several remarks, in particular formula for the boundary energy of the boundary sine-Gordon model, are collected in sections 4.6-4.7.

4.2 Boundary bootstrap

4.2.1 Solving the boundary bootstrap equations

The S-matrices for the scattering of a soliton (P^+) and an anti-soliton (P^-) on the ground state $|0\rangle_B$ of the sine-Gordon model with Dirichlet boundary conditions (4.1) read according to [1]:

$$P^{\pm}(\theta) = \cos(\xi \pm \lambda u) R_0(u) R_1(u, \xi), \tag{4.2}$$

where $\theta = iu$ is the rapidity, $\xi = 4\pi\varphi_0/\beta$ and $\lambda = 8\pi/\beta^2 - 1$. The explicit form of R_0, R_1 is given in (3.2)-(3.3). Since the theory is invariant under the simultaneous transformations $\xi \to -\xi$, and soliton$\to$anti-soliton, we choose hereafter ξ to be a generic number in the interval $0 < \xi < 4\pi^2/\beta^2$ (see the discussion in chapter 2 about the value of the upper bound).

The function R_0 contains poles in the physical strip $0 < \mathrm{Im}\theta < \pi/2$ located at $u = n\pi/2\lambda, n = 1, 2, \ldots < \lambda$. These poles come from the corresponding breather pole in the soliton-antisoliton bulk scattering, and should not be interpreted as boundary bound states [1].

When $\xi > \pi/2$, the function $P^+(\theta)$ has additional poles in the physical strip, located at $u = v_n$ with

$$0 < v_n = \frac{\xi}{\lambda} - \frac{2n+1}{2\lambda}\pi < \frac{\pi}{2}, \tag{4.3}$$

$(n = 0, 1, 2, \ldots)$ corresponding to a first set of boundary bound states which we denote by $|\beta_n\rangle$, with masses

$$m_n = m \cos v_n = m \cos\left(\frac{\xi}{\lambda} - \frac{2n+1}{2\lambda}\pi\right), \tag{4.4}$$

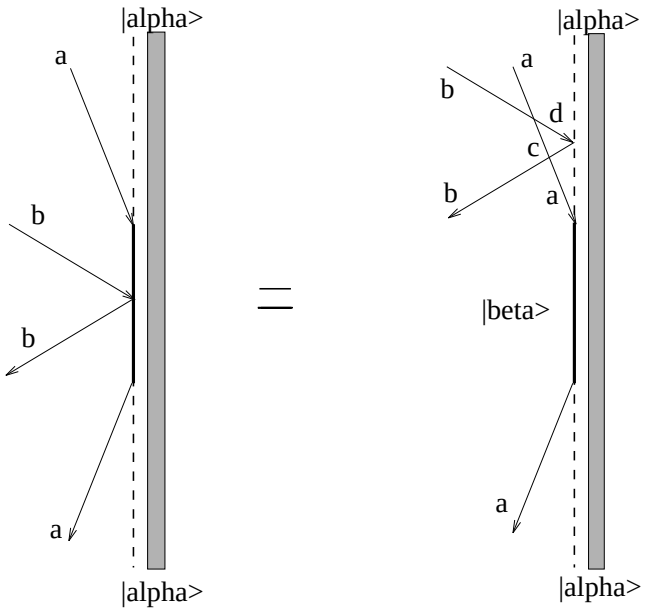

Figure 4.1: A diagrammatic representation of the bootstrap equations (4.5).

where m is the soliton mass. These bound states are easy to interpret [1, 23]. For $0 < \varphi_0 < \pi/\beta$ the ground state of the theory is characterized by the asymptotic behaviour $\varphi \to 0$ as $x \to \infty$, but other states, whose energy differs from the ground state by a boundary term only, can be obtained with $\varphi \to \{$ a multiple of $2\pi/\beta\}$ as $x \to \infty$. Since the β_n appear as bound states for soliton scattering, they all have the same topological charge as the soliton, which we take equal to unity by convention, so they are all associated with the same classical solution, a soliton sitting next to the boundary and performing a motion periodic in time ("breathing"), with $\varphi(x = 0) = \varphi_0$ and $\varphi \to 2\pi/\beta$ as $x \to \infty$ (see section 2.2.4).

To deduce the scattering matrices on the boundary bound states we use the *boundary bootstrap equations* as given in [1]. We assume that these S-matrices are diagonal, which is true if all the boundary bound states have different energies. In this case the bootstrap equations read:

$$R^b_\beta(\theta) = \sum_{c,d} R^d_\alpha(\theta) S^{ab}_{cd}(\theta + iv^\beta_{\alpha a}) S^{dc}_{ba}(\theta - iv^\beta_{\alpha a}). \tag{4.5}$$

These equations allow us to find the scattering matrix of any particle b on the boundary bound state β provided that the latter appears as a virtual state in the scattering of the particle a on the boundary state α.
The masses of the corresponding boundary states are related through

$$m_\beta = m_\alpha + m_a \cos v^\beta_{\alpha a}, \tag{4.6}$$

where $iv^\beta_{\alpha a}$ denotes the position of the pole, corresponding to the bound state β.

Let β_n stand for the n-th boundary bound state corresponding to the pole v_n in P^+ (4.3). Then (4.5) gives:

$$P^+_{\beta_n}(\theta) = P^+(\theta) a(\theta - iv_n) a(\theta + iv_n), \tag{4.7}$$

$$P^-_{\beta_n}(\theta) = b(\theta - iv_n)b(\theta + iv_n)P^-(\theta) + c(\theta - iv_n)c(\theta + iv_n)P^+(\theta), \tag{4.8}$$

where the well known bulk S-matrix elements $a(\theta) = S^{++}_{++} = S^{--}_{--}$ (kink-kink scattering), $b(\theta) = S^{+-}_{+-} = S^{-+}_{-+}$ (kink-anti-kink transmission) and $c(\theta) = S^{-+}_{+-} = S^{+-}_{-+}$ (kink-anti-kink reflection) can be found in [5].

It is easy to check that the matrix elements (4.7)-(4.8) satisfy general requirements for the boundary S-matrices, such as boundary unitarity and boundary crossing-symmetry conditions [1], e.g.

$$P^-_{\beta_n}(\frac{i\pi}{2} - \theta) = b(2\theta)P^+_{\beta_n}(\frac{i\pi}{2} + \theta) + c(2\theta)P^-_{\beta_n}(\frac{i\pi}{2} + \theta),$$
$$P^\pm_{\beta_n}(\theta)P^\pm_{\beta_n}(-\theta) = 1.$$

Finally we obtain from (4.7)-(4.8) by direct calculation:

$$P^+_{\beta_n}(\theta) = \frac{\cos(\xi - \lambda\pi - i\lambda\theta)}{\cos(\xi - \lambda\pi + i\lambda\theta)}P^-_{\beta_n}(\theta). \tag{4.9}$$

Hence the boundary Yang Baxter equation is satisfied since the ratio of the above two amplitudes has a form similar to (4.2) with $\xi \to \xi - \lambda\pi$, ξ being a free parameter.

The analytic structure of $P^\pm_{\beta_n}(\theta)$ is as follows. The function $P^+_{\beta_n}(\theta)$ has simple poles in the physical strip located at $u = \frac{\xi}{\lambda} + \frac{2N+1}{2\lambda}\pi$, $N = 0, 1, 2...$, and at $u = v_n$. It has double poles at $u = iv_n + i\frac{k\pi}{\lambda}$, $k = 1, 2, ...n$. The function $P^-_{\beta_n}(\theta)$ possesses in the physical strip the same singularities as $P^+_{\beta_n}(\theta)$ plus the set of simple poles at $u = w_N$ with

$$w_N = \pi - \frac{\xi}{\lambda} - \frac{2N-1}{2\lambda}\pi, \qquad \lambda + \frac{1}{2} - \frac{\xi}{\pi} > N > \frac{\lambda+1}{2} - \frac{\xi}{\pi}. \tag{4.10}$$

Interpreting these poles in terms of boundary bound states requires some care. First, due to the relation (4.5), one sees that if β appears as a boundary bound state for scattering of a on α, then the poles of the amplitude for scattering of b on α are also in general poles of the amplitude for scattering of b on β. It seems unlikely that these poles correspond to new bound states, although in our case they would have a natural physical meaning, for example one could try to associate them with classical solutions where $\varphi \to 4\pi/\beta$ as $x \to \infty$. Indeed there are strong constraints coming from statistics that we should not forget. For instance at the free fermion point $\beta^2 = 4\pi$, there is a bound state β_1, but although $P^+_{\beta_1}$ has again a pole at β_1, the state of mass $2m_{\beta_1}$ is not allowed from Pauli exclusion principle, as can easily be checked on the direct solution of the model (see below section 4.3.3). Therefore we take the point of view that the poles already present in the scattering on an "empty boundary" are "redundant". The only poles we interpret as new boundary bound states are (4.10) (the additional poles in $P^+_{\beta_n}$ are related to them by crossing). We denote these boundary bound states $|\delta_{n,N}\rangle$, and their masses, according to (4.6) and (4.4), are given by

$$\begin{aligned} m_{n,N} &= m(\cos v_n + \cos w_N) = m\cos\left(\frac{\xi}{\lambda} - \frac{2n+1}{2\lambda}\pi\right) - m\cos\left(\frac{\xi}{\lambda} + \frac{2N-1}{2\lambda}\pi\right) \\ &= m^b_{N+n}\sin\left(\frac{\xi}{\lambda} + \frac{N-n-1}{2\lambda}\pi\right), \end{aligned} \tag{4.11}$$

where $m_p^b = 2m \sin\left(\frac{p\pi}{2\lambda}\right)$ is the mass of the p-th breather, $p = 1, 2, \ldots < \lambda$.

To understand the physical meaning of these new boundary bound states it is helpful to consider the semi-classical limit $\lambda \to \infty$ of the sine-Gordon model. As discussed above, the boundary bound states β_n, corresponding to (4.3), are associated with solutions where a soliton is sitting next to the boundary and "breathing". An incoming anti-soliton can couple to this soliton, and together they form a breather sitting next to the boundary and performing again some (rather complicated) motion periodic in time[1]. The WKB quantization of this solution [43] shoud lead to $|\delta_{n,N}\rangle$. The topological charge of the states $|\delta_{n,N}\rangle$ is equal to 0 in our units, or, equivalently, to the charge of a free breather in the theory (4.1).

One can in principle continue to solve the bootstrap equations (4.5) recursively. For example, for the scattering of solitons or antisolitons on the boundary bound states $|\delta_{n,N}\rangle$ (4.10) one obtains the following S-matrices:

$$P^-_{\delta_{n,N}}(\theta) = P^-_{\beta_n}(\theta) a(\theta - i w_N) a(\theta + i w_N), \tag{4.12}$$

$$P^+_{\delta_{n,N}} = \frac{\cos(\xi - i\lambda\theta)}{\cos(\xi + i\lambda\theta)} P^-_{\delta_{n,N}}. \tag{4.13}$$

$P^-_{\delta_{n,N}}$ has only one simple pole in the physical strip at $u = w_N$, while $P^+_{\delta_{n,N}}$ has also simple poles at $u = v_k$, $k = n+1, n+2, ..., [\frac{\xi}{\lambda} - \frac{1}{2}]$. According to the discussion below (4.10), we do not consider these poles as associated with new boundary bound states. Therefore, the boundary bootstrap is closed for solitons and antisolitons in the sense that further recursion will not generate new boundary bound states.

So far we have obtained two sets of boundary bound states (4.4) and (4.11) by considering all the poles in the physical strip of amplitudes for scattering a soliton and anti-soliton on a boundary with or without a boundary bound state. Of course we should also consider the scattering of breathers off the boundary. The scattering of breathers on the "empty" boundary was studied in [41], and we refer the reader to this work for the explicit boundary S-matrices. By interpreting the poles of the amplitudes in [41] as boundary bound states, we find a spectrum of masses that look like (4.11) but with a slightly different range of parameters. Considering then scattering of breathers off a boundary with a bound state does not give rise to any new poles beside (4.3) and (4.10), with in the latter case an extended range of values of N (for simplicity we do not give the relevant boundary S-matrices here). Therefore the complete boundary bootstrap is closed in principle.

4.2.2 Integral representations of various S-matrices

For comparison with results obtained from regularizations of the sine-Gordon model it is useful to write integral representations of the boundary S-matrices (4.2), (4.7) and (4.8) using the well-known formula

$$\log\Gamma(z) = \int_0^\infty \frac{dx}{x} e^{-x} \left[z - 1 + \frac{e^{-(z-1)x} - 1}{1 - e^{-x}} \right], \qquad \mathrm{Re} z > 0. \tag{4.14}$$

[1]To compute this solution explicitly requires using a bulk five-soliton configuration [23], an expression which is very cumbersome.

Suppose first that $1 < 2\xi/\pi < \lambda + 1$ and denote

$$n_* = \left[\frac{\xi}{\pi} - \frac{1}{2}\right], \tag{4.15}$$

where the square brackets mean the integer part of the number. For such values of ξ there are n_*+1 poles (4.3) in the physical strip, i.e. the spectrum of excitations contains boundary bound states. Correspondingly, there is a finite number of Γ-functions in (4.2), (4.7), (4.8) whose arguments have negative real part so that formula (4.14) is not applicable. Treating such Γ-functions separately, we obtain the following results:

$$\begin{aligned} -i\frac{d}{d\theta}\log\left[\frac{P^+(\theta)}{R_0(\theta)}\right] &= \frac{2\lambda}{\pi}\int_{-\infty}^{+\infty} dx \cos\left(\frac{2\lambda\theta x}{\pi}\right) \\ &\times \left[\frac{\sinh(2\xi/\pi - 2n_* - 2)x}{\sinh x} + \frac{\sinh(\lambda - 2\xi/\pi)x}{2\sinh x\cosh\lambda x}\right], \end{aligned} \tag{4.16}$$

$$\begin{aligned} -i\frac{d}{d\theta}\log\left[\frac{P^+_{\beta_n}(\theta)}{R_0(\theta)}\right] &= \frac{2\lambda}{\pi}\int_{-\infty}^{+\infty} dx \cos\left(\frac{2\lambda\theta x}{\pi}\right) \\ &\times \frac{\sinh(\lambda - 2\xi/\pi)x - 2\cosh x\sinh(\lambda + 1 + 2n - 2\xi/\pi)x}{2\sinh x\cosh\lambda x}, \end{aligned} \tag{4.17}$$

$$\begin{aligned} -i\frac{d}{d\theta}\log\left[\frac{P^-_{\beta_n}(\theta)}{R_0(\theta)}\right] &= \frac{2\lambda}{\pi}\int_{-\infty}^{+\infty} dx \cos\left(\frac{2\lambda\theta x}{\pi}\right)\left[\frac{\sinh(2n_* + 2 - 2\xi/\pi)x}{\sinh x}\right. \\ &+ \left.\frac{\sinh(\lambda - 2\xi/\pi)x - 2\cosh x\sinh(\lambda + 1 + 2n - 2\xi/\pi)x}{2\sinh x\cosh\lambda x}\right]. \end{aligned} \tag{4.18}$$

In the derivation of analogous representation for P^- there are no subtleties because the "dangerous" Γ-functions cancel. We get

$$-i\frac{d}{d\theta}\log\left[\frac{P^-(\theta)}{R_0(\theta)}\right] = \frac{2\lambda}{\pi}\int_{-\infty}^{+\infty} dx \cos\left(\frac{2\lambda\theta x}{\pi}\right)\frac{\sinh(\lambda - 2\xi/\pi)x}{2\sinh x\cosh\lambda x}. \tag{4.19}$$

In the region $0 < 2\xi/\pi < 1$ where there are no poles and no boundary bound states in the spectrum, formula (4.19) is valid, too. The expression for P^+ can be obtained from (4.16) by setting formally $n_B \equiv n_* + 1 = 0$, which gives

$$-i\frac{d}{d\theta}\log\left[\frac{P^+(\theta)}{R_0(\theta)}\right] = \frac{2\lambda}{\pi}\int_{-\infty}^{+\infty} dx \cos\left(\frac{2\lambda\theta x}{\pi}\right)\frac{\sinh(\lambda + 2\xi/\pi)x}{2\sinh x\cosh\lambda x}. \tag{4.20}$$

Note that if $2\xi/\pi > 1$, the integral in (4.20) diverges. Finally, we complete this list by the following two expressions:

$$\begin{aligned} -i\frac{d}{d\theta}\log\left[\frac{P^\pm_{\delta_{N,n}}(\theta)}{R_0(\theta)}\right] &= -i\frac{d}{d\theta}\log\left[\frac{P^\pm_{\beta_n}(\theta)}{R_0(\theta)}\right] + \frac{2\lambda}{\pi}\int_{-\infty}^{+\infty} dx \cos\left(\frac{2\lambda\theta x}{\pi}\right) \\ \times \left[\frac{\sinh(\frac{2\xi}{\pi} - 2n_* - 2)x}{\sinh x}\right. &- \left.\frac{2\cosh x\sinh(\frac{2\xi}{\pi} + 2N - \lambda - 1)x}{2\sinh x\cosh\lambda x}\right]. \end{aligned} \tag{4.21}$$

For the integral representation of R_0 see [39].

4.3 Exact solution of the regularized boundary sine-Gordon model

4.3.1 The XXZ chain with boundary magnetic field

The XXZ model in a boundary magnetic field

$$\mathcal{H} = \frac{\pi-\gamma}{2\pi\sin\gamma}\left[\sum_{i=1}^{L-1}\left(\sigma_i^x\sigma_{i+1}^x+\sigma_i^y\sigma_{i+1}^y+\Delta(\sigma_i^z\sigma_{i+1}^z-1)\right)+h(\sigma_1^z-1)+h'(\sigma_L^z-1)\right], \quad (4.22)$$

was discussed in [44] and in [45], where its eigenstates were constructed using the Bethe ansatz. As usual, these eigenstates $\mathcal{H}|n\rangle = E|n\rangle$ are linear combinations of the states with n down spins, located at $x_1, ..., x_n$ on the chain:

$$|n\rangle = \sum f^{(n)}(x_1, ..., x_n)|x_1, ..., x_n\rangle.$$

Consider for simplicity the case $n = 1$. The wave-function $f^{(1)}(x)$ reads [45]:

$$\begin{aligned} f^{(1)}(x) &= [e^{-ik} + (h'-\Delta)]e^{-i(L-x)k} - (k \to -k) = \quad (4.23)\\ &= \left[\frac{\sinh\frac{1}{2}(i\gamma+\alpha)}{\sinh\frac{1}{2}(i\gamma-\alpha)}\right]^{L-x}\frac{\sin\gamma\sinh\frac{1}{2}(\alpha+i\gamma H')}{\sinh\frac{1}{2}(i\gamma-\alpha)\sin\frac{1}{2}(\gamma+\gamma H')} - (\alpha\to-\alpha), \end{aligned}$$

where we defined the new variables as in [45]: $\Delta = -\cos\gamma$, $k = f(\alpha,\gamma)$,

$$\gamma H = f(i\gamma, -i\ln(h-\Delta)) = -\gamma - i\ln\frac{h-i\sin\gamma}{h+i\sin\gamma} \quad (4.24)$$

(and similarly for H'), and

$$f(a,b) = -i\ln\left[\frac{\sinh\frac{1}{2}(ib-a)}{\sinh\frac{1}{2}(ib+a)}\right]. \quad (4.25)$$

When h varies from 0 to $+\infty$, γH increases monotonically from $-\pi-\gamma$ to $-\gamma$ according to (4.24) if we take the main branch of the logarithm.

Denote $h_{th} = 1-\cos\gamma$. This "threshold" value of h corresponds to $\gamma H = -\pi$; its meaning will become clear below. When h varies from $-\infty$ to 0, γH increases monotonically from $-\gamma$ to $\pi-\gamma$. For the purposes of the present work we confine our attention to the region $h, h' > 0$ and choose $\gamma \in (0, \frac{\pi}{2})$. Other regions in the parameter space can be obtained using the discrete symmetries of the Hamiltonian (4.22): $\sigma^z \to -\sigma^z$ on each site or on the odd sites only. The parameter k in (4.23) is not arbitrary, but satisfies the Bethe equation [45]:

$$e^{i(2L-2)k}\frac{(e^{ik}+h-\Delta)(e^{ik}+h'-\Delta)}{(e^{-ik}+h-\Delta)(e^{-ik}+h'-\Delta)} = 1, \quad (4.26)$$

or

$$\left[\frac{\sinh\frac{1}{2}(\alpha-i\gamma)}{\sinh\frac{1}{2}(\alpha+i\gamma)}\right]^{2L}\frac{\sinh\frac{1}{2}(\alpha-i\gamma H)\sinh\frac{1}{2}(\alpha-i\gamma H')}{\sinh\frac{1}{2}(\alpha+i\gamma H)\sinh\frac{1}{2}(\alpha+i\gamma H')} = 1. \quad (4.27)$$

Note that the wave-function (4.23) depends on H implicitely through the solution of the Bethe equation (4.27) $\alpha(H, H')$. Besides, one can multiply the amplitude (4.23) by any overall scalar factor depending on α, L, H and H'. The Bethe equations in the sector of arbitrary $n > 1$ can be found in [45].

4.3.2 The Bethe equations for the inhomogeneous XXZ chain

The real object of interest for us is actually the inhomogeneous six-vertex model with boundary magnetic field on an open strip. The inhomogeneous six-vertex model is obtained by giving an alternating imaginary part $\pm i\Lambda$ to the spectral parameter on alternating vertices of the six-vertex model [46, 47]. It was argued in [39], generalizing known results for the periodic case [46], that this model on an open strip provides in the scaling limit $\Lambda, L \to \infty$, lattice spacing $\to 0$ a lattice regularization of (4.1), with $\beta^2 = 8\gamma$ and a value of φ_0 at the boundary related to the magnetic field. The reader can find more details on the model in the references; it is actually closely related to the XXZ chain we discussed above. In particular, the wave function can be expressed in terms of the roots α_j of the Bethe equations [45, 46]:

$$\begin{aligned} &\left[\frac{\sinh\frac{1}{2}(\alpha_j+\Lambda-i\gamma)}{\sinh\frac{1}{2}(\alpha_j+\Lambda+i\gamma)}\frac{\sinh\frac{1}{2}(\alpha_j-\Lambda-i\gamma)}{\sinh\frac{1}{2}(\alpha_j-\Lambda+i\gamma)}\right]^L \frac{\sinh\frac{1}{2}(\alpha_j-i\gamma H)}{\sinh\frac{1}{2}(\alpha_j+i\gamma H)}\frac{\sinh\frac{1}{2}(\alpha_j-i\gamma H')}{\sinh\frac{1}{2}(\alpha_j+i\gamma H')} \\ = &\prod_{m\neq j}\frac{\sinh\frac{1}{2}(\alpha_j-\alpha_m-2i\gamma)}{\sinh\frac{1}{2}(\alpha_j-\alpha_m+2i\gamma)}\frac{\sinh\frac{1}{2}(\alpha_j+\alpha_m-2i\gamma)}{\sinh\frac{1}{2}(\alpha_j+\alpha_m+2i\gamma)}. \end{aligned} \tag{4.28}$$

By construction of the Bethe-ansatz wave function, $\mathrm{Re}\alpha_j > 0$. Note that the solutions of (4.28) $\alpha_j = 0, i\pi$ should be excluded because the wave function vanishes identically in this case. The analysis of solutions of eq. (4.28) is very similar to the case of the XXZ chain in a boundary magnetic field. We consider the regime $0 < \gamma < \pi/2$, which falls into the attractive regime $0 < \beta^2 < 4\pi$ in the sine-Gordon model (4.1). We set hereafter $\gamma = \pi/t$ and for technical simplicity restrict t to be positive integer. In the limit $L \to \infty$ this constraint implies that in the bulk only the strings of length from 1 to $t-1$ are allowed, along with the anti-strings (see chapter 1).

Taking the logarithm of eq. (4.28), one obtains:

$$\begin{aligned} &L\left[f(\alpha_j+\Lambda,\gamma)+f(\alpha_j-\Lambda,\gamma)\right]+f(\alpha_j,\gamma H)+f(\alpha_j,\gamma H') \\ &\qquad = 2\pi l_j+\sum_{m\neq j}\left[f(\alpha_j-\alpha_m,2\gamma)+f(\alpha_j+\alpha_m,2\gamma)\right], \end{aligned} \tag{4.29}$$

where l_j is an integer. We also recall the formula for the eigen-energy associated with the roots α_j [45, 46],

$$E = \frac{\pi-\gamma}{\pi}\sum_{\alpha_j}[f'(\alpha_j+\Lambda,\gamma)+f'(\alpha_j-\Lambda,\gamma)]. \tag{4.30}$$

4.3.3 Thirring model with boundary

Like the bulk sine-Gordon model is a bosonized version of the bulk massive Thirring model, one can expect that the boundary sine-Gordon model is a bosonized version of the Thirring model with certain boundary conditions. The quickest way to identify this boundary Thirring model is to use the Bethe ansatz equations (4.28). Write the most general $U(1)$-invariant boundary interaction

$$\begin{aligned} H_T = \int_0^L \quad & dx \quad [-i\psi_1^+\psi_{1x} + i\psi_2^+\psi_{2x} + m_0\psi_1^+\psi_2 + m_0\psi_2^+\psi_1 + 2g_0\psi_1^+\psi_2^+\psi_2\psi_1] \\ & + \quad \sum_{ij} a_{ij}\psi_i^+\psi_j(0) + \sum_{ij} a'_{ij}\psi_i^+\psi_j(L). \end{aligned} \tag{4.31}$$

The entries of the 2×2 matrices $A = \{a_{ij}\}, A' = \{a'_{ij}\}$ can be determined up to one arbitrary parameter ϕ by the hermicity of H_T and the consistency of the boundary conditions ($\det A = 0$). For the left boundary, the matrix A looks like

$$A = \frac{1}{2\sin\phi}\begin{pmatrix} e^{-i\phi} & 1 \\ 1 & e^{i\phi}\end{pmatrix} \tag{4.32}$$

and the boundary condition reads $\psi_1(0) = -e^{i\phi}\psi_2(0)$ (similarly for the right boundary).

To find the eigenvectors of the Hamiltonian (4.31), $H_T\Psi = E\Psi$, one can use the same wave-functions as for the bulk Thirring model (1.7), and modify them by analogy with the example of XXZ chain in a boundary magnetic field [45]. This way one gets the equations for the set of rapidities α_j :

$$\begin{aligned} e^{2im_0L\sinh\alpha_j} \quad &= \quad \frac{\cosh\frac{1}{2}(\alpha_j + i\phi)}{\cosh\frac{1}{2}(\alpha_j - i\phi)}\frac{\cosh\frac{1}{2}(\alpha_j + i\phi')}{\cosh\frac{1}{2}(\alpha_j - i\phi')} \\ &\times \quad \prod_{m\neq j}\frac{\sinh\frac{1}{2}(\alpha_j - \alpha_m - 2i\gamma)}{\sinh\frac{1}{2}(\alpha_j - \alpha_m + 2i\gamma)}\frac{\sinh\frac{1}{2}(\alpha_j + \alpha_m - 2i\gamma)}{\sinh\frac{1}{2}(\alpha_j + \alpha_m + 2i\gamma)}, \end{aligned} \tag{4.33}$$

where γ is related to g_0 in the usual way [18]. These equations look quite similar to (4.28). The mapping can be made complete by taking in (4.28) the limit $\Lambda\to\infty$ with the identification $m_0 = 4e^{-\Lambda}\sin\gamma$.

The derivation of these equations is rather cumbersome, therefore to illustrate the procedure we comment on the simplest case of one-particle sector, which is nevertheless sufficient to obtain the form of the boundary terms in (4.33). We make an ansatz $\Psi = \int_0^L dy\chi^\lambda(y)\psi_\lambda^+(y)|0\rangle$, where λ is the spinor index, $\chi(y)$ is the wave-function and $|0\rangle$ is the unphysical vacuum annihilated by ψ_λ.

The equation $H_T\Psi = E\Psi$ reduces to

$$-i\sigma_3\frac{\partial}{\partial x}\vec{\chi} + m_0\sigma_1\vec{\chi} + A\vec{\chi}\delta(x) + A'\vec{\chi}\delta(x-L) = E\vec{\chi}. \tag{4.34}$$

where σ_i are the Pauli matrices. We look for the solution of (4.34) in the form

$$\begin{pmatrix}\chi_1\\ \chi_2\end{pmatrix} = a(\alpha)\begin{pmatrix} e^{-\alpha/2}\\ e^{\alpha/2}\end{pmatrix}e^{im_0x\sinh\alpha} - a(-\alpha)\begin{pmatrix} e^{\alpha/2}\\ e^{-\alpha/2}\end{pmatrix}e^{-im_0x\sinh\alpha}. \tag{4.35}$$

Substituting it into (4.34) we get $E = m_0 \cosh\alpha$ and, besides, two boundary conditions to be solved. The first one, at $x = 0$, determines the form of the factor $a(\alpha) = \cosh\frac{1}{2}(\alpha - i\phi)$, while the second one at $x = L$ gives rise to the Bethe equation

$$e^{2im_0 L\sinh\alpha} = \frac{\cosh\frac{1}{2}(\alpha + i\phi)}{\cosh\frac{1}{2}(\alpha - i\phi)}\frac{\cosh\frac{1}{2}(\alpha + i\phi')}{\cosh\frac{1}{2}(\alpha - i\phi')},$$

which determines α. Comparing the Bethe equation (4.28) with (4.33) and using the relation between ξ and H obtained below in section 4.5 we find the relation between the boundary parameters ϕ and φ_0 in the Hamiltonians (4.31) and (4.1) respectively:

$$\phi = \beta\varphi_0 - \beta^2/8.$$

Thus, the integrable boundary condition for the $U(1)$-invariant boundary Thirring model equivalent to (4.1) reads:

$$\psi_2(0) = -e^{i\beta^2/8 - i\beta\varphi_0}\psi_1(0). \tag{4.36}$$

It would be interesting to obtain the result (4.36) directly from the Hamiltonian (4.1) using an extension of the Coleman-Mandelstam bosonization technique to the case with boundary. However, to our knowledge such an extension has not been developed yet, except for the free point [48].

4.4 Solutions of the Bethe ansatz equations with boundary terms

As is well known in the case of the bulk Thirring model or equivalently the periodic XXZ chain, the bound states are associated with various types of solutions of the Bethe ansatz equations involving in general complex roots (see chapter 1). By analogy, we expect the boundary bound states to correspond to new solutions made possible by the boundary terms.

Consider first the example of the XXZ chain as given in section 4.3.1. Since our goal is to study purely boundary effects, we will look for the solutions of the Bethe equations that give rise to a wave-function localized at $x = 0$ or $x = L$ and exponentially decreasing away from the boundary.

The states described by such wave-functions will be referred to as the "boundary bound states" below. For this, one should have α purely imaginary in (4.23). We consider here the limit of L large, when the left and the right boundaries can be treated independently and the overlap of the corresponding wave-functions is negligibly small (for the physical applications it is necessary to take the scaling limit anyway). In the limit $L \to \infty$ it is easy to check that there are two such solutions to (4.27): $\alpha = i\alpha_0 = -i\gamma H + i\varepsilon(L, H, H')$ and $\alpha = i\alpha_0' = -i\gamma H' + i\varepsilon'(L, H, H')$, where $\varepsilon \sim \exp(-2\kappa L)$ and we defined $\kappa > 0$ as

$$e^{-\kappa} = \left|\frac{\sin\frac{1}{2}(-\gamma H - \gamma)}{\sin\frac{1}{2}(-\gamma H + \gamma)}\right|$$

(similar relations are assumed for ε', κ'). Solution α_0' gives a wave-function (4.23) localized at $x = L$: $f^{(1)}(x) \sim e^{-\kappa'(L-x)}$. Solution α_0 gives a wave-function localized at $x = 0$, $f^{(1)}(x) \sim e^{-\kappa x}$, provided we renormalize the wave-function (4.23):

$$f^{(1)} \to f^{(1)} \left[\sinh \frac{1}{2}(\alpha - i\gamma H) \sinh \frac{1}{2}(\alpha + i\gamma H) \right]^{1/2}. \tag{4.37}$$

In the special case $H = H'$ there is only one proper solution $\alpha = i\alpha_0 = -i\gamma H + i\varepsilon(L, H)$ with $\varepsilon \sim \exp(-\kappa L)$. The wave-function (4.23) behaves as the superposition of the "left" and the "right" boundary bound states, $f^{(1)} \sim (e^{-\kappa x} + e^{-\kappa(L-x)})$. Note that the boundary bound state appears in the above example only when the boundary magnetic field is large enough:[2] namely, $h > h_{th}$. This follows from the fact that α should be such that $0 < \alpha_0 < \pi$.

Now, consider the equations for the inhomogeneous model (4.28). The basic boundary 1-string solution to (4.28) is $\alpha = i\alpha_0 = -i\gamma H + i\epsilon$, provided that $0 < \alpha_0 < \pi$. This solution is possible due to an argument very similar to the one used in the bulk: as $L \to \infty$, the two first terms of (4.28) decrease exponentially fast, while the third increases exponentially fast, and $\epsilon \sim \exp(-2\kappa L)$ with

$$e^{-\kappa} = \frac{\sinh^2 \frac{\Lambda}{2} + \sin^2 \frac{\alpha_0 - \gamma}{2}}{\sinh^2 \frac{\Lambda}{2} + \sin^2 \frac{\alpha_0 + \gamma}{2}}. \tag{4.38}$$

Recall that for the bulk problem when there is no boundary term, the right hand side of (4.28) would have to decrease exponentially, forcing the existence of a "partner" root at $\alpha - 2i\gamma$.

One can construct similarly boundary n-strings which consist of the points $i\alpha_0$, $i\alpha_0 + 2i\gamma, ..., i\alpha_0 + 2i(n-1)\gamma$ (see figure 4.2). By convention $n = 0$ means there is no boundary string, that is all complex solutions are in the usual bulk strings. The possible values of n are restricted by the fact that the upper point of the complex should be below $i\pi$: $\max(n) = [\frac{\pi - \alpha_0}{2\gamma}] + 1$, where the square bracket denotes the integer part. To show that the boundary n-string is indeed a solution to (4.28), we introduce infinitesimal corrections ε_i to the positions of the points of complex [20]. Taking the modulus of both sides of (4.28) with $\alpha_j = i\alpha_0 + 2ik\gamma$ and multiplying equations for $k = 0, ..., n-1$ we obtain $\exp\{-2L(\kappa_1 + \kappa_2 + ... + \kappa_n)\} \sim \varepsilon_1$, where ε_1 denotes the correction to the point $i\alpha_0$. The behavior of the remaining ε_k follows from ε_1 by recursion. For example, for the 2-string ε_2 is given by $|\varepsilon_1 - \varepsilon_2| \sim \exp(-2L\kappa_2)$.

Note that associated with each boundary n-string there is also the solution to (4.28) obtained by complex conjugation of all α's. The existence of such a "mirror image" is the

[2] More generally, the criterion of existence of boundary bound state solutions allows us to determine threshold fields for any anisotropy Δ. For this, let us examine (4.26). The parameter k is defined modulo 2π, therefore we restrict it to lie withing $k \in (0, 2\pi)$. Two possibilities $k = ia$ and $k = \pi + ia$, where $a > 0$, lead to two different threshold fields, determined by the fact that the denominator in (4.26) should vanish:

$$h_{th}^{(1)} = \Delta + 1, \qquad h_{th}^{(2)} = \Delta - 1,$$

and the regions where boundary bound states could in principle exist are $h < \Delta - 1, \quad h > \Delta + 1$ (one has to be carefull here and check that these solutions of BE indeed correspond to the *stable* states of the model). When $\Delta > 1$, there are two different threshold fields, in agreement with the results of Jimbo et al [49]. In the region of interest, $|\Delta| < 1$, there is only one threshold field $h_{th}^{(1)}$.

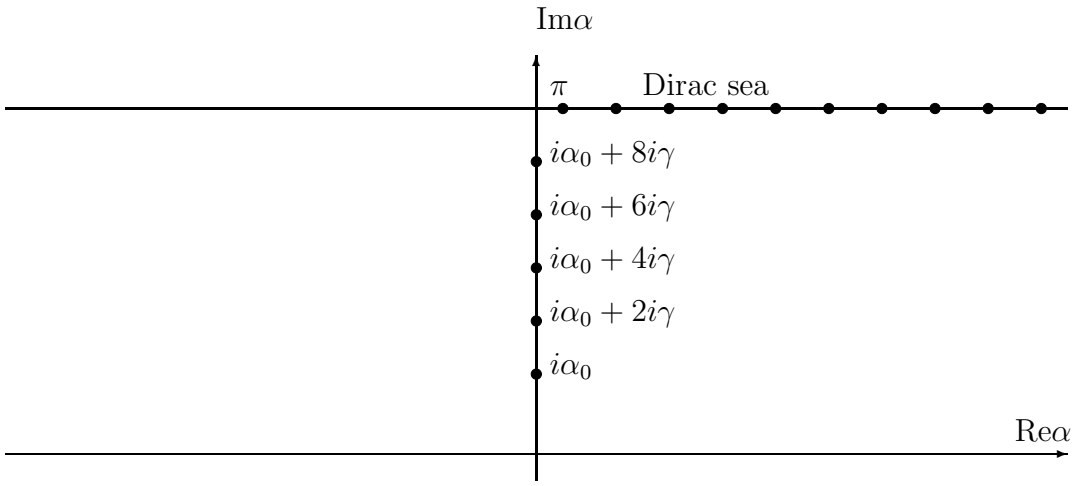

Figure 4.2: The first type of boundary string. In the ground state the boundary string of maximum allowed length is filled.

consequence of the symmetry of equations (4.28) and it is of no importance to physics. In the bulk case, it is easy to show [50] that all solutions are invariant under complex conjugation, but this result does not hold here. In fact, a solution which has both the boundary n-string and its mirror image would lead to a vanishing wave-function.

Additional boundary strings can be obtained by adding the roots $i\alpha_s$ below $i\alpha_0$ so that $i\alpha_s = i\alpha_0 - 2is\gamma$, with $s = 1, 2, ..., N$ (see figure 4.3). Together with the boundary n-string above α_0, they form the complex which we call boundary (n, N)-string. To analyze the existence of such complexes as the solutions of (4.28) we introduce as before the infinitesimal corrections ε_s to the roots α_s, where now $s = n, n-1, ..., 1, -1, -2, ..., -N$. Then, the equations (4.28) with $\alpha_j = i\alpha_s$ tell us that the range of N should be

$$\frac{\alpha_0}{2\gamma} < N < \frac{\pi + \alpha_0}{2\gamma}. \tag{4.39}$$

In other words, the inequality (4.39) states that the lowest root of the boundary string should be below the axis $\mathrm{Im}\alpha = 0$ and above the axis $\mathrm{Im}\alpha = -i\pi$. Another constraint follows if we multiply the equations (4.28) for all the roots of boundary (n, N)-string. This gives $\exp(-2L\sum \kappa_s) = \varepsilon_1$. So, one should have $\sum \kappa_s > 0$. The latter sum can be easily evaluated if one uses the expression (4.38) simplified in the limit $\Lambda \to \infty$: $\kappa = 4e^{-\Lambda} \sin\gamma \sin\alpha_0$. The constraint obtained in such a way forces the number of roots above $\mathrm{Im}\alpha = 0$ axis in the boundary string to be greater than the number of roots below $\mathrm{Im}\alpha = 0$.

We have not been able to find any reasonable additional solution to the Bethe ansatz equations. The two sets of boundary strings we have encountered appear to be in one to one

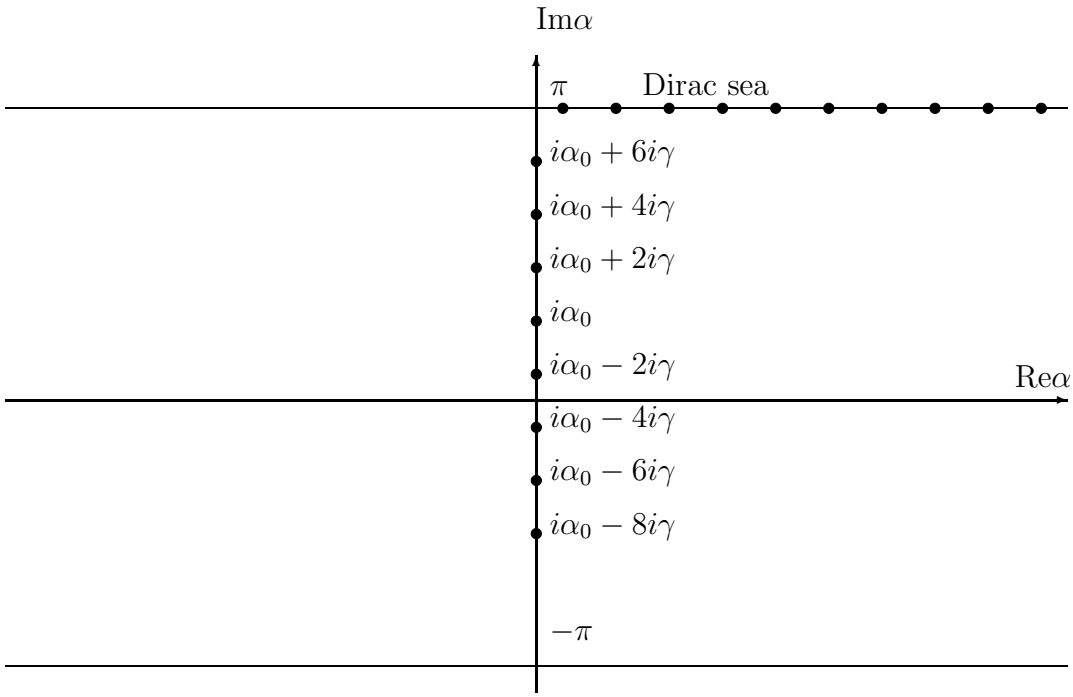

Figure 4.3: The second type of boundary string.

correspondence with the boundary bound states identified in section 4.2 using the bootstrap approach. To clarify this identification we now compute related masses and S-matrices.

4.5 S-matrices and bound state properties from the exact solution

4.5.1 Bare and physical Bethe ansatz equations

The *bare* Bethe equations follow from taking the derivative of (4.29). Defining $2L(\rho_k+\rho_k^h)d\alpha$ to be the number of roots in the interval $d\alpha$, one obtains coupled integral equations for the densities of strings $\rho_1, ..., \rho_{t-1}$ and anti-strings ρ_a:

$$\begin{aligned} 2\pi(\rho_k+\rho_k^h) &= \frac{1}{2}p_k' - f_{ka}'*\rho_a - \sum_{l=1}^{t-1} f_{kl}'*\rho_l + \frac{1}{2L}(u_k - \omega f_{n;k}'^{(L)} - \omega' f_{n';k}'^{(R)}) \\ 2\pi(\rho_a+\rho_a^h) &= -\frac{1}{2}p_a' + f'*\rho_a + \sum_{l=1}^{t-1} f_{al}'*\rho_l + \frac{1}{2L}(u_a + \omega f_n'^{(L)} + \omega' f_{n'}'^{(R)}) \end{aligned} \qquad (4.40)$$

where $*$ denotes convolution:

$$f*g(\alpha) = \int_{-\infty}^{\infty} d\beta f(\alpha-\beta)g(\beta).$$

These densities are originally defined for $\alpha > 0$, but the equations allow us to define $\rho_k(-\alpha) \equiv \rho_k(\alpha)$ in order to rewrite the integrals to go from $-\infty$ to ∞. If we totally neglect the boundary terms (terms $\sim L^{-1}$) in (4.40), we will end up with the same equations as for the periodic inhomogeneous six-vertex model [46]. The various kernels and sources in (4.40) are defined as follows:

$$p_a(\alpha) = f(i\pi+\alpha+\Lambda,\gamma) + f(i\pi+\alpha-\Lambda,\gamma),$$
$$p_k(\alpha) = \sum_{\alpha_i} f(\alpha_i+\Lambda,\gamma) + f(\alpha_i-\Lambda,\gamma),$$

where the sum in the last expression is taken over the rapidities of the bulk k-string roots centered on α.

The kernels f_{kl} are the phase shifts of bulk k-string on bulk l-string obtained by summing (4.25) over the rapidities of string roots. The boundary terms are:

$$u_a(\alpha) = -2f'(2\alpha,2\gamma) - f'(\alpha+i\pi,\gamma H) - f'(\alpha+i\pi,\gamma H') - 2\pi\delta(\alpha),$$

$$u_k(\alpha) = \sum_{\alpha_i}[2f'(2\alpha_i,2\gamma) + f'(\alpha_i,\gamma H) + f'(\alpha_i,\gamma H')] - 2\pi\delta(\alpha),$$

(the sum above is over the roots of bulk k-string centered on α),

$$f_n^{(L,R)}(\alpha) = \sum_{\alpha_i} f(i\pi+\alpha-\alpha_i,2\gamma) + f(i\pi+\alpha+\alpha_i,2\gamma),$$

and α_i denotes the rapidities of the roots in the boundary n-string.

$$f_{n;k}^{(L,R)}(\alpha) = \sum_{\alpha_i} \sum_{\alpha_j} f(\alpha_j - \alpha_i, 2\gamma) + f(\alpha_j + \alpha_i, 2\gamma),$$

where α_i denotes the roots in the boundary n-string, while α_j denotes the roots in the bulk k-string centered on α. The parameters ω, ω' are equal to 1 or 0, depending on whether the boundary string is present or not. In our ferromagnetic case the ground state of the periodic inhomogeneous XXZ chain is filled with anti-strings.

The physical Bethe equations are obtained [51, 52] by eliminating the "non-physical" density ρ_a from the right-hand side of (4.40). This is done simply by solving for ρ_a in the last equation in (4.40) and substituting it into the others. The result is

$$\begin{aligned} 2\pi(\rho_k + \rho_k^h) &= \frac{1}{2}p'_k + \frac{1}{2}\frac{f'_{ak}}{2\pi - f'} * p'_a + + \frac{f'_{ak}}{2\pi - f'} * 2\pi\rho_a^h \\ &- \sum_{l=1}^{t-1} \left(f'_{kl} + \frac{f'_{ak} f'_{al}}{2\pi - f'} \right) * \rho_l + \frac{1}{2L} U_{n,n';k}, \qquad (4.41) \\ 2\pi(\rho_a + \rho_a^h) &= -\frac{1}{2}\frac{2\pi p'_a}{2\pi - f'} - \frac{f'}{2\pi - f'} * 2\pi\rho_a^h + \sum_{l=1}^{t-1} \frac{f'_{al}}{2\pi - f'} * 2\pi\rho_l + \frac{1}{2L} U_{n,n';a}, \end{aligned}$$

where

$$U_{n,n';a} = 2\pi \frac{u_a + \omega f_n'^{(L)} + \omega' f_{n'}'^{(R)}}{2\pi - f'}, \qquad (4.42)$$

$$U_{n,n';k} = u_k - \omega f_{n;k}'^{(L)} - \omega' f_{n';k}'^{(R)} - f'_{ak} * U_{n,n';a}/2\pi, \qquad (4.43)$$

and different products (ratios) of kernels are defined through their Fourier transforms.

4.5.2 The mass spectrum of boundary bound states

We assume at first that the ground state is built by filling up the Dirac sea with anti-strings, as in the case of the periodic XXZ chain. We will see below that this is not always true. The presence of the boundary strings in the Bethe equations deforms the distribution of roots and modifies the density of the Dirac sea ρ_a by a term $\delta\rho_a/2L$ of order L^{-1}. With the boundary n-string, the Bethe equation for the density of the Dirac sea particles $\tilde{\rho}_a$ is

$$\frac{1}{2}p'_a(\alpha) - \frac{1}{2L}u_a(\alpha) = \int_{-\infty}^{+\infty} f'(\alpha - \beta)\tilde{\rho}_a(\beta)d\beta - 2\pi\tilde{\rho}_a(\alpha) + \frac{1}{2L}f'_n(\alpha), \qquad (4.44)$$

where f_n was defined above. Subtracting from (4.44) the equation for the density of the Dirac sea alone,

$$\frac{1}{2}p'_a(\alpha) - \frac{1}{2L}u_a(\alpha) = \int_{-\infty}^{+\infty} f'(\alpha - \beta)\rho_a(\beta)d\beta - 2\pi\rho_a(\alpha), \qquad (4.45)$$

one obtains the equation for $\delta\rho_a$:

$$0 = -\int_{-\infty}^{+\infty} f'(\alpha-\beta)\delta\rho_a(\beta)d\beta + 2\pi\delta\rho_a(\alpha) - f_n'(\alpha), \tag{4.46}$$

where

$$\delta\rho_a \equiv 2L(\tilde{\rho}_a - \rho_a).$$

The solution to (4.46) can be written in terms of the Fourier transform

$$\delta\hat{\rho}_a(k) = \int d\alpha e^{ik\alpha}\delta\rho_a(\alpha)$$

as follows:

$$\delta\hat{\rho}_a(k) = \frac{\hat{f}_n'(k)}{2\pi - \hat{f}'(k)}. \tag{4.47}$$

For the boundary n-string $i\alpha_0 + 2i\gamma s$, $s = 0, 1, ..., n-1$, we obtain

$$\hat{f}_n'(k) = -2\pi\frac{4\cosh\gamma k\sinh n\gamma k\cosh(\alpha_0+\gamma n-\gamma)k}{\sinh\pi k}, \tag{4.48}$$

$$\delta\hat{\rho}_a(k) = -\frac{2\cosh\gamma k\sinh n\gamma k\cosh(\alpha_0+\gamma n-\gamma)k}{\sinh\gamma k\cosh(\pi-\gamma)k}, \tag{4.49}$$

where we used

$$\hat{f}'(k) = 2\pi\frac{\sinh(\pi-2\gamma)k}{\sinh\pi k}.$$

Expressions (4.48), (4.49) are valid for the n-strings with $n = 1, 2, ..., \left[\frac{t+H}{2}\right]$. For the longest n-string with $n = \left[\frac{t+H}{2}\right]+1 \equiv n_*+1$ the Fourier transforms $\hat{f}_n', \delta\hat{\rho}_a$ differ from (4.48), (4.49):

$$\begin{aligned}\hat{f}_*'(k) &= 2\pi\frac{2\sinh(\pi-2\gamma)k\cosh(\alpha_0+2\gamma n_*-\pi)k}{\sinh\pi k} \\ &- 2\pi\frac{4\cosh\gamma k\sinh n_*\gamma k\cosh(\alpha_0+\gamma n_*-\gamma)k}{\sinh\pi k},\end{aligned} \tag{4.50}$$

$$\begin{aligned}\delta\hat{\rho}_a(k) &= \frac{\sinh(\pi-2\gamma)k\cosh(\alpha_0+2\gamma n_*-\pi)k}{\sinh\gamma k\cosh(\pi-\gamma)k} \\ &- \frac{2\cosh\gamma k\sinh n_*\gamma k\cosh(\alpha_0+\gamma n_*-\gamma)k}{\sinh\gamma k\cosh(\pi-\gamma)k}.\end{aligned} \tag{4.51}$$

The conserved $U(1)$ charge in the boundary XXZ chain is the total projection of the spin on the z-axis. In the thermodynamic limit the charge of the boundary n-string with respect to the vacuum is determined by [45]:

$$Q_n = n + \int_0^{+\infty} 2L\tilde{\rho}_a d\alpha - \int_0^{+\infty} 2L\rho_a d\alpha = n + \frac{1}{2}\int_{-\infty}^{+\infty}\delta\rho_a d\alpha = n + \frac{1}{2}\delta\hat{\rho}_a(0). \tag{4.52}$$

Using (4.49), we obtain for the n-string $Q_n = 0$, and for the longest boundary string Eq. (4.51) yields $Q_* = \pi/2\gamma$. Similarly, the mass of the boundary strings in the thermodynamic limit according to (4.30) is given by

$$m_n = h_n + \int_0^{+\infty} 2L\tilde{\rho}_a h_a d\alpha - \int_0^{+\infty} 2L\rho_a h_a d\alpha = h_n + \frac{1}{2}\int_{-\infty}^{+\infty} h_a \delta\rho_a d\alpha, \tag{4.53}$$

where the expression for h_a is

$$\hat{h}_a(k) = \frac{\pi-\gamma}{\pi}\hat{p}'_a = -2(\pi-\gamma)\frac{2\sinh\gamma k\cos\Lambda k}{\sinh\pi k}$$

and the soliton mass [46]

$$m = 2e^{-\frac{\Lambda\pi}{2(\pi-\gamma)}}.$$

We obtain in the limit $\Lambda \to \infty$

$$m_n = m\left[\sin\frac{\pi}{2\lambda}(2n-1-H) + \sin\frac{\pi}{2\lambda}(H+1)\right], \tag{4.54}$$

$$m_* = m\sin\frac{\pi}{2\lambda}(H+1). \tag{4.55}$$

Since the parameter H varies in the interval $-\lambda - 1 < H < -1$, the mass of the longest string m_* (4.55) is always negative, while the other boundary strings have positive masses (4.54). This means that the vacuum we have been working with is an unstable one in the region $-t < H < -1$ ($h > h_{th}$). To cure the situation we define a new correct ground state by attributing the longest boundary string to the Dirac sea. The boundary excitations are obtained by succeessive removing of particles from the top of the longest boundary string. The charge and mass of such excitations with respect to the correct ground state are given by

$$Q_n = -\frac{\pi}{2\gamma}, \qquad m_n = m\cos\frac{\pi}{2\lambda}(\lambda+1+H-2n), \qquad n = 0,1,...,n_*. \tag{4.56}$$

Note that the number of excitations (4.56) is equal to the number of roots in the longest boundary string, n_*+1. The charge of such boundary excitations is equal to the charge of the hole in the Dirac sea. We identify a hole with a sine-Gordon soliton, and the boundary excitations described above, with the boundary bound states $|\beta_n\rangle$ (4.4). Their masses and charge (4.56) and the counting coincide provided that

$$t + H + 1 = \frac{2\xi}{\pi}, \tag{4.57}$$

and the lattice charge Q is properly normalized. This expression is in fact valid for all values of $h > 0$.

In the above discussion we considered the boundary bound states related to one of the boundaries (say, the left one). In principle, one should include into the ground state the longest boundary string $i\alpha'_0 + 2i\gamma l$, $\quad l = 0,1,...,\left[\frac{t+H'}{2}\right]$, corresponding to the right boundary as well. The energy of the excitations due to both boundary strings is a superposition

of energies of the form (4.56). When $H = H'$, these two boundary strings overlap and the usual Bethe wave-function vanishes. However on physical grounds we do not expect anything special to happen when the boundaries are identical. So, in such a case one should use as a wave function a properly renormalized version of the limit $H \to H'$ of the usual Bethe wave function.

When the magnetic field varies, the above picture indicates a qualitative change in the structure of the ground state at values $H = -t, -t+2, -t+4, ...$ At these values, the mass of the bound state with the highest mass approaches the soliton mass and it becomes unstable. As discussed in [53] and [1] for the Ising case, this decay corresponds to large boundary fluctuations that propagate deeply into the bulk.

The mass of the boundary (n, N)-string with respect to the correct vacuum can be calculated analogously. The result is:

$$m_{n,N} = m\cos(\frac{\xi}{\lambda} - \frac{\pi}{2\lambda}) + m\cos(\frac{\xi}{\lambda} - \frac{2n+1}{2\lambda}\pi) - m\cos(\frac{\xi}{\lambda} + \frac{2N-1}{2\lambda}\pi), \tag{4.58}$$

where we used (4.57) to express H in terms of ξ. This result seems rather confusing, because the above mass does not correspond in general to one of the bound state masses found in the bootstrap apporach. It can be considered as a sum of such masses, hinting that the (n, N) string describes actually coexisting bound states, but the calculation of corresponding boundary S-matrix does not allow such an interpretation. We are forced (but see the conclusion) to consider that only the (n, N)-strings with $n = n_* + 1$ occur, that is the physical excitations are built by adding roots to the ground state configuration below $i\alpha_0$. The charge and energy of such excitations with respect to the correct vacuum is given by

$$Q_N = \frac{\pi}{2\gamma} - \frac{\pi}{2\gamma} = 0, \qquad m_N = m\cos(\frac{\xi}{\lambda} - \frac{\pi}{2\lambda}) - m\cos(\frac{\xi}{\lambda} + \frac{2N-1}{2\lambda}\pi), \tag{4.59}$$

These coincide with the charge and mass of the boundary bound states $|\delta_{n=0,N}\rangle$ (4.11). The range of N (4.39) agrees with the range of corresponding parameter in (4.10).

4.5.3 Boundary S-matrices

It remains to check that the boundary S-matrices obtained above by the bootstrap approach coincide with those of the lattice model. To extract the boundary S-matrices from the Bethe equations we will follow the discussion of [39]. Briefly, the idea of the method is the following. The physical excitations of the lattice model in the limit $\Lambda \to \infty$ can be thought of as relativistic quasi-particles with rapidities θ_i. The integrability implies that the set $\{\theta_i\}$ is conserved. Moreover, if the scattering matrices are diagonal, each particle preserves its rapidity. Assuming that this is the case, the quantization of a gas of $\mathcal{N}$ quasi-particles on an interval of lenght L results in the integral equations for the set of allowed rapidities [39]:

$$2\pi(\rho_b + \rho_b^h) = m_b \cosh\theta + \sum_{c=1}^{p} \varphi_{bc} * \rho_c + \frac{1}{2L}\Theta_b, \tag{4.60}$$

where subscript stands for the type of particle, and

$$\begin{aligned}\varphi_{bc}(\theta) &= -i\frac{d}{d\theta}\ln S_{bc}(\theta) \\ \Theta_b(\theta) &= -i\frac{d}{d\theta}\ln R_{\beta}^{b(L)}(\theta) - i\frac{d}{d\theta}\ln R_{\beta'}^{b(R)}(\theta) + i\frac{d}{d\theta}\ln S_{bb}(2\theta) - 2\pi\delta(\theta).\end{aligned} \tag{4.61}$$

Equations (4.60) should be compared with the physical BE (4.41), which gives bulk and boundary S-matrices. We will confine our attention to the boundary S-matrices only, keeping track of those terms in (4.42), (4.43), (4.61), which depend on the boundary magnetic field (the field-independent terms contribute to R_0 and their agreement has been shown in [39]). The discussion for the left boundary is completely parallel to that of the right one. Also, it is sufficient to consider only b =soliton and b =anti-soliton in (4.60). We identify a hole in the anti-string distribution in (4.41) with a soliton in (4.60), and $(t-1)$-string with an anti-soliton. Below we give explicit expressions only for the kernels in (4.41) which we need for our analysis. The other expressions are listed in [39].

Suppose first that $h < h_{th}$ $(-t-1 < H < -t)$. This corresponds to the case without boundary excitations in the spectrum, $\xi < \pi/2$. Choose $\omega = \omega' = 0$ in (4.41). Then

$$\hat{u}_a^{(L)}(k) = 2\pi\frac{\sinh(2\pi+\gamma H)k}{\sinh\pi k} + \dots$$

(we omitted the H-independent terms and H'-dependent ones),

$$\hat{U}_a^{(L)} = 2\pi\frac{\sinh(2\pi+\gamma H)k}{2\sinh\gamma k\cosh(\pi-\gamma)k} + \dots .$$

Using (4.61) we compare this expression with (4.20) (recall that the rapidity α should be renormalized $\alpha \to \theta = t\alpha/2\lambda$) and find complete agreement under the identification (4.57). Similarly, one can use

$$\hat{u}_{t-1}^{(L)} = -2\pi\frac{\sinh(\pi+\gamma H)k\sinh(\pi-\gamma)k}{\sinh\pi k\sinh\gamma k} + \dots ,$$

$$\hat{U}_{t-1}^{(L)} = -2\pi\frac{\sinh(2+H)\gamma k}{2\sinh\gamma k\cosh(\pi-\gamma)k} + \dots$$

to compare U_{t-1} with (4.19) and obtain agreement as well.

Next, suppose that $h > h_{th}$ $(-t < H < -1)$. To obtain the boundary S-matrices for scattering on the ground state $|0\rangle_B$ set $\omega = \omega' = 1$ and choose the boundary string to be the longest string, $n = n_* + 1$ in (4.41). Then, using (4.50), $\hat{f}'_{n_*+1;t-1} = -\hat{f}'_*$ and

$$\hat{u}_a^{(L)} = 2\pi\frac{\sinh\gamma Hk}{\sinh\pi k} + \dots ,$$

$$\hat{u}_{t-1}^{(L)} = \hat{u}_a^{(L)} - 2\pi\frac{\sinh(H+2[\frac{1-H}{2}])\gamma k}{\sinh\gamma k} + \dots \tag{4.62}$$

we obtain

$$\frac{\hat{U}^{(L)}_{n_*+1;a}}{2\pi} = \frac{\sinh\gamma H k}{2\sinh\gamma k\cosh(\pi-\gamma)k} + \frac{\sinh(\pi-2\gamma)k\cosh(H+t-2n_*)\gamma k}{\sinh\gamma k\cosh(\pi-\gamma)k} -$$

$$-\frac{2\cosh\gamma k\sinh n_*\gamma k\cosh(H-n_*+1)\gamma k}{\sinh\gamma k\cosh(\pi-\gamma)k} + \dots,$$

$$\hat{U}^{(L)}_{n_*+1;t-1} = \hat{U}^{(L)}_{n_*+1;a} - 2\pi\frac{\sinh(H+2[\frac{1-H}{2}])\gamma k}{\sinh\gamma k} + \dots,$$

which agrees with (4.16), (4.19) under the identification (4.57). Note that the last relation, which follows directly from (4.42), (4.43) and (4.62), is valid also for $\hat{U}_{n;a}$ and $\hat{U}_{n;t-1}$ with any n. In the same manner one can calculate the boundary S-matrices for scattering on the boundary n-strings and check that they indeed coincide with (4.17), (4.18) under the condition (4.57). For this, one needs to take $\omega = \omega' = 1$ in (4.41) and use (4.48), $\hat{f}'_{n;t-1} = -\hat{f}'_n$. Finally one can compute also the boundary S-matrix for the scattering on the (n_*+1, N)-strings, again in agreement with the bootstrap results.

4.6 Conclusion

The question of boundary bound states even in the simple Dirichlet case appears rather difficult: using the XXZ lattice regularization or equivalently the Thirring model, we have only been able to recover the $|\beta_n\rangle$ and $|\delta_{n=0,N}\rangle$ boundary bound states. A way out is to consider solutions of the Bethe ansatz equations made of an (n, N) string superposed with the n_*+1 string that describes the ground state. This is not allowed in principle in the model we consider because the Bethe wave function vanishes when two roots are equal. However, putting formally such a solution in the equations gives the masses of the $|\delta_{n,N}\rangle$ states and the S-matrix also agrees with the bootstrap results! But the meaning of this is not clear to us.

4.7 Remarks

Finally let us mention that one can calculate the ground state energy in the thermodynamic limit by solving the equation (4.44) for the ground state density and using (4.30):

$$E_{gr} = \int_0^{+\infty} 2L\tilde{\rho}_a(\alpha)h(\alpha)d\alpha.$$

As a result, we get the combination $E_{gr} = E_{bulk} + E_{boundary}$, where E_{bulk} is the well-known sine-Gordon ground state energy [54]:

$$E_{bulk} = -\frac{Lm^2}{4}\tan\frac{\pi\gamma}{2(\pi-\gamma)}$$

and $E_{boundary}$ is the contribution of the boundary terms ($\Lambda \to \infty$):

$$E_{boundary} = \frac{m}{2}\left[\frac{\sin\frac{(H+2)\gamma\pi}{2(\pi-\gamma)}}{\sin\frac{\pi^2}{2(\pi-\gamma)}} + 1 + \cot\frac{\pi^2}{4(\pi-\gamma)}\right].$$

We see that the ground state energy of the boundary sine-Gordon model is a smooth function of the boundary magnetic field for the whole range of h in the XXZ regularization, hence of φ_0. The changes in ground state structure do not affect E, as is expected since in such a unitary model there is no (one dimensional) boundary transition.

The finite size corrections to the ground state energy themshelves (the genuine Casimir effect) can be computed using the technique developed in [54]. We will show how such a calculation can be carried out in the next chapter. It is also interesting to consider the inhomogeneous 6-vertex model with an imaginary boundary magnetic field ensuring commutation with $U_q sl(2)$ [55]. This should lead to a solution of minimal models with integrable boundary conditions [56].

Chapter 5

Boundary energy in integrable quantum field theories

The main purpose of this chapter is to study the ground state energy of 1+1 integrable relativistic quantum field theories with boundaries. This involves several questions. One is the energy associated with a boundary for an infinite system, the other is the way the energy of the theory on an interval varies with its length - the "genuine" Casimir effect. The elegant method of Destri and de Vega [54] for the periodic systems leads directly to the expression for the ground state energy from which the infinite size contribution and the finite size correction can be easily extracted. The heart of the DDV method is a non-linear integral equation (5.45) being derived from the Bethe equations. We generalize the Destri-de-Vega method to the systems with boundaries and apply it to compute the ground state energy for the boundary sine-Gordon model. This chapter is a part of a more complete work [56].

5.1 TBA for a QFT defined on cylinder

For a Quantum Field Theory defined on a torus, the standard way to compute its ground state energy is through the Thermodynamic Bethe Ansatz [8]. If the theory is defined on a circle of circumference R, one switches to a modular transformed point of view where now the theory is defined on a circle of very long circumference L and at temperature $T = 1/R$. The free energy F of the theory in the "R channel" can be computed using TBA, and it is simply related to the ground state energy $E^0(R)$ of the theory in the "L channel" by $F = -TLE^0(R)$. The limit $R \to 0$ corresponds to the UV limit and is described by a conformal field theory. It is known that $E^0(R)$ behaves as $E^0(R) \sim \pi c/6R$ in this limit [57], where c is the *central charge* of the underlying conformal field theory [58].[1]

Consider now a quantum field theory on a cylinder of finite length R and circumference L, with some boundary conditions (a, b) at the ends of the cylinder.

[1] More precisely, one has

$$E^0(R) = \frac{2\pi}{R}\left(\Delta + \overline{\Delta} - \frac{c}{12}\right)$$

where $(\Delta, \overline{\Delta})$ are the scaling dimensions of the ground state.

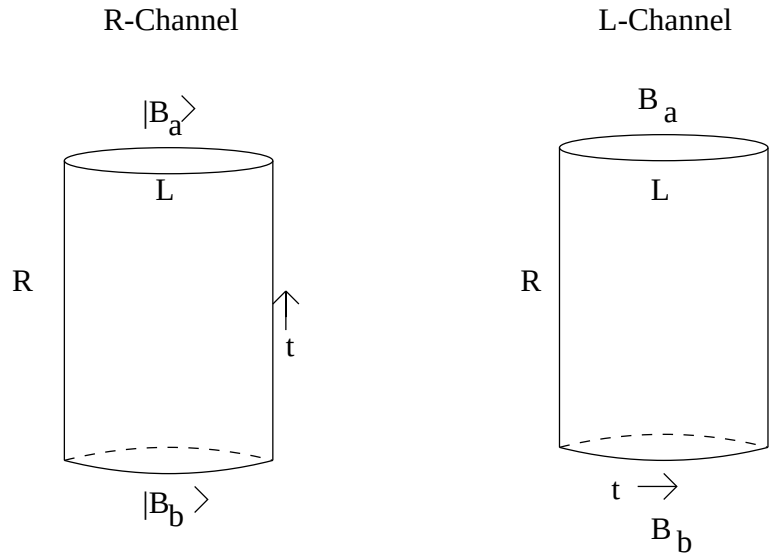

Figure 5.1: Cylindrical geometry in the R and L channels.

Depending on quantization scheme, we have two possible ways to compute the partition function of the system (see figure 5.1). The first possibility consists in choosing as direction of time the horizontal axis and therefore the partition function will be expressed as

$$Z_{ab} = Tr\, e^{-LH_{ab}}\,, \tag{5.1}$$

where H_{ab} is the Hamiltonian relative to the system with boundary conditions (a, b). In the second method the time evolution takes place along the vertical axis and therefore the partition function is given by the matrix element of the time evolution operator between the boundary states, i.e.

$$Z_{ab} = \langle B_a \mid e^{-RH} \mid B_b \rangle = e^{RF}\,, \tag{5.2}$$

where now H is the Hamiltonian of the bulk system. The ground state energy $E_{ab}(R)$ is, by definition, the leading term arising in the large L limit of the first expression, eq. (5.1), i.e.

$$Z_{ab} \sim e^{-LE^0_{ab}(R)}\,. \tag{5.3}$$

However, in view of the equivalence of the two quantization schemes, we can compute this quantity by looking at the large L limit of the second expression, eq. (5.2). In the large R limit, $R \to \infty$, the partition function (5.2) becomes

$$Z_{ab} \to \langle B_a|0\rangle e^{-RE^0} \langle 0|B_b\rangle \tag{5.4}$$

where $|0\rangle$ is the ground state of Hamiltonian H on the circle. It is the only state that contributes in the limit $R \to \infty$; other states do not propagate along the cylinder. The scalar products $g_a = \langle 0|B_a\rangle$ and $g_b = \langle 0|B_b\rangle$ are called the *ground state degeneracy*. The quantity $S(0) = \ln(g_a g_b)$, corresponding to the *zero-temperature entropy*, is one other universal term

that appears in the expansion of the free energy [59]. For periodic boundary conditions one must have $g_a g_b = 1$.

Since eq. (5.2) employs the boundary states of the model, let us shortly recall their basic properties (for more detail see the original reference [1]). In the QFT description of the model, the information on boundary conditions is encoded into a boundary state $\mid B\rangle$, which for infinite length L reads [1]:

$$\mid B\rangle = g \exp\left[\int_0^\infty \frac{d\theta}{2\pi} K(\theta) A^\dagger(-\theta) A^\dagger(\theta)\right] \mid 0\rangle. \tag{5.5}$$

Here g is an overall normalization related to the boundary entropy. For simplicity, we ignore possible additional contributions to the boundary state from zero momentum particles. From the point of view of QFT, the boundary state can be therefore regarded as a particular state of the Hilbert space of the bulk theory, made of a superposition of pairs of particles of equal and opposite momentum ("Cooper pairs"). All information relative to a particular boundary condition is encoded into the function $K(\theta)$ which can be seen as the elementary amplitude to create a virtual pair of particles.

In this chapter we address the question of computing the ground state energy of the sine-Gordon model with Dirichlet boundary conditions. Instead of deriving a TBA in the R channel, we adopt the beautiful approach of Destri and de Vega [54]. This requires working for a while with the lattice theory, here chosen to be the XXZ model with boundary magnetic fields.

5.2 TBA for the inhomogeneous XXZ model with boundary fields

like in the previous chapter, we start from the inhomogeneous 6-vertex model with boundary fields h as a regularization of the boundary sine-Gordon model with Dirichlet boundary conditions, with the only difference that now we consider the antiferromagnetic regime.

In the inhomogeneous antiferromagnetic 6-vertex model with anisotropy parameter γ, one gives an alternating imaginary part $\pm i\Lambda$ to the spectral parameter on alternating vertices [46, 47]. The scaling limit is given by taking $\Lambda \to \infty$, $N \to \infty$, and the lattice spacing $\Delta \to 0$, such that $R \equiv N\Delta$ remains finite. In the bulk, this provides a regularization of the sine-Gordon model with Lagrangian

$$L_{SG} = \int_0^R dx \ \left[\frac{1}{2}(\partial\phi)^2 + \mu^2 \cos\beta_{SG}\phi\right] \tag{5.6}$$

where $\mu \propto \frac{1}{\Delta}\exp(-\text{const}\Lambda)$, $\beta_{SG}^2 = 8(\pi - \gamma)$, and the field is fixed at $x = 0$ and $x = R$ (Dirichlet boundary conditions) to a value that is simply related to h (see previous chapter, eq. (4.57)).

The wave function of the inhomogeneous six-vertex model can be expressed in terms of a set of "roots" α_j, where $j = 1 \dots n$. They must be solutions of the set of equations (4.29):

$$N\left[f(\alpha_j + \Lambda, \gamma) + f(\alpha_j - \Lambda, \gamma)\right] + 2f(\alpha_j, \gamma H) =$$

$$2\pi l_j + \sum_{m=1,m\neq j}^{n} \left[f(\alpha_j - \alpha_m, 2\gamma) + f(\alpha_j + \alpha_m, 2\gamma) \right], \tag{5.7}$$

where l_j is an integer and all α_j are positive. The function f is defined as

$$f(a,b) = 2\tan^{-1}\left(\cot\frac{b}{2}\tanh a\right)$$

and

$$H \equiv \frac{1}{\gamma} f(i\gamma, -i\ln(h+\cos\gamma)). \tag{5.8}$$

By construction of the Bethe-ansatz wave function, $\alpha_j > 0$. Even though there is a solution of (5.7) with one vanishing root for any N and n, we emphasize that $\alpha_j = 0$ is **not** allowed because the wave function vanishes identically in this case. Observe that equations (5.7) are formally satisfied as well by the opposite of the roots, $-\alpha_j$. Often in what follows we shall consider that the roots take both signs in order to rewrite equations in a way which is similar to the bulk case.

For simplicity, we restrict to the case $\gamma = \frac{\pi}{t}$ where t is an integer, and restrict to the choice $\epsilon = -1$ [46]. In the sine-Gordon model, this falls in the repulsive regime. We make the standard assumption that all the solutions of interest are collections of "k-strings" for $k = 1, 2 \ldots t-1$ and antistrings a. A k-string is a group of α_j in the pattern $\alpha^{(k)} - i\pi(k-1), \alpha^{(k)} - i\pi(k-3), \ldots, \alpha^{(k)} + i\pi(k-1)$ where $\alpha^{(k)}$ is real. The antistring has $\alpha_j = \alpha^{(a)} + i\pi$, where $\alpha^{(a)}$ is real.

The thermodynamic limit is obtained by sending $N \to \infty$. In this case, we can define densities of the different kinds of solutions. The number of allowed solutions of (5.7) of type k in the interval $(\alpha, \alpha + d\alpha)$ is $2N(\rho_k(\alpha) + \rho_k^h(\alpha))d\alpha$, where ρ_k is the density of "filled" solutions (those which appear in the sum in the right-hand-side of (5.7)) and ρ_k^h is the density of "holes" (unfilled solutions). The densities ρ_a and ρ_a^h are defined likewise for the antistring. The "bare" Bethe ansatz equations follow from taking the derivative of (5.7). For $\gamma = \pi/t$ they can be written in the form:

$$\begin{aligned} 2\pi(\rho_k + \rho_k^h) &= a_k(\alpha) - \dot{\phi}_{k,t-1} * \rho_a + \sum_{l=1}^{t-1} \dot{\phi}_{kl} * \rho_l + \frac{1}{2N} u_k \\ 2\pi(\rho_a + \rho_a^h) &= 2\pi(\rho_{t-1} + \rho_{t-1}^h) + \frac{1}{2N}(u_a - u_{t-1}) \end{aligned} \tag{5.9}$$

These densities are originally defined for $\alpha > 0$, but the equations allow us to define $\rho_k(-\alpha) \equiv \rho_k(\alpha)$ in order to rewrite the integrals to go from $-\infty$ to ∞. The kernels in these equations are defined most easily in terms of their Fourier transforms

$$\hat{f}(x) = \int_{-\infty}^{\infty} \frac{d\alpha}{2\pi} e^{i\alpha t x/\pi} f(\alpha), \quad f(\alpha) = \frac{t}{\pi}\int_{-\infty}^{\infty} e^{-i\alpha t x/\pi}\hat{f}(x)dx. \tag{5.10}$$

One has

$$\hat{\dot{\phi}}_{kl}(x) = \delta_{ab} - 2\frac{\cosh x \sinh(t-k)x \sinh lx}{\sinh x \sinh tx}, \tag{5.11}$$

for $k \geq l$ with $\dot{\phi}_{lk} = \dot{\phi}_{kl}$, and

$$\begin{aligned}
\hat{a}_k &= \frac{\sinh(t-k)x}{\sinh tx} \cos \Lambda t x/\pi \\
\hat{u}_k &= 2\frac{\sinh(t-H)x \sinh kx}{\sinh x \sinh tx} + \frac{\sinh(t-2k)x/2}{\sinh tx/2} - 1 \\
\hat{u}_a &= 2\frac{\sinh Hx}{\sinh tx} - \frac{\sinh(t-2)x/2}{\sinh tx/2} - 1,
\end{aligned} \tag{5.12}$$

with in particular $a_1(\alpha) = \frac{1}{2}\left[\dot{f}(\alpha+\Lambda,\gamma) + \dot{f}(\alpha-\Lambda,\gamma)\right], \phi_{11}(\alpha) = -f(\alpha, 2\gamma)$. The boundary manifests itself in the first term in u_k; notice that even for $h = 0$, it still modifies the equations. A few technicalities account for the other terms (these are relevant here because we are interested in subleading boundary effects). The second term in u_k arises from the fact that the sum in (5.7) does not include the term $m = j$; the integration over densities includes such a contribution and so it must be subtracted off by hand. The third term in u_k arises because ρ and ρ^h are defined for allowed solutions, while as already explained, $\alpha = 0$ is not allowed because it does not give a valid wavefunction. Since it is a valid solution of (5.7) but is not included in the densities, we must subtract an explicit $\frac{2\pi}{2N}\delta(\alpha)$ (corresponding to $1/2N$ in Fourier space). Explicitly, one has

$$u_1 = 2\dot{f}(\alpha, \gamma H) + 2\dot{f}(2\alpha, 2\gamma) - 2\pi\delta(\alpha). \tag{5.13}$$

For compactness we rewrite (5.9) as

$$2\pi\sigma^{(k)}(\rho_k + \rho_k^h) = a_k(\alpha) + \sum_l \dot{\phi}_{kl} * \rho_l + \frac{1}{2N}u_k, \tag{5.14}$$

where $\sigma^{(k)} = -1$ for the antistring.

The energy reads, with proper hamiltonian normalization,

$$\frac{E^{latt}}{2N} = -\frac{1}{t}\sum_k \int_{-\infty}^{\infty} a_k(\alpha)\rho_k(\alpha)d\alpha. \tag{5.15}$$

It is easy to write the thermodynamic Bethe ansatz for this model. One finds that the TBA equations, since they are obtained by a variational method, do not depend on boundary terms, and read as usual

$$-\frac{2}{t}a_k(\alpha) = T\ln\left(1+e^{\epsilon_k}\right) - T\sum_l \sigma^{(l)}\frac{A_{kl}}{2\pi} * \ln\left(1+e^{-\epsilon_l}\right), \tag{5.16}$$

where

$$A_{kl}(\alpha) = 2\pi\sigma^{(k)}\delta_{kl}\delta(\alpha) - \dot{\phi}_{kl}\,. \tag{5.17}$$

The free energy does depend on the boundary term and reads

$$\begin{aligned}
F^{latt} = &- TN\sum_k \int_{-\infty}^{\infty} \sigma^{(k)} a_k(\alpha)\ln\left(1+e^{-\epsilon_k}\right)\frac{d\alpha}{2\pi} \\
&- \frac{T}{2}\sum_k \int_{-\infty}^{\infty} \sigma^{(k)} u_k \ln\left(1+e^{-\epsilon_k}\right)\frac{d\alpha}{2\pi}.
\end{aligned} \tag{5.18}$$

In the above formulas the temperature T corresponds in the two-dimensional point of view to having a cylinder of radius $L = 1/T$. We can deduce from this result the ground state energy. Indeed recall that the ground state is obtained by $\rho_k = 0, k \neq 1$ and $\rho_1^h = 0$ so

$$E^{latt} = -N \int_{-\infty}^{\infty} a_1(\alpha) |\epsilon_1^-| \frac{d\alpha}{2\pi} - \frac{1}{2} \int_{-\infty}^{\infty} u_1 |\epsilon_1^-| \frac{d\alpha}{2\pi}, \tag{5.19}$$

where from (5.16) we have

$$\hat{\epsilon}_1{}^- = -\frac{1}{t} \frac{\cos(\Lambda t x/\pi)}{\cosh x}. \tag{5.20}$$

Replacing and using (5.12) we find

$$\begin{aligned} E_{bulk}^{latt} &= -\frac{N}{\pi} \int_{-\infty}^{\infty} \cos^2\left(\frac{\Lambda t x}{\pi}\right) \frac{\sinh(t-1)x}{\cosh x \sinh tx} \\ E_{bdry}^{latt} &= -\frac{1}{2\pi} \int_{-\infty}^{\infty} \frac{\cos(\Lambda t x/\pi)}{\cosh x} \left(2\frac{\sinh(t-H)x}{\sinh tx} + \frac{\sinh(t-2)x/2}{\sinh tx/2} - 1 \right) \end{aligned} \tag{5.21}$$

where we used the formula

$$\int_{-\infty}^{\infty} a(\alpha) b(\alpha) d\alpha = 2t \int_{-\infty}^{\infty} \hat{a}(x) \hat{b}(-x) dx \,.$$

In the continuum limit $\Lambda \to \infty$ the energy contains various terms. We keep only the finite part which is obtained by closing the above integrals in the upper half plane and selecting the pole at $x = i\frac{\pi}{2}$, leading to

$$\begin{aligned} E_{bulk} &= R\frac{m^2}{4} \cot\frac{t\pi}{2} \\ E_{bdry} &= -\frac{m}{2} \left(2\frac{\sin(t-H)\pi/2}{\sin t\pi/2} - \cot\frac{t\pi}{4} - 1 \right), \end{aligned} \tag{5.22}$$

where m is the soliton mass,

$$m = 2e^{-t\Lambda/2} \,. \tag{5.23}$$

All these results trivially generalize to the case of two different boundary fields by splitting the H dependent terms into the sum of an H and an H' term. The bulk result agrees with what is obtained by other methods. As in the bulk case, when t is even, there are additional logarithmic terms. The boundary entropy is actually the same in the UV and IR limits.

5.3 The Destri De Vega equations for the boundary sine-Gordon model

We now would like to compute the complete Casimir effect in a theory with boundary. TBA in the R channel is pretty intricate in the non diagonal case. We adopt an alternative method elaborated by Destri and De Vega (DDV) in the periodic case.

5.3.1 The DDV equations with boundary conditions

Consider eq. (5.7) which we rewrite as

$$2Np(\alpha_j) + p_{bdry}(\alpha_j) + \sum_{\alpha_m>0} \phi(\alpha_j - \alpha_m) + \phi(\alpha_j + \alpha_m) = 2\pi n_j, \tag{5.24}$$

where the sum runs over all roots (including $m = j$) and we introduced the notations

$$p(\alpha) \equiv \frac{1}{2}\left[f(\alpha + \Lambda, \gamma) + f(\alpha - \Lambda, \gamma)\right], \quad p_H(\alpha) \equiv f(\alpha, \gamma H), \quad \phi(\alpha) \equiv \phi_{11}(\alpha), \tag{5.25}$$

$$p_{bdry}(\alpha) = 2p_H(\alpha) - \phi(2\alpha). \tag{5.26}$$

The ground state is obtained by filling the real positive solutions, $\alpha_j = 0$ excepted. This corresponds to the choice $n_j = 1, 2, \ldots$. Recall that if α_j is solution of (5.24) with some n_j, so is formally $-\alpha_j$ (with $-n_j$). Given the set of roots $\{\alpha_j > 0\}$ representing the ground state, one can construct the *counting function* as follows:

$$f(\alpha) \equiv 2iNp(\alpha) + ip_{bdry}(\alpha) + i\sum_{\alpha_m>0} \phi(\alpha - \alpha_m) + \phi(\alpha + \alpha_m), \tag{5.27}$$

Define then

$$Y(\alpha) \equiv e^{f(\alpha)}. \tag{5.28}$$

We have $Y(\alpha_j) = Y(-\alpha_j) = 1$ for every root α_j from the ground state, as well as $Y(0) = 1$. Therefore we can rewrite (5.27) as

$$f(\alpha) = 2iNp(\alpha) + ip_{bdry}(\alpha) - i\phi(\alpha) - \int_C \phi(\alpha - \alpha')\frac{\dot{Y}(\alpha')}{1 - Y(\alpha')}\frac{d\alpha'}{2\pi}, \tag{5.29}$$

where $i\phi(\alpha)$ at the right-hand side takes care of the unwanted contribution of the pole $\alpha' = 0$ and the contour C consists of two parts as shown in figure 5.2, C_1 above and C_2 below the real axis.

Like in the bulk case [54], simple manipulations allow us to rewrite this non-linear integral equation as

$$\begin{aligned} f(\alpha) &= 2iNP(\alpha) + iP_{bdry}(\alpha) + \int_{C_1} \Phi(\alpha - \alpha') \ln\left(1 - e^{f(\alpha')}\right) d\alpha' \\ &+ \int_{C_2} \Phi(\alpha - \alpha') \ln\left(1 - e^{-f(\alpha')}\right) d\alpha'. \end{aligned} \tag{5.30}$$

In equation (5.30) one has

$$\Phi(\alpha) = -\frac{t}{2\pi^2}\int_{-\infty}^{+\infty} dx e^{-itx\alpha/\pi} \frac{\sinh(t-2)x}{2\sinh(t-1)x\cosh x}, \tag{5.31}$$

together with

$$P(\alpha) = \int_{-\infty}^{+\infty} dx \frac{e^{-itx\alpha/\pi} - 1}{-ix} \frac{\cos(\Lambda t x/\pi)}{2\cosh x} \tag{5.32}$$

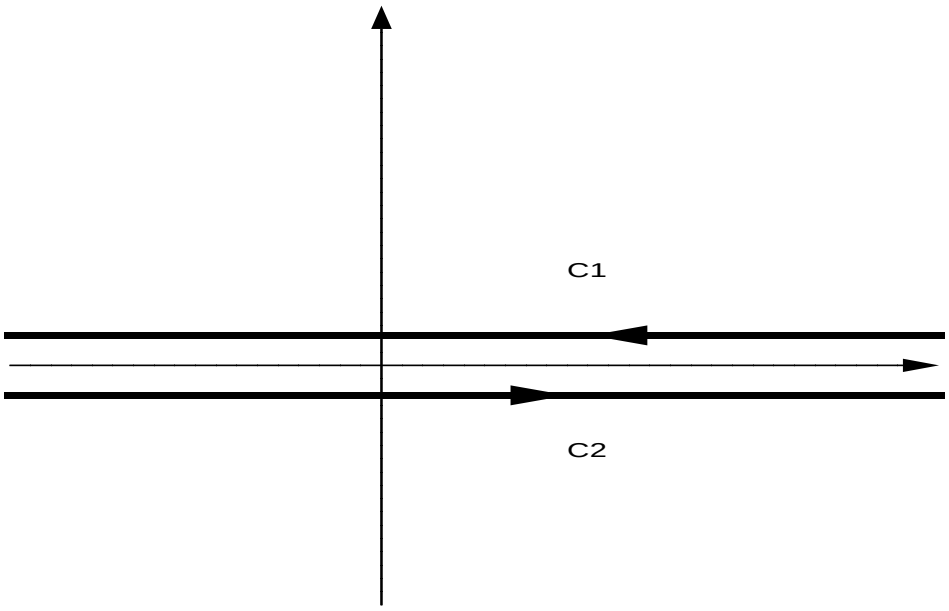

Figure 5.2: Contours of integration in the DDV method.

and

$$\begin{aligned} P_{bdry} &= \int_{-\infty}^{+\infty} dx \frac{e^{-itx\alpha/\pi}-1}{-ix}\left[\frac{\sinh(t-H)x}{\sinh(t-1)x\cosh x}\right. \\ &+ \left.\frac{\sinh(t-2)x/2\cosh tx/2}{\sinh(t-1)x\cosh x}+\frac{\sinh(t-2)x}{2\sinh(t-1)x\cosh x}\right] \end{aligned} \tag{5.33}$$

Obtaining (5.30) requires some care with the definition of logarithms. One proceeds as follows. Before integrating by parts in the integral over C_2 one factors out $\frac{d}{dx}\ln Y(x)$:

$$-\frac{\dot{Y}(x)}{1-Y(x)} = \frac{d}{dx}\ln[1-Y^{-1}] + \frac{d}{dx}\ln Y(x).$$

Then both integrals over C_1 and C_2 can be taken by parts, resulting in

$$\begin{aligned} f(\alpha) &- \int_{-\infty}^{+\infty}\dot{\phi}(\alpha-\alpha')f(\alpha')\frac{d\alpha'}{2\pi} = 2iNp(\alpha)+ip_{bdry}(\alpha)-i\phi(\alpha) \\ &- \int_{-\infty}^{+\infty}\dot{\phi}(\alpha-\alpha'-i0)\ln[1-Y(\alpha'+i0)]\frac{d\alpha'}{2\pi} \\ &+ \int_{-\infty}^{+\infty}\dot{\phi}(\alpha-\alpha'+i0)\ln[1-Y^{-1}(\alpha'-i0)]\frac{d\alpha'}{2\pi}, \end{aligned}$$

(surface terms from C_1 and C_2 cancel against each other provided N, Λ are finite). To make the source term vanish at infinity we take the derivative of both sides in the latter equation, after which it can be Fourier-transformed and "dressed" by the factor $(1-\hat{\dot{\phi}})^{-1}$. Finally,

one goes back in the rapidity space and integrates the equation, using $f(0) = 0$, to obtain (5.30).

The energy of the ground state configuration can be expressed as

$$\begin{aligned} E^{latt} &= -\frac{2}{t}\sum_{\alpha_j>0}\dot{p}(\alpha_j) = -\frac{1}{t}\sum_{\alpha_j}\dot{f}(\alpha_j-\Lambda,\gamma)+\dot{f}(-\alpha_j-\Lambda,\gamma) \\ &= \frac{1}{t}\dot{f}_\gamma(\Lambda)+\frac{1}{t}\int_C \dot{f}_\gamma(\alpha-\Lambda)\frac{\dot{Y}(\alpha)}{1-Y(\alpha)}\frac{d\alpha}{2i\pi}, \end{aligned} \tag{5.34}$$

where $f(\alpha,\gamma)\equiv f_\gamma(\alpha)$. One finds after exactly the same manipulations as above,

$$\begin{aligned} E &= \frac{1}{t}\dot{f}_\gamma(\Lambda)-\frac{1}{t}\int_{-\infty}^{+\infty} f''_\gamma(\alpha-\Lambda+i0)\ln[1-Y(\alpha+i0)]\frac{d\alpha}{2i\pi} \\ &+ \frac{1}{t}\int_{-\infty}^{+\infty} f''_\gamma(\alpha-\Lambda-i0)\ln[1-Y^{-1}(\alpha-i0)]\frac{d\alpha}{2i\pi}+\frac{1}{t}\int_{-\infty}^{+\infty} f''_\gamma(\alpha-\Lambda)f(\alpha)\frac{d\alpha}{2i\pi}. \end{aligned} \tag{5.35}$$

Substituting (5.30) instead of $f(\alpha)$ in the last term of the latter, we obtain

$$\begin{aligned} E^{latt} &= E^{latt}_{bulk}+E^{latt}_{bdry}-\frac{i}{t}\int_{-\infty}^{+\infty} s(y-\Lambda+i0)\ln[1-Y(y+i0)]\frac{dy}{2\pi} \\ &+ \frac{i}{t}\int_{-\infty}^{+\infty} s(y-\Lambda-i0)\ln[1-Y^{-1}(y-i0)]\frac{dy}{2\pi}, \end{aligned} \tag{5.36}$$

where we defined $s(y)$ by

$$s(y) = i\int_{-\infty}^{+\infty}\frac{kdk}{2\cosh\gamma k}e^{-iky} = \frac{t^2}{4}\frac{\tanh(ty/2)}{\cosh(ty/2)}. \tag{5.37}$$

The last two terms in (5.36) represent finite-size corrections to the ground state energy, while

$$\begin{aligned} E^{latt}_{bulk}+E^{latt}_{bdry} &= \frac{1}{t}\dot{f}_\gamma(\Lambda)-\frac{1}{t}\int_{-\infty}^{+\infty}\frac{dk}{2\pi}e^{-ik\Lambda}\hat{\dot{f}}_\gamma(k)\frac{2N\hat{\dot{p}}(k)+\hat{\dot{p}}_{bdry}(k)-\hat{\dot{\phi}}(k)}{2\pi-\hat{\dot{\phi}}(k)} \\ &\equiv \frac{1}{t}\dot{f}_\gamma(\Lambda)-\frac{2N}{t}\int_{-\infty}^{+\infty}\dot{f}_\gamma(\alpha-\Lambda)\rho(\alpha)d\alpha, \end{aligned} \tag{5.38}$$

where the function $\rho(\alpha)$ defined so satisfies the following equation:

$$2\pi\rho(\alpha) = \dot{p}(\alpha)+\dot{\phi}*\rho(\alpha)+\frac{1}{2N}\left(\dot{p}_{bdry}(\alpha)-\dot{\phi}(\alpha)\right), \tag{5.39}$$

which can be checked by solving this linear equation in Fourier space. Introduce $\rho_1(\alpha) = \rho(\alpha)-\delta(\alpha)/2N$. Then

$$E^{latt}_{bulk}+E^{latt}_{bdry} = -\frac{2N}{t}\int_{-\infty}^{+\infty}\dot{f}_\gamma(\alpha-\Lambda)\rho_1(\alpha)d\alpha \tag{5.40}$$

and, by virtue of (5.39), ρ_1 satisfies the equation

$$2\pi\rho_1(\alpha) = \dot{p}(\alpha)+\dot{\phi}*\rho_1(\alpha)+\frac{1}{2N}\left(\dot{p}_{bdry}(\alpha)-2\pi\delta(\alpha)\right). \tag{5.41}$$

Hence ρ_1 is the density of the ground state configuration (5.9) (see also (5.13)) and E^{latt}_{bulk} and E^{latt}_{bdry} coincide with the quantities computed in the previous section.

5.3.2 The continuum DDV equations

Having checked the correct values of bulk and boundary energies, we now let the cutoff $\Lambda \to \infty$ according to $\Lambda = \frac{2}{t}\log(2/m\Delta)$ with the size of the system $R = N\Delta$ and the physical mass $m = \frac{2}{\Delta}e^{-t\Lambda/2}$ fixed, and work only with the renormalized theory. In that limit one has, evaluating all integrals in Fourier transforms and keeping the leading terms,

$$s(\alpha+\Lambda) + s(\alpha-\Lambda) = -\frac{t^2}{2} m \sinh\theta, \qquad NP(\theta) = mR\sinh\theta, \tag{5.42}$$

where we set

$$\theta = \frac{t\alpha}{2}. \tag{5.43}$$

Recall indeed that when one studies the excitations of the model, a relativistic dispersion relation is obtained provided the rapidity in the relativistic theory and the "bare rapidity" of the Bethe excitations are related by (5.43). We redefine implicitely all functions to depend on θ from now on. The energy therefore reads now,

$$\begin{aligned} E &= E_{bulk} + E_{bdry} + \frac{1}{2}\int_{C_1} m\sinh\theta \ln\left(1-e^{f(\theta)}\right)\frac{d\theta}{2i\pi} \\ &+ \frac{1}{2}\int_{C_2} m\sinh\theta\ln\left(1-e^{-f(\theta)}\right)\frac{d\theta}{2i\pi}, \end{aligned} \tag{5.44}$$

where f is solution of the integral equation

$$\begin{aligned} f(\theta) &= 2imR\sinh\theta + iP_{bdry}(\theta) + \int_{C_1}\Phi(\theta-\theta')\ln\left(1-e^{f(\theta')}\right)d\theta' \\ &+ \int_{C_2}\Phi(\theta-\theta')\ln\left(1-e^{-f(\theta')}\right)d\theta', \end{aligned} \tag{5.45}$$

and

$$\Phi(\theta) = -\int_{-\infty}^{\infty}\frac{dx}{2\pi^2}\frac{\sinh(t-2)x}{\cosh x\sinh(t-1)x}e^{2ix\theta/\pi}, \tag{5.46}$$

which can be identified with

$$\Phi(\theta) = -\frac{1}{2i\pi}\frac{d}{d\theta}\ln S_{++}(\theta), \tag{5.47}$$

where S_{++} is the soliton-soliton S matrix element (see eq. (1.37)).

5.3.3 The Casimir effect

We define the effective central charge by the formula

$$E = E_{bulk} + E_{bdry} - \frac{\pi c_{eff}}{24R}. \tag{5.48}$$

From (5.44) we find

$$c_{eff}(mR) = -\frac{6R}{i\pi^2}\left\{\int_{C_1} m\sinh\theta \ln\left(1-e^{f(\theta)}\right)d\theta + \int_{C_2} m\sinh\theta\ln\left(1-e^{-f(\theta)}\right)\right\}d\theta. \quad (5.49)$$

To study the ultraviolet behaviour of the above expression, let us use $f(\overline{\theta}) = \overline{f(\theta)}$ and rewrite (5.45) as

$$f(\theta) = 2imR\sinh\theta + iP_{bdry}(\theta) - 2i\int_{-\infty}^{\infty}\Phi(\theta-\theta')\ \mathrm{Im}\ln\left[1-e^{f(\theta'+i0)}\right]d\theta', \quad (5.50)$$

and (5.49) as

$$c_{eff}(mR) = \frac{12mR}{\pi^2}\int_{-\infty}^{\infty}d\theta\sinh\theta\ \mathrm{Im}\ln\left[1-e^{f(\theta+i0)}\right]. \quad (5.51)$$

It might be useful to remind the reader of the form of the corresponding bulk equations [54]:

$$c_{eff}(mR) = \frac{6mR}{\pi^2}\int_{-\infty}^{\infty}\sinh\theta\ \mathrm{Im}\ln\left[1+e^{f(\theta+i0)}\right]d\theta, \quad (5.52)$$

with f satisfying

$$f(\theta) = imR\sinh\theta + i\omega - 2i\int_{-\infty}^{\infty}\Phi(\theta-\theta')\mathrm{Im}\ln\left[1+e^{f(\theta'+i0)}\right]d\theta', \quad (5.53)$$

and ω is the twist of the 6-vertex model. Note the deep similarity between these two systems; the factors of 2 can obviously be absorbed in a redefinition of mR and the minus sign in the arguments of logarithms in a redefinition of f, so the only essential difference is that the twist angle ω is replaced by P_{bdry}. It is well known that the twist corresponds to a soliton fugacity [39] so we see that the boundary acts by some effective, rapidity dependent fugacity.

In the limit when $R \to 0$, only the region $|\theta|$ large contributes to c_{eff}. Let us focus on the limit $\theta \gg 1$, the results for negative θ following by symmetry. Then one finds $f \approx f_K$, where

$$f_K(\theta) = imRe^{\theta} + iP_{bdry}(\infty) - 2i\int_{-\infty}^{\infty}\Phi(\theta-\theta')\ \mathrm{Im}\ln\left[1-e^{f_K(\theta'+i0)}\right]d\theta', \quad (5.54)$$

together with

$$c_K(mR) = \frac{6}{\pi^2}\int_{-\infty}^{\infty}mRe^{\theta}\mathrm{Im}\ln\left[1-e^{f_K(\theta+i0)}\right]d\theta. \quad (5.55)$$

It is now useful to recall some well known results about dilogarithms [52]. Define

$$L(x) \equiv \int_0^x du\left[\frac{\ln(1+u)}{u} - \frac{\ln u}{1+u}\right]. \quad (5.56)$$

Assume

$$-i\ln F(x) = \phi(x) + 2\int_{-\infty}^{\infty}dy\ G(x-y)\ \mathrm{Im}\ln\left[1+F(y+i0)\right], \quad (5.57)$$

with G an even function. Then one has

$$\mathrm{Im}\int_{-\infty}^{\infty} dx\phi'(x)\ln\left[1+F(x+i\epsilon)\right] = \frac{1}{2}\mathrm{Re}\left\{L[F(-\infty)]-L[F(\infty)]\right\}$$
$$+\frac{1}{2}\mathrm{Im}\left\{\phi(\infty)\ln\left[1+F(\infty)\right]-\phi(-\infty)\ln\left[1+F(-\infty)\right]\right\}, \qquad (5.58)$$

(where we did not write the $i0$ part of some arguments for simplicity). Set $F = e^{f_K - i\pi}$ and denote $P_{bdry}(\infty) \equiv \sigma$. Then, according to (5.54): $\phi = mRe^{\theta} + \sigma - \pi, \quad G = -\Phi$. We have $\phi(-\infty) = \sigma - \pi$, $\phi(\infty) = \infty$. One has also $F(\infty + i0) = 0$, and from this and (5.54) one can get the value of F at $-\infty$:

$$\begin{aligned}\frac{f_K(-\infty)}{i} &= \sigma - 2\ \mathrm{Im}\ln\left[1-e^{f_K(-\infty+i0)}\right]\int_{-\infty}^{\infty}\Phi(\theta)d\theta \\ &= \sigma + \frac{t-2}{t-1}\ \mathrm{Im}\ln\left[1-e^{f_K(-\infty+i0)}\right]. \qquad (5.59)\end{aligned}$$

So, if $e^{f_K(-\infty+i0)} = e^{i\omega}$ one may use $\mathrm{Im}\ln(1\pm e^{i\omega}) = \frac{1}{2i}\ln(\pm e^{i\omega})$ to find

$$e^{i\omega} = -\exp\left\{2i\frac{t-1}{t}\sigma + 2i\frac{\pi}{t}\right\}. \qquad (5.60)$$

From (5.58) it follows that

$$\mathrm{Im}\int_{-\infty}^{\infty} mRe^{\theta}\ln(1-e^{f_K(\theta+i0)})d\theta = \frac{1}{2}\ \mathrm{Re}L(-e^{i\omega}) - \frac{1}{2}(\sigma-\pi)\left(\frac{t-1}{t}\sigma - \pi + \frac{\pi}{t}\right).$$

In the region $\theta \ll 1$ we have $f \approx f_A$, and similar calculations yield

$$\mathrm{Im}\int_{-\infty}^{\infty} mRe^{-\theta}\ln(1-e^{f_A(\theta+i0)})d\theta = -\frac{1}{2}\ \mathrm{Re}L(-e^{-i\omega}) + \frac{1}{2}(\pi-\sigma)\left(-\frac{t-1}{t}\sigma + \pi - \frac{\pi}{t}\right).$$

Collecting both $\theta \gg 1$ and $\theta \ll 1$ contributions we obtain

$$\begin{aligned}c_{UV} &= \frac{6}{\pi^2}\left\{\frac{1}{2}\left[L(-e^{2i\omega})+L(-e^{-2i\omega})\right] + \frac{t-1}{t}(\sigma-\pi)^2\right\} = \\ &= \frac{6}{\pi^2}\left[\frac{\pi^2}{6} - \frac{t-1}{t}(\sigma-\pi)^2\right]. \qquad (5.61)\end{aligned}$$

From (5.33) we get

$$P_{bdry}(\infty) \equiv \sigma = 2\pi - \frac{\pi}{2}\frac{H+H'}{t-1}. \qquad (5.62)$$

Finally, from this we find

$$c_{UV} = 1 - 6\frac{t-1}{t}\left(1 - \frac{H+H'}{2(t-1)}\right)^2. \qquad (5.63)$$

In the case with no boundary field, $H = H' = t-1$ so $c_{UV} = 1$ as expected.

Remark. So far we tacitly assumed that $0 < H < t-1$. In general, from relation (5.8) it follows that when $h > 0$, H varies between $-t-1$ and -1, while when $h < 0$, $-1 < H < t-1$. To generalize our results, we should use the most general form of p_H:

$$\hat{\dot{p}}_H(k) = \int_{-\infty}^{\infty} \dot{p}_H(\alpha) e^{ik\alpha} d\alpha = 2\pi \ \mathrm{sign}(H) \frac{\sinh(\pi - \omega_H)k}{\sinh \pi k}, \quad -\pi < \gamma H < \pi, \tag{5.64}$$

where we defined $\omega_H \equiv |\gamma H|$. For $-2\pi < \gamma H < -\pi$ set $\omega_H = 2\pi + \gamma H$ and $\mathrm{sign}(H) = 1$ in (5.64). Then (5.62) generalizes to

$$\sigma = 2\pi - \frac{\pi}{2} \frac{\omega_H + \omega'_H}{\pi - \gamma}$$

if H and H' are both positive or $-2t < (H, H') < -t$, and

$$\sigma = 2\pi - \frac{\pi}{2} \frac{4\pi - \omega_H - \omega'_H}{\pi - \gamma}$$

if they are both negative, but greater than $-t$. In the case when $0 < H < t-1$ and $-t < H' < -1$ (that is, $h < 0, h' > 0$) we get:

$$\sigma = \pi + \frac{\pi}{2} \frac{\omega'_H - \omega_H - 2\gamma}{\pi - \gamma}.$$

So, when $\omega'_H - \omega_H = 2\gamma$ we have $\sigma = \pi$ and $c_{UV} = 1$, as in the free case. The condition $\omega'_H - \omega_H = 2\gamma$ is equivalent to $h = -h'$, as could be seen from (5.8). That $c = 1$ when the two surface field are real and opposite is well known from lattice studies [60].

5.4 Remarks

A particularly interesting case is when the XXZ chain or the inhomogeneous 6-vertex model commutes with the quantum group $U_q sl(2)$. In that case $h = -h' = 2i \sin \gamma$ and the net result is that all H dependent terms simply disappear from the equations, so, in particular

$$E_{bdry} = \frac{m}{2} \left(\cot \frac{t\pi}{4} + 1 \right). \tag{5.65}$$

At the $N = 2$ supersymmetric point, $t = 3$, the boundary energy vanishes, a result well expected from supersymmetric considerations. More generally, it vanishes if $t = 4n + 3$, n an integer. Notice that the bulk energy vanishes for t an odd number (as a consequence of the generalized fractional $N = 2$ supersymmetries studied in [61]).

In the quantum group symmetric case [55] one has $H + H' = 2t$ so from (5.63)

$$c = 1 - \frac{6}{t(t-1)}, \tag{5.66}$$

the expected result for the restricted sine-Gordon model [62, 63, 64].

Chapter 6

Surface excitations and surface energy of the antiferromagnetic XXZ chain by the Bethe ansatz approach

We study an open XXZ chain in the regime $\Delta > 1$ with a boundary magnetic field h and discuss some of its peculiar features due to the presence of boundary. In the Bethe ansatz formalism, boundary bound states are represented by the "boundary strings" as described in chapter 4. We find that for certain values of h the ground state wave function contains boundary strings, and from this infer the existence of two "critical" fields in agreement with [49]. An expression for the vacuum surface energy in the thermodynamic limit is derived and found to be an analytic function of h. We argue that boundary excitations appear only in pairs with "bulk" excitations or with boundary excitations at the other end of the chain. The case where the magnetic fields at the left and the right boundaries are antiparallel has non-trivial differences with the case of the parallel fields. The Ising ($\Delta = \infty$) and isotropic ($\Delta = 1$) limits are discussed thoroughly and found helpful for the intuitive understanding of the behavior of the boundary XXZ chain at arbitrary Δ. This section is based on the work [65].

6.1 Introduction

In this chapter we study the XXZ chain with even number of spins L in a boundary magnetic field,

$$\mathcal{H} = \frac{1}{2}\left\{\sum_{i=1}^{L-1}\left(\sigma_i^x\sigma_{i+1}^x + \sigma_i^y\sigma_{i+1}^y + \Delta\sigma_i^z\sigma_{i+1}^z\right) + h_1\sigma_1^z + h_2\sigma_L^z\right\}, \tag{6.1}$$

in the regime $\Delta > 1$, $h_1 \geq 0$, $h_2 \leq 0$, focusing on the effects peculiar to systems with boundaries [53]. At $h_1 = h_2 = 0$ this model describes one-dimensional antiferromagnet with non-magnetic impurities, accessible experimentally. We exploit the Bethe ansatz solution for this model, first derived in [45], together with the well-known results for the periodic chain [20, 66]. We find new "boundary string" solutions to the Bethe equations, similar to the boundary strings existing in the $|\Delta| < 1$ regime [40]. For certain values of the boundary

magnetic field the ground state configuration contains boundary 1-strings. Boundary excitations are obtained by removing (or adding, depending on the sign of h) boundary strings from the ground state wave-function. Their energy was first obtained in [49] by the algebraic approach.

A peculiar feature of the Bethe ansatz solution of the periodic chain is that the excitations (holes in the Dirac sea) appear only in pairs [14]. We argue that similarly the boundary excitations can appear only in pairs with bulk excitations or with boundary excitations at the other end of the spin chain. There is no such restriction in the soultion of the semi-infinite chain by the algebraic approach [49].

Using the Bethe ansatz solution we calculate the surface energy (see e.g.,[67]):

$$E_{surf}(L, \Delta, h) = E_{gr} - E^0_{gr}, \tag{6.2}$$

in the thermodynamic limit $L = \infty$. Here E_{gr} is the ground state energy of (6.1) and E^0_{gr} is that of the periodic chain. We give an interpretation of our results in the limits $\Delta \to \infty$ and $\Delta \to 1$, corresponding to the 1D Ising and XXX models respectively. Finally, we comment on the structure of the ground state when the boundary magnetic fields are parallel.

6.2 The Bethe ansatz equations

Let us first set up the Bethe ansatz (BA) notations and list the relevant results about the XXZ chain [45, 66]. In [45] the eigenstates of (6.1) were constructed for arbitrary Δ. As usual in the BA picture, the n-magnon eigenstates $|n\rangle$, satisfying $\mathcal{H}|n\rangle = E|n\rangle$, are linear combinations of the states with n spins down, located at sites $x_1, ..., x_n$:

$$|n\rangle = \sum f^{(n)}(x_1, ..., x_n)|x_1, ..., x_n\rangle.$$

The wave-function

$$f(x_1, ..., x_n) = \sum_P \varepsilon_P A(p_1, ..., p_n) e^{i(p_1 x_1 + ... + p_n x_n)}, \tag{6.3}$$

contains n parameters $p_j \in (0, \pi)$ which are subject to quantization conditions, called Bethe equations (BE):

$$e^{2iLp_j} \cdot \frac{e^{ip_j} + h_1 - \Delta}{1 + (h_1 - \Delta)e^{ip_j}} \cdot \frac{e^{ip_j} + h_2 - \Delta}{1 + (h_2 - \Delta)e^{ip_j}} = \prod_{l \neq j}^{n} e^{i\Phi(p_j, p_l)}. \tag{6.4}$$

The summation in (6.3) is over all permutations and negations of p_j. The energy and spin of the n-magnon state are given by [45]:

$$E = \frac{1}{2}\left[(L-1)\Delta + h_1 + h_2\right] + 2\sum_{j=1}^{n}(\cos p_j - \Delta), \qquad S_z = \frac{L}{2} - n. \tag{6.5}$$

It is convenient to rewrite BE using the following mappings:

$$\Delta = \cosh\gamma \geq 1, \qquad \gamma \geq 0, \tag{6.6}$$

$$p = -i \ln \frac{\cosh \frac{1}{2}(i\alpha + \gamma)}{\cosh \frac{1}{2}(i\alpha - \gamma)}, \tag{6.7}$$

(our definition of $p(\alpha)$ differs from that of [20, 66] by the shift $\alpha \to \alpha + \pi$ and it was chosen in such a way that $p(\alpha)$ be an odd function that maps $-\pi < \alpha < \pi$ to $-\pi < p < \pi$),

$$h = \cosh\gamma + \frac{\sinh \frac{\gamma}{2}(1-H)}{\sinh \frac{\gamma}{2}(1+H)} = \sinh(\gamma) \cdot \coth \frac{\gamma}{2}(H+1), \qquad h_{lim} < |h| < \infty, \tag{6.8}$$

$$h = \cosh\gamma - \frac{\cosh \frac{\gamma}{2}(1-H)}{\cosh \frac{\gamma}{2}(1+H)} = \sinh(\gamma) \cdot \tanh \frac{\gamma}{2}(H+1), \qquad |h| < h_{lim}. \tag{6.9}$$

The latter two mappings are defined on $H \in (-\infty, \infty)$ and are necessary to cover the region $-\infty < h < \infty$, with positive h corresponding to $H \in (-1, \infty)$. The value $h_{lim} \equiv h(\infty) = \sinh\gamma$ lies between two critical fields $h_{cr}^{(1)}, h_{cr}^{(2)}$ defined as follows [49]:

$$h_{cr}^{(1)} = \Delta - 1, \qquad h_{cr}^{(2)} = \Delta + 1. \tag{6.10}$$

Both critical fields correspond to $H = 0$, and the gap $h_{cr}^{(1)} < h < h_{cr}^{(2)}$ corresponds to $0 < H < \infty$. In these notations eq. (6.4) becomes:

$$\left[\frac{\cosh \frac{1}{2}(i\alpha_j + \gamma)}{\cosh \frac{1}{2}(i\alpha_j - \gamma)}\right]^{2L} B(\alpha_j, H_1) B(\alpha_j, H_2) = \prod_{m \neq j} \frac{\sinh \frac{1}{2}(i\alpha_j - i\alpha_m + 2\gamma) \sinh \frac{1}{2}(i\alpha_j + i\alpha_m + 2\gamma)}{\sinh \frac{1}{2}(i\alpha_j - i\alpha_m - 2\gamma) \sinh \frac{1}{2}(i\alpha_j + i\alpha_m - 2\gamma)}, \tag{6.11}$$

where

$$B(\alpha, H) = \frac{\cosh \frac{1}{2}(i\alpha + \gamma H)}{\cosh \frac{1}{2}(i\alpha - \gamma H)}, \qquad h_{lim} < |h| < \infty, \tag{6.12}$$

$$B(\alpha, H) = \frac{\sinh \frac{1}{2}(i\alpha + \gamma H)}{\sinh \frac{1}{2}(i\alpha - \gamma H)}, \qquad |h| < h_{lim}, \tag{6.13}$$

are called boundary terms. The energy eq. (6.5) takes the form:

$$E = \frac{1}{2}\left[(L-1)\cosh\gamma + h_1 + h_2\right] - 2\sinh\gamma \sum_{j=1}^{n} p'(\alpha_j), \qquad p'(\alpha) = \frac{\sinh\gamma}{\cosh\gamma + \cos\alpha}. \tag{6.14}$$

In the thermodynamic limit $L \to \infty$ the real roots α_j of BE form a dense distribution in the open interval $(0, \pi)$ with density $\rho(\alpha)$, $dI = 2L(\rho + \rho_h)d\alpha$ being the number of roots in the interval $d\alpha$. The logarithm of eq. (6.11) is:

$$2Lp(\alpha_j) + \frac{1}{i}\ln B(\alpha_j, H_1) + \frac{1}{i}\ln B(\alpha_j, H_2) + \phi(2\alpha_j) = \sum_{l=1}^{n} \phi(\alpha_j - \alpha_l) + \phi(\alpha_j + \alpha_l) + 2\pi I_j, \tag{6.15}$$

where I_j form an increasing sequence of positive integers, and

$$\phi(\alpha) = -i \ln \frac{\sinh \frac{1}{2}(2\gamma + i\alpha)}{\sinh \frac{1}{2}(2\gamma - i\alpha)}, \qquad \phi(0) = 0. \tag{6.16}$$

Taking the derivative of eq. (6.15) and defining ρ for negative α by $\rho(\alpha) = \rho(-\alpha)$, we obtain

$$p'(\alpha) + \frac{1}{2L} p'_{bdry}(\alpha) = \int_{-\pi}^{\pi} \phi'(\alpha - \beta)\rho(\beta) d\beta + 2\pi(\rho(\alpha) + \rho_h(\alpha)), \tag{6.17}$$

with

$$p'_{bdry}(\alpha) = -i \frac{B'(\alpha, H_1)}{B(\alpha, H_1)} - i \frac{B'(\alpha, H_2)}{B(\alpha, H_2)} + 2\phi'(2\alpha) - 2\pi\delta(\alpha) - 2\pi\delta(\alpha - \pi). \tag{6.18}$$

The presence of delta-functions in (6.18) is due to the fact that $\alpha_j = 0$ and $\alpha_j = \pi$ are always solutions to (6.11), which should be excluded, since they make the wave-function (6.3) vanish identically.

6.3 Solution for the bulk part

In eq. (6.17) the "boundary terms" are down by the factor $1/2L$. Neglecting p'_{bdry} and setting $\rho_h = 0$, we obtain the equation for the ground state density of the periodic XXZ chain [68]. Solving it by the Fourier expansion

$$f(\alpha) = \sum_{l=-\infty}^{\infty} \hat{f}(l) e^{il\alpha}, \qquad \hat{f}(l) = \frac{1}{2\pi} \int_{-\pi}^{\pi} f(\alpha) e^{-il\alpha} d\alpha, \tag{6.19}$$

and using (6.14), we recover the result for the ground state energy of the periodic chain [68]:

$$2\pi\hat{\rho}_{per}(n) = \frac{\hat{p}'(n)}{1 + \hat{\phi}'(n)}, \qquad \hat{\phi}'(n) = e^{-2\gamma|n|}, \qquad \hat{p}'(n) = (-1)^n e^{-\gamma|n|} \tag{6.20}$$

$$E^0_{gr} = \frac{L\Delta}{2} - 2L \sinh\gamma \int_{-\pi}^{\pi} \rho_{per}(\alpha) p'(\alpha) d\alpha = \frac{L\Delta}{2} - L \sinh\gamma \sum_{n=-\infty}^{\infty} \frac{e^{-\gamma|n|}}{\cosh \gamma n}. \tag{6.21}$$

The spin of the ground state is $S_z = L/2 - L\int_{-\pi}^{\pi} \rho_{per} d\alpha = 0$, which is the well-known result [68].

An elementary "bulk" excitation above the vacuum in the model (6.1) is a hole in the distribution of I_j, but only a pair of holes can occur for the periodic chain, as argued in [14]. Thus physical excitations contain an even number of holes. The energy of the hole with rapidity θ can be easily computed:

$$\varepsilon_h(\theta) = \sinh\gamma \sum_{n=-\infty}^{\infty} \frac{(-1)^n e^{in\theta}}{\cosh \gamma n} > 0, \tag{6.22}$$

and the spin with respect to the vacuum is $S_z = 1/2$. (Our result, eq. (6.22), differs from the conventional one by the shift $\theta \to \theta + \pi$, but the dispersion relation is unchanged by rapidity reparametrization.)

Analogous arguments can be applied to analyze "bulk" string solutions with complex values of α. Although there exists an infinite hierarchy of complex strings of arbitrary length, and quartets, their energy vanishes with respect to the vacuum [50].

6.4 Boundary excitations

So far we discussed the bulk excitations, which are essentially the same as in the periodic chain. Let us now turn to the new solutions of eq. (6.11), boundary strings. The analysis is close to that of section 4.4. Boundary excitations have their wave-function (6.3) localized at the left or right ends of the chain, and in the limit $L \to \infty$ the two boundaries may be considered separately. Let us study first the left boundary, $h_1 > 0$. The fundamental boundary 1-string consists of one root located at $\alpha_0 = -i\gamma H_1$ for $0 < h_1 < h_{cr}^{(1)}$, and at $\alpha_0 = \pi - i\gamma H_1$ for $h_{cr}^{(2)} < h_1 < \infty$ (in both cases $-1 < H_1 < 0$). It is a solution of BE due to the mutual cancellation of the decreasing modulus of the first term in (6.11) and the increasing modulus of the second term $B(\alpha, H_1)$ as $L \to \infty$ and $\alpha \to \alpha_0$. When $h_{cr}^{(1)} < h_1 < h_{cr}^{(2)}$, no such solution exists. Introduction of such a string into the vacuum with the density of roots $\rho(\alpha)$ defined from

$$p'(\alpha) + \frac{1}{2L} p'_{bdry}(\alpha) = \int_{-\pi}^{\pi} \phi'(\alpha - \beta)\rho(\beta)d\beta + 2\pi\rho(\alpha), \tag{6.23}$$

leads to the redistribution of roots by $\delta\rho \equiv 2L(\tilde{\rho} - \rho)$ satisfying the equation

$$0 = \int_{-\pi}^{\pi} \phi'(\alpha - \beta)\delta\rho(\beta)d\beta + \phi'(\alpha - \alpha_0) + \phi'(\alpha + \alpha_0) + 2\pi\delta\rho. \tag{6.24}$$

From the latter we find

$$2\pi\delta\hat{\rho}(n) = -\frac{2\cos n\alpha_0 e^{-2\gamma|n|}}{1 + e^{-2\gamma|n|}}. \tag{6.25}$$

For the energy and spin of the boundary 1-string with respect to this vacuum we obtain:

$$\tilde{\varepsilon}_b = -2\sinh(\gamma)p'(\alpha_0) - \sinh\gamma \int_{-\pi}^{\pi} \delta\rho p'(\alpha)d\alpha = -\sinh\gamma \sum_{n=-\infty}^{\infty} \frac{(-1)^n e^{in\alpha_0}}{\cosh\gamma n}, \tag{6.26}$$

$$S_z = -\frac{1}{2}.$$

We see that the energy (6.26) is negative, so the correct ground state wave-function (6.3) should contain the boundary 1-string root α_0 when the value of h_1 is not in the gap $h_{cr}^{(1)} < h_1 < h_{cr}^{(2)}$. The ground state density $\tilde{\rho}$ in this case satisfies the equation

$$p'(\alpha) + \frac{1}{2L}(p'_{bdry}(\alpha) - \phi'(\alpha - \alpha_0) - \phi'(\alpha + \alpha_0)) = \int_{-\pi}^{\pi} \phi'(\alpha - \beta)\tilde{\rho}(\beta)d\beta + 2\pi\tilde{\rho}(\alpha). \tag{6.27}$$

The boundary excitation is obtained by removing from vacuum (6.27) the root α_0, which means that it has the energy $-\tilde{\varepsilon}_b > 0$ and spin 1/2, equal to the spin of the bulk hole. Substituting the value of α_0 into (6.26), we get the boundary excitation energy, which precisely agrees with the one obtained in [49]:

$$\varepsilon_b(h_1) = \sinh\gamma \sum_{n=-\infty}^{\infty} \frac{(-1)^{\kappa n} e^{\gamma H_1 n}}{\cosh\gamma n}, \qquad -1 < H_1 < 0, \tag{6.28}$$

with $\kappa = 1$ if $h_1 < h_{cr}^{(1)}$ and $\kappa = 2$ if $h_1 > h_{cr}^{(2)}$.

From (6.22) and (6.28) we see that for $h_1 < h_{cr}^{(1)}$ the energy of the boundary excitation is smaller than the bottom of the energy band of bulk excitations, and becomes equal to it at $h_1 = h_{cr}^{(1)}$ (see Figure 6.1). So in this regime we may interpret the boundary excitation as the bound state of the kink, which gets unbound at $h_1 = h_{cr}^{(1)}$. For $h_1 > h_{cr}^{(2)}$ the energy of the boundary bound state is bigger than the top of the energy band. Therefore it is stable, in spite of its huge energy.

Besides the fundamental boundary 1-string, there exists an infinite set of "long" boundary strings, consisting of roots $\alpha_0 - 2ik\gamma, \alpha_0 - 2i(k-1)\gamma, ..., \alpha_0 + 2ni\gamma$ with $n, k \geq 0$. We will call such solution an (n,k) boundary string (thus the fundamental boundary string considered above is the (0,0) string). One can use the same arguments as given in section 4.4 to show that the (n,k) string is a solution of BE when its "center of mass" has positive imaginary part and the lowest root $\alpha_0 - 2ik\gamma$ lies below the real axis. Thus, sufficiently long boundary string solutions exist even in the region $h_{cr}^{(1)} < h_1 < h_{cr}^{(2)}$. However, a direct calculation shows that their energy vanishes with respect to the vacuum, so they represent charged vacua. [1] (Analogous phenomenon occurs for the "long" strings in the bulk [50]: if the imaginary part of α lies outside the strip $-2\gamma < \mathrm{Im}\alpha < 2\gamma$, the root α gives no contribution to the energy.) For $0 < h_1 < h_{cr}^{(1)}$ and $h_{cr}^{(2)} < h_1 < \infty$ the (n,0) strings also represent charged vacua, while (n,k) strings with $k \geq 1$ have the same energy (6.28) as the boundary bound state found above, and hence represent charged boundary excitations. [2]

Consider now the right boundary, $h_2 < 0$ ($H_2 < -1$). Now the fundamental boundary 1-string solution $\alpha_0 = -i\gamma H_2$ exists for any value of h_2 in the interval $-h_{lim} < h_2 < 0$ (resp. $\alpha_0 = \pi - i\gamma H_2$ for $h_2 < -h_{lim}$). Explicit calculation shows that it has non-vanishing energy only if $-2 < H_2 < -1$, which corresponds to $-h_{cr}^{(1)} < h_2 < 0$ (resp. $h_2 < -h_{cr}^{(2)}$). For such values of h_2 the energy of the 1-string with respect to the vacuum (6.23) is positive and equal to $\varepsilon_b(-h_2)$ (see eq. (6.28)), and its spin is $S_z = -1/2$. In some sense the pictures are dual for the positive and negative h cases: there exist two states when $|h|$ is not between $|h_{cr}^{(1)}|$ and $|h_{cr}^{(2)}|$, one with boundary 1-string and one without. One of them is the ground state and another is the excited state at the boundary, and these states exchange their roles when the sign of h changes. The analysis of long boundary strings is very similar to that at

[1] As an example, consider the boundary (1,0)-string consisting of the roots $\alpha_0 + 2i\gamma, \alpha_0$. It exists if $-1 < H_1 < 1$, although the (0,0)-string exists only if $-1 < H_1 < 0$. The (1,0)-string has charge $S_z = -1$ and vanishing energy with respect to the vacuum.

[2] *E.g.*, (1,1) string with roots $\alpha_0 + 2i\gamma, \alpha_0, \alpha_0 - 2i\gamma$ has $S_z = -3/2$ and energy given by (6.28) with respect to the physical vacuum.

the left boundary, and therefore will be omitted. The net result is again that long boundary strings represent charged vacua or charged boundary excitations.

In all examples shown above, the charge of boundary excitations turned out to be half-integer. One can easily check that this is true for all boundary strings representing charged excitations. Since the charge of physical excitations is obviously restricted to be an integer (see (6.5)), we conclude that a boundary excitation can appear only paired with the bulk excitation of half-integer charge (i.e. containing an odd number of holes), or with a boundary excitation at the other end of the chain. We give a qualitative interpretation of this fact below.

6.5 The surface energy

To compute the vacuum surface energy, eq. (6.2), of the model (6.1), one should use eq. (6.14) in the limit $L = \infty$ with the root density determined from eqs. (6.23) or (6.27) and the boundary terms (6.12) or (6.13), depending on the value of h. Define for convenience

$$g(\Delta) = \frac{\Delta}{2} + 2\sinh\gamma \sum_{n=1}^{\infty} \frac{e^{-2n\gamma} - 1}{\cosh 2n\gamma}. \tag{6.29}$$

We consider separately the following intervals for positive h_1 and negative h_2:

1) $|h_{1,2}| < h_{cr}^{(1)}$. The ground state contains one boundary 1-string, corresponding to h_1. The spin of the ground state can be found to be $S_z = 0$. Using eqs. (6.13), (6.18) and (6.27), and subtracting the bulk contribution (6.21) we get

$$E_{surf} = \frac{1}{2}(h_1 + h_2) - g(\Delta) - \sinh\gamma \sum_{n=1}^{\infty} (-1)^n \frac{e^{-\gamma H_1 n} - e^{\gamma H_2 n}}{\cosh\gamma n}. \tag{6.30}$$

2) $|h_{1,2}| > h_{cr}^{(2)}$. The ground state contains one boundary 1-string and has $S_z = 0$. From eqs. (6.12) and (6.27) it follows:

$$E_{surf} = \frac{1}{2}(h_1 + h_2) - g(\Delta) - \sinh\gamma \sum_{n=1}^{\infty} \frac{e^{-\gamma H_1 n} - e^{\gamma H_2 n}}{\cosh\gamma n}. \tag{6.31}$$

3) $h_{cr}^{(1)} < |h_{1,2}| < h_{lim}$. The ground state has no boundary strings and its spin is zero. From (6.23) and (6.13) one obtains the same expression as in case 1.

4) $h_{lim} < |h_{1,2}| < h_{cr}^{(2)}$. From (6.23) and (6.12) one obtains the same expression as in case 2. The ground state has the same structure as in case 3.

A qualitative plot of the surface energy as a function of h ($h = h_1 = -h_2$) is given in Figure 6.2. The apparent difference between (6.30) and (6.31) is an artefact of our parametrization of h in terms of H. In fact, E_{surf} is an analytic function of h in the domain $h \in (0, \infty)$,

which can be seen after substituting H as a function of h according to (6.8)-(6.9). In this sense the fields $h_{cr}^{(1,2)}$ are not actually "critical." We find for $h_1 = h_2 = 0$ the value

$$E_{surf} = -\frac{\Delta}{2} + 4\sinh\gamma\left(\frac{1}{4} + \sum_{n=1}^{\infty}\frac{e^{2n\gamma}-1}{1+e^{4n\gamma}} + \sum_{n=1}^{\infty}\frac{(-1)^n}{1+e^{2n\gamma}}\right). \tag{6.32}$$

Note that one can obtain the boundary magnetization $\langle\sigma_1^z\rangle$ [49] immediately from the formula for the surface energy (6.30)-(6.31) by differentiating it in h_1.

6.6 The Ising $\Delta = \infty$ and rational $\Delta = 1$ limits

In the extreme anisotropic limit $\Delta \to \infty$, $h \sim \Delta$ of the XXZ chain (6.1) one gets the one-dimensional Ising model:

$$\mathcal{H} = \frac{1}{2}\left\{\sum_{i=1}^{L-1}\Delta\sigma_i^z\sigma_{i+1}^z + h_1\sigma_1^z + h_2\sigma_L^z\right\}, \tag{6.33}$$

In this limit from (6.8)-(6.9) one has

$$h \approx \Delta \pm e^{-\gamma H}, \tag{6.34}$$

and the gap between $h_{cr}^{(1)}$ and $h_{cr}^{(2)}$ dissapears, so for any h there exists a boundary bound state. The energy of the "bulk" hole (6.22) becomes θ-independent and equal to Δ, since only $n = 0$ term contributes to the sum when $\gamma \to \infty$. The energy of the boundary bound state (6.28) becomes $\varepsilon_b = \Delta \pm e^{-\gamma H_1} = h_1$. This suggests the following interpretation in terms of the Ising chain. In the Ising ground state the i-th spin has the value $(-1)^i$. Local bulk excitation of the smallest energy 2Δ can be obtained by flipping one spin (the first and last spins excepted). The arising two surfaces (domain walls) separating the flipped spin from its right and left neighbours are called kinks and carry the energy Δ each. Kink corresponds to a hole in the Bethe ansatz picture, and kinks obviously appear only in pairs, which demonstrates that holes can exist only in pairs, too. The charge of the one-spin-flipped state is equal to one, in agreement with the charge of two holes in BA. In addition to charge 1 excitation, one has charge 0 excitation of the same energy obtained by flipping any even number of spins in a row. In the BA this corresponds to the "2 holes and 2-string" state. In the Ising model the left (right) boundary bound state is obtained by flipping the first (last) spin. Such a state has the energy $h_1 + \Delta$ above the vacuum energy, where h_1 is the contribution of the boundary term in (6.33) and Δ is the energy of the kink created due to the boundary-bulk interaction. Thus flipping the boundary spin actually gives a combination of the boundary excitation and the bulk kink. Still another possibility is to flip all spins, creating two boundary bound states, one at each boundary. This explains why, in the BA picture, a boundary excitation can exist only if paired with a hole in the Dirac sea or with another boundary excitation. The vacuum surface energy (6.2) of the Ising chain in the thermodynamic limit is $(\Delta - h_1 + h_2)/2$. The $\Delta/2$ contribution here is the bulk interaction energy that we lost when we disconnected the periodic chain, and $\pm h_{1,2}/2$ is the contribution

of each of the boundary terms. Taking the limit $\gamma \to \infty$ in eqs. (6.30)- (6.31), we obtain the expected result $E_{surf} \to (\Delta - h_1 + h_2)/2$.

In the isotropic (rational) limit $\Delta \to 1$ (*i.e.*, $\gamma \to 0$) one gets the XXX chain in a boundary magnetic field, which was discussed in the BA framework in [42] for $0 < h_{1,2} < 2$. From (6.8)-(6.9) one has in this limit

$$h = \frac{2}{1+H}. \tag{6.35}$$

There is only one critical field $h_{cr} = 2$, which is the limit of $h_{cr}^{(2)}$. Passing from summation to integration in eq. (6.31), we obtain for $0 < h_1 < \infty$, $0 < -h_2 < \infty$:

$$\begin{aligned} E_{surf} &= \frac{1}{2}(h_1 + h_2) - \frac{1}{2} + \frac{\pi}{2} - \int_0^\infty dx \frac{e^{-(\frac{2}{h_1}-1)x} - e^{(\frac{2}{h_2}-1)x} + e^{-x}}{\cosh x} = \\ &= \frac{1}{2}(h_1 - h_2) - \frac{1}{2} + \frac{\pi}{2} - \int_0^\infty dx \frac{e^{-(\frac{2}{h_1}-1)x} + e^{(\frac{2}{h_2}+1)x} + e^{-x}}{\cosh x}, \end{aligned} \tag{6.36}$$

where the second line was obtained from the first one after a simple manipulation. This agrees with the results of [42]. For $h_1 = h_2 = 0$ one has from (6.36) $E_{surf} = (\pi - 1)/2 - \ln 2$.

6.7 The case of parallel magnetic fields

Another aspect is the structure of the ground state in the regime $h_{1,2} > 0$. Assuming that, for example, for $h_{1,2} > h_{cr}^{(2)}$ the ground state contains both left and right boundary 1-strings to minimize the energy, we end up after a short calculation with a half-integer spin of the vacuum, which signals that such a state cannot, in fact, be the vacuum. Hence, the ground state must have a more intricate structure. Appealing to the Ising limit $\gamma \to \infty$, one sees that for $h_{1,2} > \Delta$ the ground state must have both boundary spins directed opposite to the magnetic field, and therefore contain a kink in the bulk (recall that L is even). On the other hand, for $h_{1,2} < \Delta$ the lowest energy configuration is such that the boundary spins are antiparallel, which means that the physical vacuum contains what was called a boundary excitation at one of the ends. This suggests that for finite Δ the correct ground state wave-function of the Hamiltonian (6.1) should contain a bulk hole with the minimal possible energy (i.e. the kink with zero rapidity $\theta = 0$) and both boundary 1-strings when $h_{1,2} > h_{cr}^{(2)}$. Such a state has spin zero. Changing the rapidity of this stationary kink away from zero, one obtains in such a way an excited state whose energy can be arbitrarily close to the vacuum one, which means that there is a new gapless branch in the spectrum. [3] Similarly, when $h_{cr}^{(1)} < h_{1,2} < h_{cr}^{(2)}$, for the ground state to have the integer charge it should also contain a kink in the bulk. When $h_{1,2} < h_{cr}^{(1)}$ the physical vacuum contains only one of the two boundary 1-strings and no stationary kink in the bulk (when $h_1 = h_2$ there are two possibilities to have either left or right boundary 1-string in the vacuum, corresponding to

[3] In the Ising limit $\gamma \to \infty$ the energy of the kink is independent of rapidity, and therefore this branch degenerates to the vacuum.

the obvious two-fold degeneracy of the Ising ground state in this case). Such a state has a smaller energy for $h_{1,2} < h_{cr}^{(1)}$ than the one with a hole in the bulk and two boundary strings, while for $h_{1,2} > h_{cr}^{(2)}$ the state with the bulk hole is energetically preferable, since in this case $\varepsilon_b > \varepsilon_h$ (see Fig.12 and [49]). This situation is in some sense analogous to the case of the periodic antiferromagnetic XXZ chain with odd L, where the ground state contains a kink. According to the above discussion the surface energy in the case $h_{1,2} > h_{lim}$ is:

$$E_{surf} = \frac{1}{2}(h_1 + h_2) - g(\Delta) + \varepsilon_h(0) - \sinh\gamma \left(1 + \sum_{n=1}^{\infty} \frac{e^{-\gamma H_1 n} + e^{-\gamma H_2 n}}{\cosh \gamma n}\right). \tag{6.37}$$

In the rational ($\gamma \to 0$) limit $\varepsilon_h(0)$ vanishes and eq. (6.37) becomes

$$E_{surf} = \frac{1}{2}(h_1 + h_2) - \frac{1}{2} + \frac{\pi}{2} - \int_0^{\infty} dx \frac{e^{-(\frac{2}{h_1}-1)x} + e^{-(\frac{2}{h_2}-1)x} + e^{-x}}{\cosh x}. \tag{6.38}$$

This expression agrees with the one obtained in [42]. Note that the authors of [42] obtained eq. (6.38) under the assumption that $0 < h_{1,2} < h_{cr}$, while our derivation shows that this result is valid for $0 < h_{1,2} < \infty$. In the Ising limit eq. (6.37) gives the correct result $E_{surf} = (3\Delta - h_1 - h_2)/2$. Observe that for the XXX chain the following equality holds (see (6.36) and (6.38)): $E_{surf}(h_1, h_2) = E_{surf}(h_1, -h_2)$. This is the consequence of the decomposition $E_{surf} = f(h_1) + f(h_2) + const$, which takes place in the limit $L = \infty$ when two boundaries are independent, and the obvious property of the semi-infinite chain $f(-h) = f(h)$. The same statements are true for the surface energy of XXZ chain apart from the $\varepsilon_h(0)$ contribution (see (6.37)).

6.8 Remarks

We would like to mention also that within the BA technique it is possible to calculate also the boundary S-matrix for the scattering of kinks (represented by holes in the Dirac sea) in the ground state of the Hamiltonian (6.1) or in the excited boundary state. Such a calculation has been performed in [42] for the boundary XXX chain and in chapter 4 above for the boundary sine-Gordon model. For the boundary XXZ chain these S-matrices have been obtained by Jimbo et al. [49] by the algebraic approach.

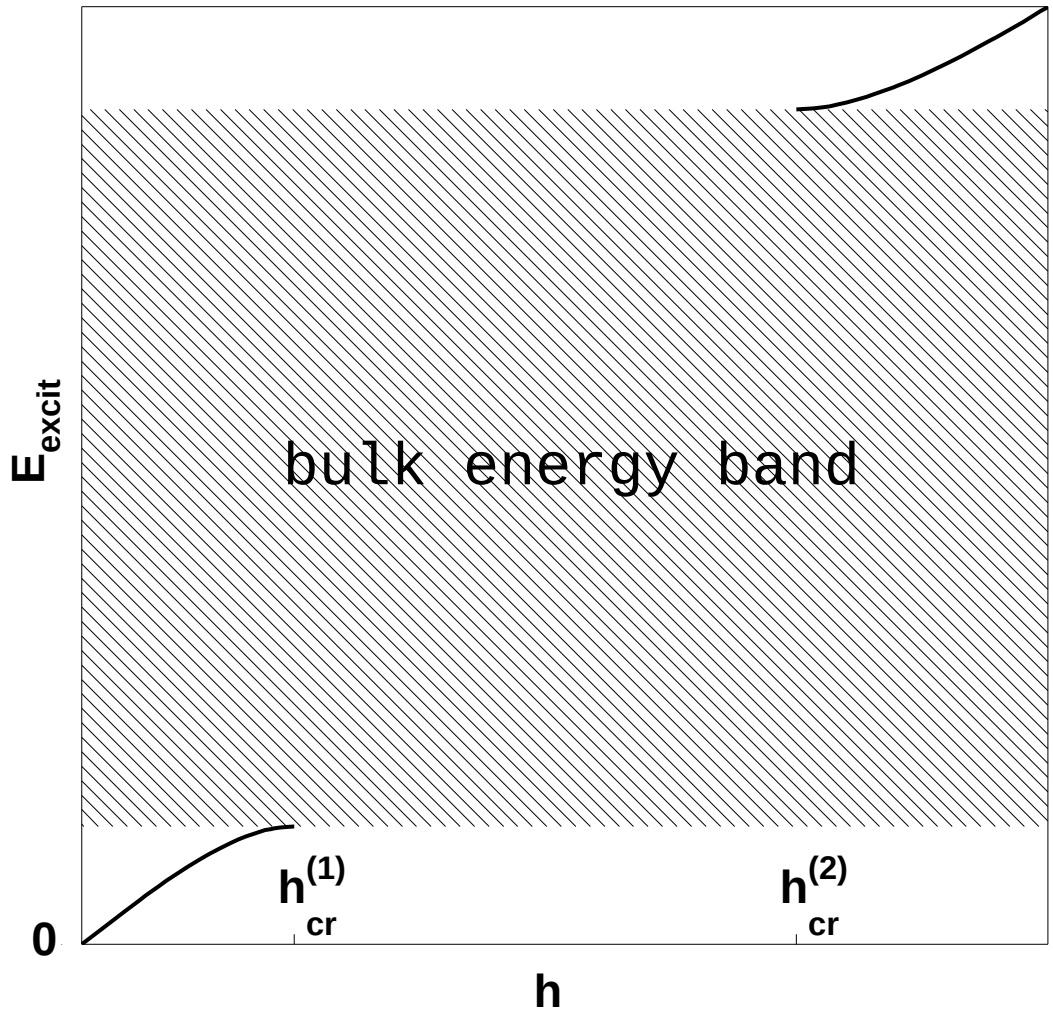

Figure 6.1: Solid line: a schematic plot of the energy of the boundary excitation, $\varepsilon_b(h)$, as a function of the boundary magnetic field h. Shaded area: the energy band of the bulk excitations.

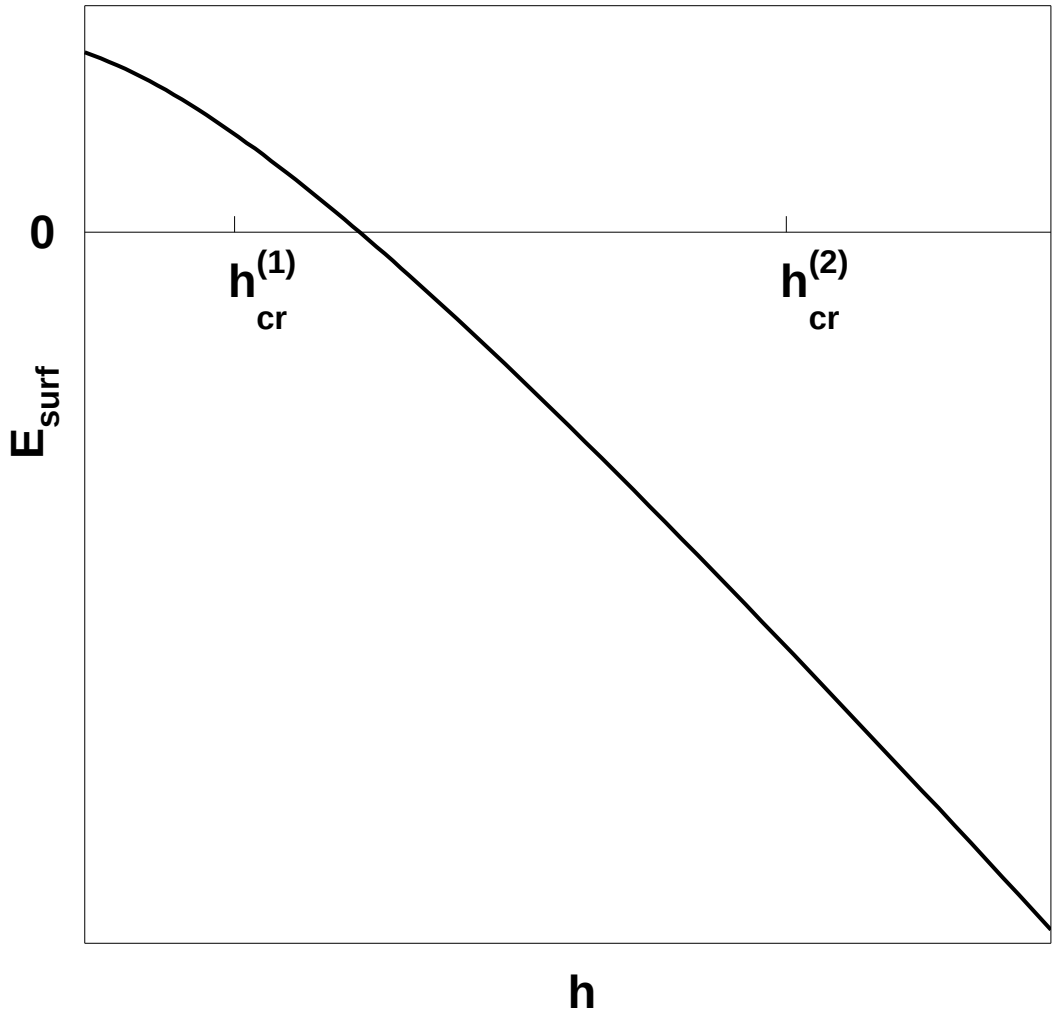

Figure 6.2: A schematic plot of the vacuum surface energy as a function of the boundary magnetic field $h = h_1 = -h_2$.

Chapter 7

Calculation of correlation functions for the problems with impurities

We show how to compute analytically time and space dependent correlations in one-dimensional quantum integrable systems with an impurity. Our approach is based on a description of these systems in terms of massless scattering of quasiparticles [69]. Correlators follow then from matrix elements of local operators between multiparticle states – the *massless form-factors*. Although, in general an infinite sum of these form-factors has to be considered, we find that for the current, spin and energy operators only a few (two or three) are necessary to obtain an accuracy of more than 1%. Our results are valid for `arbitrary impurity strength`, in contrary to the perturbative expansions in the coupling constants. As an example, we compute the frequency dependent condunctance, at zero temperature, in a Luttinger liquid with an impurity, and also discuss the succeptibility in the Kondo model and the time-dependent properties of the two-state problem with dissipation. This chapter is based on [70].

7.1 Introduction

In this chapter we present the technique to calculate current-current correlation functions in the quantum field theories of the form

$$H = \frac{1}{2}\int_0^\infty dx\ [8\pi g\Pi^2 + \frac{1}{8\pi g}(\partial_x\phi)^2] + \mathcal{B}, \tag{7.1}$$

where $\mathcal{B}$ is a problem dependent boundary interaction and the fields are defined on the positive half-line. The method we adopt is based on the form-factor formalism [71] and provides us with the series expansions of correlators. One has to insert intermediate n-particle states in the correlator $\langle 0|j_\mu j_\nu|0\rangle = \sum_n \langle 0|j_\mu|n\rangle\langle n|j_\nu|0\rangle$; then the well-known technique for integrable models [72] gives the exact values for the above scalar products between the vacuum and n-particle states (the form-factors). The integral representation for each term of the series is available. Moreover, the observed `rapid convergence at any scale from small to large distances` allows us to truncate the series after a few terms (typically two

or three) to obtain a 1% accuracy. There are few novelties that deserve our attention: first, we have to deal with the *massless* form-factors, following the pioneering work [73]. Second, we work in a half-plane geometry. An instructive example, although somewhat simple and abstract, is an Ising model in a boundary magnetic field [74].

The role, played by integrability in our approach is two-folded. First, it gives us the `exact` expressions for the form-factors and other necessary quantities. Second, it provides us with a basis of particles (intermediate states) which allow us to truncate the series expansion of correlators due to the rapid convergence. Thus, the integrability insures the relatively small contribution of the multi-particle terms.

To pave our path through the calculations, we consider some simple model of the free massless 1-dimensional scalar field with the boundary interaction of the form $\mathcal{B} = M_B \cosh\phi$. This model can be viewed as the massless limit of the integrable sinh-Gordon model with boundary interaction:

$$S = \int dxdt \left[\frac{1}{2}(\partial_\mu\phi)^2 - \frac{m^2}{g^2}\cosh(g\phi)\right] - M_B \int dt \cosh\left(\frac{g\phi}{2}\right)|_{x=0} \tag{7.2}$$

The advantage of this approach, as opposed to starting with the free massless boson quantized in the plane-wave basis, is the following: in the massless limit, obtained by scaling the energy and momentum of particles along with the boundary mass M_B to infinity, we get the convenient basis of massless particle states which are particular combinations of plane waves that scatter diagonally off the boundary. Corresponding classical solutions are presented in [31]. Working with these massless particles at first sight adds some complexity, but it is paid off by the final simple and manageable results, while in the plane wave picture one has to do infinite summations and the final result is difficult to extract.

We apply our technique to find the correlation functions in three models of condensed matter physics: the Kondo model, the spin-boson model (two-level system with dissipation), and the Luttinger liquid with impurity (realized as the quantum Hall liquid with constriction). A common feature to all these models is that they can be reduced to a model described by massless excitations in the bulk interacting with an impurity at the boundary. The boundary interaction $\mathcal{B}$ in the first and second models is $\mathcal{B} = \lambda\,(S_+e^{i\phi(0)/2} + S_-e^{-i\phi(0)/2})$, and the third model has $\mathcal{B} = M\cos\phi(0)$. The absence of a mass gap leads to a power law behaviour for the current correlators in both the ultra-violet and the infra-red regime. The cross-over between these two regimes is non-trivial because of the renormalisation group flow induced by the impurity. For each model that we study, correlation functions can be related to the measurable quantities in the model dependent way. For example, for the Luttinger liquid, the Kubo formula [75] gives the *AC conductivity*:

$$\sigma_{\mu\nu}(\omega) = \int_0^\infty dx \int_0^\infty \langle 0|j_\nu(0)j_\mu(t+ix)|0\rangle e^{-i\omega t}dt \tag{7.3}$$

The *perturbative* analysis of [76] shows that the conductivity scaling function, depending on the impurity strength, flows from the insulating at $T = 0$ to the perfect conductance at $T = \infty$ in the repulsive regime. The alternative *exact* methods, which do not employ the knowledge of correlation functions, have been developed in [77] to find the static DC

conductivity at non-zero temperature and voltage. These methods do not allow, however, the determination of the AC conductivity. The experimental data [78], as well as the numerical Monte-Carlo simulations [79, 80] for the Luttinger liquids with impurity are available.

7.2 Integrable models in condensed matter physics

In this section we introduce and review three prominent models of condensed matter physics: the Kondo model, the spin-boson model (two-level system with dissipation), and the Luttinger liquid with impurity. The results of application of our technique for computing correlators to these models are partially shown here and in part further. When bosonized, all three models look alike in the bulk (free massless boson), but have different boundary interactions $\mathcal{B}$: $\lambda\ (S_+e^{i\phi(0)/2} + S_-e^{-i\phi(0)/2})$ for the first and second, and $M\cos\phi(0)$ for the third one.

7.2.1 Kondo model

The Kondo model describes the free bulk electrons interacting with an impurity via the spin:

$$H_K = \sum_{k,\sigma} \varepsilon(k) c^+_{k\sigma} c_{k\sigma} + J\vec{s}(0)\vec{S}_{imp} \tag{7.4}$$

Here, $\vec{S}_{imp} = \frac{1}{2}\vec{\sigma}$ is the impurity spin, $\vec{\sigma}$ are Pauli matrices, and $\vec{s}(0)$ is the spin induced by the electrons at the point of impurity,

$$\vec{s}(0) = \frac{1}{2}\sum_{\sigma\sigma'} \psi^+_\sigma(0)\vec{\sigma}_{\sigma\sigma'}\psi_{\sigma'}(0), \qquad \psi_\sigma(0) = L^{-1/2}\sum_k c_{k\sigma}. \tag{7.5}$$

A useful generalization of (7.4) is an anisotropic Kondo model [81]:

$$H_K = \sum_{k,\sigma} \varepsilon(k) c^+_{k\sigma} c_{k\sigma} + J_\pm[\sigma_+\psi^+_\downarrow\psi_\uparrow(0) + \sigma_-\psi^+_\uparrow\psi_\downarrow(0)] + J_z\sigma_z \sum_{k,k',\sigma=\pm} \sigma c^+_{k\sigma}c_{k'\sigma}, \tag{7.6}$$

which reduces to (7.4) if $J_z = J_\pm$.

We need also the bosonized version of (7.6). For it, two bosonic fields are necessary: one associated with charge and one with spin. The charge-density field decouples completely and only the spin-density has interaction at the boundary. The Hamiltonian for the spin-density field is of the form

$$H_K = \frac{1}{2}\int_0^\infty dx[8\pi g\Pi^2 + \frac{1}{8\pi g}(\partial_x\phi)^2] + \lambda\ (S_+e^{i\phi(0)/2} + S_-e^{-i\phi(0)/2}). \tag{7.7}$$

The coupling constant λ is related to $J_\pm$. The S_z term in the Hamiltonian has been eliminated by a unitary rotation, but dependence on J_z is implicit in g. The case $g = 1$ corresponds to the isotropic Kondo model.

The quantities of interest in the Kondo model are the spin-spin correlation functions for the induced electron spin in the bulk (screening cloud problem [82]) and for the impurity

spin on the boundary, $\langle S^z_{imp}(t)S^z_{imp}(0)\rangle$. We consider here mostly the latter ones, since they are relevant for the dissipative two-level problem. But the screening cloud problem can be approached by the form-factors technique, too, and for partial results we refer to [70]. The *dynamic susceptibility*, or the *response function* is given by

$$\chi''(\omega) \equiv \frac{1}{2}\int dt e^{i\omega t}\langle [S^z(t), S^z(0)]\rangle. \tag{7.8}$$

In [70] it was shown how to express the spin correlators in terms of the bosonic field correlators of (7.7). In particular, for the response function we have[1]

$$\chi''(\omega) = \frac{1}{(2g\pi)^2}\frac{1}{\omega^2}\mathrm{Im}\left[\mathcal{G}(-i\omega,\beta_B) - \mathcal{G}(-i\omega,-\infty)\right], \tag{7.9}$$

where

$$\langle \partial_{\bar z}\phi(x,y')\partial_z\phi(x,y'')\rangle_\lambda = \int_0^\infty dE\mathcal{G}(E,\beta_B)\exp\left[-2Ex - iE(y'-y'')\right], \tag{7.10}$$

and the boundary temperature β_B is related to λ. The foregoing technique (see section 7.4) allows us to compute the quantity $\mathcal{G}(E,\beta_B)$ in the form of series expansion. Every term of the series is known analytically. In practice, it is enough to keep only few first terms of these series to obtain a very good accuracy of 1% or more. E.g., for the Toulouse limit, corresponding to $g = \frac{1}{2}$, the series get truncated and we obtain the exact result

$$\begin{aligned}\chi''(\omega) &= \frac{2}{\pi^2}\frac{T_B}{\omega}\mathrm{Im}\left(\int_0^\omega dx \frac{1}{(x+iT_B)(\omega - x + iT_B)}\right)\\ &= \frac{1}{\pi^2}\frac{4T_B^2}{\omega^2+4T_B^2}\left[\frac{1}{\omega}\ln\left(\frac{T_B^2+\omega^2}{T_B^2}\right) + \frac{1}{T_B}\tan^{-1}\frac{\omega}{T_B}\right].\end{aligned}$$

For the less simple $g = 1/3$ case the leading contribution to the response function reads

$$\delta\chi''(\omega)^{(1)} = -\frac{9\mu^2 d^2}{8\pi\omega}\mathcal{R}e\left[\frac{\tanh\left(\frac{1}{2}\log(\frac{\omega}{\sqrt{2}T_B}) - \frac{i\pi}{8}\right)}{\tanh\left(\frac{1}{2}\log(\frac{\omega}{\sqrt{2}T_B}) + \frac{i\pi}{8}\right)} - 1\right] \tag{7.11}$$

where $\mu \approx 3.14$, $d \approx 0.1414$. Similar computations give rise to the results in figure 7.1 where we plotted $\chi''(\omega)/\omega$ for the values $g = 3/5, 1/2, 1/3, 1/4$. Notice the emergence of the peak for $g < 1/3$. It is remarkable that this peak appears at $g = 1/3$ and not at $g = 1/2$ as was expected from other means of calculations.

Using eq. (7.9) and the general form of $\mathcal{G}(E,\beta_B)$ given below, we can find the exact static succeptibility χ_0 which is given by the Shiba's relation [83]:

$$\lim_{\omega\to 0}\frac{\chi''(\omega)}{\omega} = 2\pi g\chi_0^2. \tag{7.12}$$

Omitting the details, we list the result:

$$\chi_0 = \frac{1}{\pi^2 g T_B}. \tag{7.13}$$

(but see [70] for the complete account of this derivation).

[1] In the most of this chapter it is tacitly assumed that $\hbar = 1$.

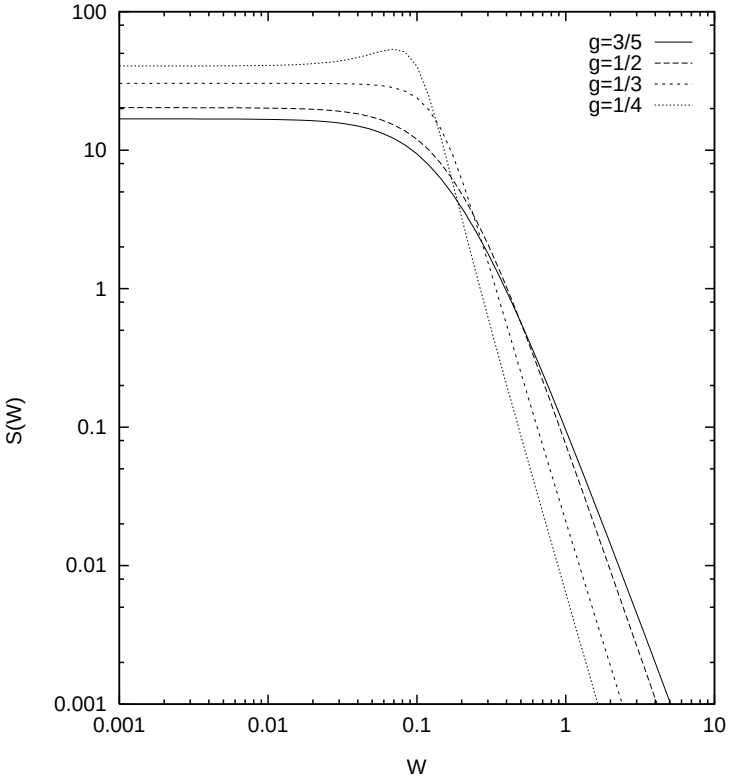

Figure 7.1: Plot of $\chi''(\omega)/\omega$ for the values $g = 3/5, 1/2, 1/3, 1/4$

7.2.2 Quantum systems with dissipation

The effect of dissipation on quantum tunnelling has been addressed in the pioneering work of Caldeira and Leggett [84]. Suppose first one has a system with friction, or dissipation, described by the equation of motion

$$M\ddot{q} + \eta\dot{q} + \frac{\partial V}{\partial q} = F_{ext}(t), \tag{7.14}$$

with the potential V admitting a quasi-stationary state that can tunnel into the continuum. Then, speaking loosely, the question one asks is whether there is a qualitative change in the behavior of such a system for $\eta = 0$ and $\eta \neq 0$?

It is an interesting problem in general how to introduce friction in the formalism of quantum mechanics. In [84] the following phenomenological model is suggested, in analogy with (7.14):

$$C\ddot{\phi} + R_n^{-1}\dot{\phi} + \frac{\partial U}{\partial \phi} = 0 \tag{7.15}$$

It is usually refered as RSJ (resistively shunted junction) model. The nature of the resistance R_n is not clear, however. It is introduced in the model phenomenologically.

As the analysis of [84] shows, the net effect of the friction is that the WKB exponent for the tunnelling rate is increased by dissipation and tunnelling rate decreases:

$$P \sim \exp\left(\frac{-cV_0}{h\omega_{eff}}\right) \tag{7.16}$$

As a consequence of interactions, the characteristic frequency of classical system ω_0 (defined by the product LC) is renormalized to ω_{eff}.

As for experimental applications, the theory of [84] describes a trapped flux in SQUID (superconducting interference device). The phase of the flux, ϕ, is a quantum degree of freedom governed by the potential

$$U(\phi) = \frac{(\phi - \phi_x)^2}{2L} - I_c\Phi_0 \cos\left(\frac{2\pi\phi}{\phi_0}\right), \tag{7.17}$$

where ϕ_x is an external flux, L is a self-inductance of the device, I_c is a critical current and $\Phi_0 = h/2e$ is a flux quantum. The kinetic energy is given by $K = \frac{1}{2}C\dot{\phi}^2$ with C a capacitance. Another experimental realization can be found in the single Josephson junction biased by a fixed external current I_0. The quantum degree of freedom now is the phase difference of Cooper pair across the junction, φ, and the potential is

$$U = -\frac{I_0\Phi_0}{2\pi}\varphi - \frac{I_c\Phi_0}{2\pi}\cos\varphi. \tag{7.18}$$

Another fundamental system has been studied in [85]. Here, instead of tunnelling into the continuum, a double well problem is being considered with the tunnelling between two separated wells. Since the particle can be localized in either of two wells, the system is refered

to as a two-level system. More generally, it could be not necessarily a continuum degree of freedom with two spacially separated states, but also an isospin degree of freedom with two states, e.g. a strangeness quantum number in particle physics. Examples and applications include the strangeness oscillations of a neutral K-meson beam, or an inversion resonance of the NH_3 molecules.

The isolated two-level system can be modeled by a Hamiltonian

$$H_0 = -\frac{1}{2}\Delta_0\sigma_x + \frac{1}{2}\varepsilon\sigma_z \tag{7.19}$$

where Δ_0 is a matrix element for tunneling, and ε is a "detuning" parameter called *bias* (e.g. in the double-well problem it is the difference of the ground state energies of the wells). It is obvious that the model (7.19) is the effective Hamiltonian in the quasiclassical description of the double-well problem.

The dynamics of the two-level system with the Hamiltonian (7.19) can be easily solved. It is well-known that in the absense of bias, $\varepsilon = 0$, system shows coherent behavior with the probability distribution

$$P(t) \equiv P_R - P_L = \cos(\Delta_0 t), \tag{7.20}$$

where P_L (P_R) is the probabilty of finding particle in the left (right) well, and we assumed that initially the particle was localized in the right well. In the presence of non-zero bias the oscillatory behavior (7.20) is destroyed.

Another factor that can potentially destroy the coherence is an interaction with the environment with sufficiently strong coupling. Environment couples through the σ_z term in (7.19) and can be modeled the by following *spin-boson* Hamiltonian [85]:

$$H_{sb} = H_0 + \frac{1}{2}q_0\sigma_z\sum_i C_i x_i + \sum_i\left(\frac{1}{2}m_i\omega_i x_i^2 + \frac{p_i^2}{2m_i}\right) \tag{7.21}$$

The environment is modeled by the set of N harmonic oscillators (phonons) described by the last term in (7.21), and, of course, we are interested in the thermodynamic limit $N \to \infty$. With the non-zero coupling to environment, q_0, one state of the two-state system becomes more preferable than the other, depending on the "mood" of the environment. At $T = 0$, classically, all the oscillators are at $x_i = 0$ and have no effect on the two-state system. However, quantum-mechanically the problem becomes non-trivial even at $T = 0$ due to the quantum fluctuations. The question of theoretical interest can be formulated as follows: Can there exist oscillatory behavior (7.20) in a macroscopic system (7.21), or the coherence will be destroyed by the interaction with environment?

The time-dependent quantities of interest which are useful in the analysis of this problem are conveniently encoded in the following:

$$P(t) = \langle\sigma_z\rangle, \tag{7.22}$$

$$C(t) = \frac{1}{2}\langle[\sigma_z(t), \sigma_z(0)]\rangle. \tag{7.23}$$

Here, $P(t)$ measures how the average of spin varies with time, provided that at $t = 0$ it was in a certain state, while $C(t)$ describes the probability to be in a state $\sigma_z(t)$ given that the system was in a state $\sigma_z(0)$ at $t = 0$. The operators are understood in the Heisenberg representation $\sigma_z(t) = e^{-iH_{sb}t}\sigma_z e^{iH_{sb}t}$.

It turns out that the effect of phonon bath on the two-level system is very non-trivial and depends on the form of the *spectral function of the environment*,

$$J(\omega) = \frac{\pi}{2}\sum_i \frac{C_i^2}{m_i\omega_i}\delta(\omega - \omega_i) \tag{7.24}$$

It is usually assumed that $J(\omega) = \eta\omega^s \exp(-\omega/\omega_c)$ where ω_c is a cut-off frequency. According to the analysis of [85], we have, at $T = 0$, the weakly damped coherent oscillations for $s > 1$, and the complete localization for $s < 1$. For $s = 1$ the analysis becomes more complicated and the result depends on the value of the dimensionless coupling constant α,

$$\alpha = \frac{\eta q_0^2}{2\pi} \tag{7.25}$$

The $s = 1$ case is usually refered to as the *ohmic regime*. For $\alpha \geq 1$ and $s = 1$ it is believed that the system is completely localized [85], while for $\alpha < 1$ the situation is not clear yet. It is known that there exists a critical point at the value of α equal or about $\alpha_c = \frac{1}{2}$ where a phase transition in the ground state occurs. For α less than this critical value the damped oscillations are observed, while above it there is an incoherent relaxation.

The value $\alpha = \frac{1}{2}$, called the Toulouse limit, is an exactly solvable point. At this point the model can be mapped onto the following model:

$$H_T = \sum_k kc_k^+ c_k + V\sum_k (d^+ c_k + c_k^+ d) \tag{7.26}$$

where d^+, d create and annihilate a localized state (corresponding to the spin degree of freedom in the spin-boson model), while c_k^+, c_k are the creation and annihilation operators for the fermions in continuum (corresponding to the bath).[2] The Toulouse model is a particular case, $U = 0$, of a more general exactly solvable *resonance-level model* [86], which can be mapped onto the spin-boson model :

$$H_{RL} = H_T + U\sum_{k,k'}(c_k^+ c_{k'} - \frac{1}{2})(d^+ d - \frac{1}{2}) \tag{7.27}$$

The correspondence is given by the simple relations

$$\sigma_+ = d^+, \qquad \sigma_- = d, \qquad \sigma_z = d^+ d - \frac{1}{2} \tag{7.28}$$

and V is directly proportional to the hopping Δ_0, while U is related to α as follows [87] :

$$\alpha \sim \left(1 - \frac{U}{\pi}\right)^2 \tag{7.29}$$

[2] The bias ε corresponds to the energy of localized state.

The exact solution of the Toulouse model gives the following behavior at $\alpha = \frac{1}{2}$:

$$P(t) = \exp(-t/\tau). \tag{7.30}$$

A particularly useful fact for us is that the long-time behavior, $t \gg \omega_c^{-1}$, of the spin-boson model in the ohmic regime with $\frac{1}{2} < \alpha < 1$ is the same as the long-time behavior of the anisotropic Kondo model [3] (7.6). This result can be established rigorously by means of the bosonization [87]. The harmonic oscillators in the spin-boson model play the role of the spin-density excitations in the Kondo case, and the impurity spin ($S_{imp} = \frac{1}{2}$) corresponds to the discrete degree of freedom in (7.21). We have :

$$\begin{aligned} \Delta_0 &\sim J_\pm \\ \alpha &\sim (1 - \frac{1}{2}\rho J_z)^2. \end{aligned} \tag{7.31}$$

The point $\alpha = 1$ maps into $J_z = 0$, in such a way separating the ferro and antiferromagnetic regimes in the Kondo model. Note that the mapping works only for $J_\pm, J_z$ small enough, i.e. α close to 1. The regions where α is far from 1 can be approached by the renormalization group analysis [88]. By continuity, the results should hold at least up to the strong coupling fixed point, $\alpha = \frac{1}{2}$, where the exact solution (7.30) holds. Note that the analysis of the previous section, in particular figure 7.X suggests that the incoherent relaxation takes place in fact up to $\alpha = 1/3$. This is supported by a recent RG numerical study [89].

7.2.3 Quantum Hall liquid with constriction

Transport in one-dimensional interacting electron systems in the presence of impurities is an instructive problem with a broad rangle of experimental applications. Important ingredients, defining a proper physical model, are the Coulomb correlations in the vicinity of a tunneling point, as well as the electron interactions in the "feeding leads". Namely, when the leads are one-dimensional, they ought to be described by a Luttinger liquid, rather than the Fermi liquid since the latter is de-stabilized by interactions. In real 1D wires the impurities away from the point contact will complicate matters, tending to localize electrons. This localization makes it difficult to realize 1D Luttinger liquids in experiment.

However, systems are available [79, 78] which are free of undesirable localization – where the leads feeding a point contact are 2D fractional quantum Hall (QH) fluids. In the appropriate regime of the QH liquid the incoming current will be carried by *edge states*. Wen has demonstrated [90] that the gapless edge excitations of a QH system are *chiral* Luttinger liquids. Let us recall briefly the logic behind Wen's theory. The long-length-scale physics of the bulk 2D QH state is described by the massive 2+1 dimensional Chern-Simons theory

$$S_{bulk} = \frac{i}{4\pi\nu} \int a_\mu \partial_\nu a_\lambda \varepsilon_{\mu\nu\lambda} d^2x d\tau. \tag{7.32}$$

[3] Only the low-lying excitations are relevant in this limit.

The coefficient ν is uniquely fixed by the quantized Hall conductivity. [4] In the presence of a boundary, say at $y = 0$, one can integrate out the bulk degrees of freedom. The resulting 1D action for the edge field reads

$$S^R_{edge} = -\frac{1}{4\pi\nu}\int dxd\tau(\partial_x\varphi_R)(i\partial_\tau + v\partial_x)\varphi_R, \tag{7.33}$$

where v is the velocity of edge excitation (we set $v = 1$ hereafter). The boson field φ was introduced as $a_j = \partial_j\varphi$ to solve an incompressibility constraint on the electron density, $\varepsilon_{ij}\partial_i a_j = 0$. Similarly, one writes for another edge

$$S^L_{edge} = -\frac{1}{4\pi\nu}\int dxd\tau(\partial_x\varphi_L)(-i\partial_\tau + v\partial_x)\varphi_L. \tag{7.34}$$

The charge density along the edge is given by $\rho(x) = \partial_x\varphi/2\pi$, and the momentum operator conjugate to φ is $\Pi = \rho/\nu$. Adding an extra electron to the edge is equivalent to creating a soliton in φ with electron creation operator being

$$\Psi(x) \sim \exp[2\pi i\int^x \Pi(x')dx'] = e^{i\varphi(x)/\nu}. \tag{7.35}$$

A quasiparticle of fractional charge νe is created by $e^{i\varphi(x)}$ (speaking loosely, an electron is composed of ν^{-1} quasiparticles).

Due to the chirality, backscattering is only possible when opposite edges of the sample are close together, i.e. at the point contact. Thus, localization in such leads is absent. The analog of impurity that causes backscattering is a narrow constriction which brings left and right edges close enough for Laughlin quasiparticles to tunnel, as illustrated in figure 7.2. This is achieved by applying a gate voltage V_G across the narrow region in the Hall bar.

Suppose that tunneling takes place at $x = 0$. The edges are no longer independent, but rather coupled via the tunneling term in the total action:

$$S = S^L_{edge}(\varphi_L) + S^R_{edge}(\varphi_R) + \int d\tau V_{imp}(\varphi_L, \varphi_R)_{x=0}. \tag{7.36}$$

The most general form of the tunneling term is

$$V = \Psi^+_L\Psi_R(0) + \text{h.c.} = \sum_{m=1}^{\infty} v_m e^{im[\varphi_L(0)-\varphi_R(0)]} + \text{c.c.} \tag{7.37}$$

where v_m are tunneling amplitues. The term with $m = 1$ corresponds to quasiparticle tunneling, while $m = \nu^{-1}$ term – to the electron tunneling. In what follows we choose $\nu = 1/3$. As was argued in [76], for this value of ν only the term $m = 1$ in (7.37) is relevant, corresponding to the transfer of the $Q = e/3$ Laughlin quasiparticle. For generic filling fraction, many types of quasiparticles contribute as relevant charge transfer. So, the

[4] For simplicity, we choose ν^{-1} to be an odd integer to have only one branch of edge state.

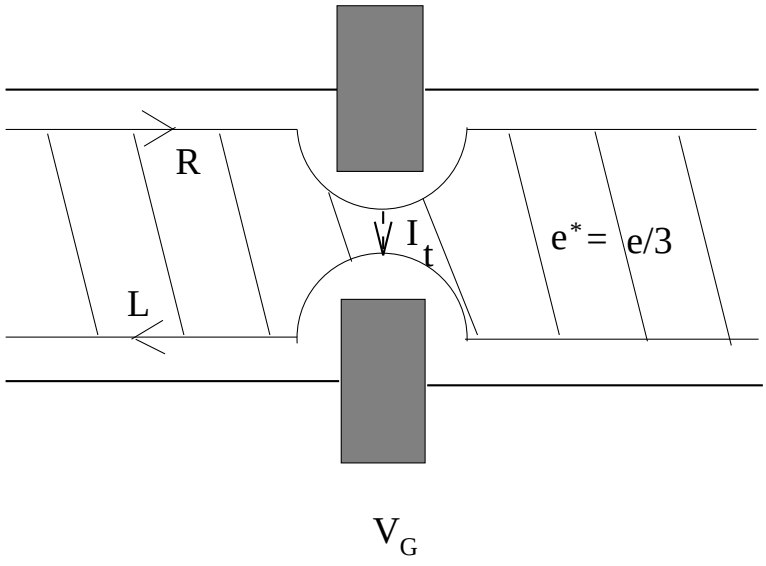

Figure 7.2: Quantum Hall bar with tunneling between the edge states.

model of interest has the following Hamiltonian (in a slightly different notations for further convinience):

$$H = \frac{1}{2}\int_{-\infty}^{\infty} dx[8\pi\nu\Pi^2 + \frac{1}{8\pi\nu}(\partial_x\varphi)^2] + \lambda\delta(x)\cos(\varphi_L - \varphi_R), \tag{7.38}$$

where the L and R components depend on x, t as $\varphi_L(x+t), \varphi_R(x-t)$. One can tune the tunneling amplitude λ by varying the gate voltage V_G. The Hall voltage V between the two edges of the QH liquid can be introduced in the model by adding the term $-e(Q_L - Q_R)V/2\hbar$ to the Hamiltonian. This substitution has an effect of placing the charge carriers injected into the left and right edges at different chemical potentials. As can be easily seen, by shifting the fields $\varphi_{L,R}$ we can bring the voltage dependence in the boundary term: $\cos(\varphi_L - \varphi_R + \omega t)$. We will deal with the $V = 0$ and $T = 0$ case only.

As discussed in [77], in order to map (7.38) to a boundary problem on a half-line, it is convenient to proceed in two steps. First introduce :

$$\begin{aligned} \phi^e(x+t) &= \frac{1}{\sqrt{2}}\left[\varphi_L(x,t) + \varphi_R(-x,t)\right] \\ \phi^o(x+t) &= \frac{1}{\sqrt{2}}\left[\varphi_L(x,t) - \varphi_R(-x,t)\right] \end{aligned} \tag{7.39}$$

which are both left moving. The even and odd charges are related to the charges of the original left- and right-moving edges by

$$\Delta Q = Q_L - Q_R = \sqrt{2}Q^o, \qquad Q_L + Q_R = \sqrt{2}Q^e. \tag{7.40}$$

The backscattering current is related to Q^o, whereas the total charge on both edges, Q^e, is conserved even in the presence of impurity. It is clear that the interaction term does not

affect the even field, which therefore remains free. As for the odd term, it can be mapped onto a boundary problem as follows. Define :

$$\begin{aligned} \phi^o_L(x,t) &= \sqrt{2}\phi^o(x+t), \quad x>0, \\ \phi^o_R(x,t) &= \sqrt{2}\phi^o(-x+t), \quad x>0. \end{aligned} \tag{7.41}$$

The odd hamiltonian then reads :

$$H = \frac{1}{2}\int_0^\infty [8\pi g(\Pi^o)^2 + \frac{1}{8\pi g}(\partial_x\phi^o)^2] + \lambda\delta(x)\cos\frac{1}{2}\phi^o, \tag{7.42}$$

and in the following we will write $\phi \equiv \phi^o$ and g instead of ν. Thus, for this problem, $\mathcal{B} = \lambda\cos\frac{1}{2}\phi(x=0,t)$.

The quantity of interest in this case is the AC conductance at vanishing temperature. A standard way of representing it is through the Kubo formula (7.3). It is usually easiest to calculate (7.3) using Matsubara formalism [91]. First, one defines current-current correlator in the Matrubara formalism :

$$\begin{aligned} \sigma_{\alpha\beta}(\omega) &= \frac{i}{\omega}\Pi_{\alpha\beta}(\omega) \\ \Pi_{\alpha\beta}(x,\tau) &= -\langle T_\tau j_\alpha(x,\tau) j_\beta(x,0)\rangle \\ \Pi_{\alpha\beta}(x,i\omega_M) &= \int_0^\beta d\tau e^{i\omega_M\tau}\Pi_{\alpha\beta}(x,\tau) \end{aligned} \tag{7.43}$$

Then, one substitutes $i\omega_M \to \omega + i\delta$ into $\Pi_{\alpha\beta}$ and sends $\delta \to 0$. Eventually, we get for the real part of conductivity tensor :

$$\mathrm{Re}\sigma_{\alpha\beta} = -\frac{1}{\omega}\mathrm{Im}\Pi_{\alpha\beta}(\omega). \tag{7.44}$$

The imaginary part of the spectral function in the latter formula can be expanded as follows:

$$-\mathrm{Im}\Pi_{\alpha\beta}(\omega) = \pi(1-e^{-\beta\omega})e^{\beta\Omega}\sum_{n,m} e^{-\beta E_n}\langle n|j_\alpha|m\rangle\langle m|j_\beta|n\rangle\delta(\omega+E_n-E_m). \tag{7.45}$$

In the limit of zero temperature, $\beta \to \infty$, the sum over n contains only one term – the ground state, so one has :

$$-\mathrm{Im}\Pi_{\alpha\beta}(\omega) = \pi\sum_m \langle 0|j_\alpha|m\rangle\langle m|j_\beta|0\rangle\delta(\omega-E_m). \tag{7.46}$$

In the above formulas $j_{\alpha,\beta} \equiv j$ is the physical current in the unfolded system, $j = \partial_t(\varphi_L - \varphi_R)$. Without impurity, the AC conductance of the Luttinger liquid is frequency independent, $G = g$. When adding the impurity, it becomes $G = \frac{g}{2} + \Delta G$. After some simple manipulations using the folding, one finds :

$$\begin{aligned} \Delta G(\omega_M) &= \frac{1}{8\pi\omega_M L^2}\int_0^L dxdx' \int_{-\infty}^\infty dy e^{i\omega_M y} \\ &\quad [\langle\partial_z\phi(x,y)\partial_{\bar{z}'}\phi(x',0)\rangle + \langle\partial_{\bar{z}}\phi(x,y)\partial_{z'}\phi(x',0)\rangle], \end{aligned} \tag{7.47}$$

where $z = x + iy$.

7.3 Boundary sinh-Gordon model

We discuss in this section one other boundary integrable model, the boundary sinh-Gordon model with $\mathcal{B} = M\cosh\phi(0)$. It is related to the boundary sine-Gordon model by the analytic continuation in the coupling constant g, but we do not make use of this fact here. Instead, we use it as a toy model for studying the correlation functions. It is fairly straighforward then how to tackle more complicated models. The advantage of the sinh-Gordon model is its technical simplicity: the particle spectrum of this model consists of only one scalar particle – a sinh-Gordon boson. The bulk sinh-Gordon model is well-studied in the literature.

7.3.1 The boundary reflection coefficient

We need to know the boundary reflection coefficient for sinh-Gordon model:

$$S_{ShG} = \int dxdt \left[\frac{1}{2}(\partial_\mu\phi)^2 - \frac{m^2}{g^2}\cosh(g\phi)\right] - \frac{M_B}{g^2}\int dt \cosh\left(\frac{g\phi(x=0)}{2}\right) \tag{7.48}$$

For this we use the fact that the action (7.48) is related to that of sine-Gordon model

$$S_{SG} = \int dxdt \left[\frac{1}{2}(\partial_\mu\phi)^2 + \frac{m^2}{\beta^2}\cos(\beta\phi)\right] + \frac{M_B}{\beta^2}\int dt \cos\left(\frac{\beta\phi(x=0)}{2}\right) \tag{7.49}$$

by the analytic continuation in coupling constant $g = i\beta$. Recall that the sinh-Gordon model has only one particle with neutral charge. A useful observation is that the bulk scattering matrix for this particle,

$$S(\theta, B) = \frac{\tanh\frac{1}{2}(\theta - i\frac{\pi B}{2})}{\tanh\frac{1}{2}(\theta + i\frac{\pi B}{2})}, \qquad B = \frac{2g^2}{8\pi + g^2} \tag{7.50}$$

can be obtained from the scattering matrix of the lightest breather of the sine-Gordon model [5] by the mentioned above analytic continuation in coupling constant. We assume that the same is true for the boundary reflection matrices. Partial confirmation of this can be found in [92], where this statement was proven in the semi-classical limit. So, we will use the result obtained in [41] for the reflection coefficient of the lightest breather in the boundary sine-Gordon model. The general solution of Ghoshal has two free boundary parameters [41]:

$$R_{mass}(\theta) = U(\eta, \theta)U(i\vartheta, \theta)R_0(\theta) \tag{7.51}$$

One can argue that for the boundary term of the form $M\cos(\beta\phi/2)$ one should set $\eta = 0$, the other parameter ϑ being related to M_B. So, the reflection coefficient for the boundary sinh-Gordon model with boundary interaction $M_B\cosh(g\phi/2)$ obtained from (7.51) by the analytic continuation reads:

$$R_{mass}(\theta) = \frac{\tanh\frac{1}{2}(\theta + \frac{\vartheta B}{2} - \frac{i\pi}{2})}{\tanh\frac{1}{2}(\theta - \frac{\vartheta B}{2} + \frac{i\pi}{2})} \frac{\cosh\frac{1}{2}(\theta + \frac{i\pi}{2})\cosh\frac{1}{2}(\theta - \frac{i\pi B}{4})\cosh\frac{1}{2}(\theta + \frac{i\pi B}{4} - \frac{i\pi}{2})}{\cosh\frac{1}{2}(\theta - \frac{i\pi}{2})\cosh\frac{1}{2}(\theta + \frac{i\pi B}{4})\cosh\frac{1}{2}(\theta - \frac{i\pi B}{4} + \frac{i\pi}{2})} \tag{7.52}$$

The massless limit of (7.52) is obtained by sending θ and ϑ to infinity. We have in the massles limit

$$R(\theta) = -\tanh\frac{1}{2}(\theta - \theta_B - \frac{i\pi}{2}) \tag{7.53}$$

where θ is now massless rapidity related to the momentum as in (7.64). This is as well the massless limit of the sine-Gordon reflection matrix. The boundary parameter θ_B is related to the boundary mass M_B in the way unknown to us. Note that in terms of momentum expression (7.53) looks like

$$R(p) = \frac{p - ip_B}{p + ip_B}$$

The definition of $K(\theta)$ in the massive case [1]

$$K_{mass}(\theta) = R_{mass}\left(\frac{i\pi}{2} - \theta\right)$$

becomes in the massless limit

$$K(\theta) = R\left(\frac{i\pi}{2} + \theta\right) \tag{7.54}$$

This follows from

$$\begin{aligned} K(\theta) &= \lim_{\theta_0\to\infty} K_{mass}(\theta_0 + \theta) = \lim_{\theta_0\to\infty} R_{mass}(\frac{i\pi}{2} - \theta_0 - \theta) = \\ &= \lim_{\theta_0\to\infty} S(2\theta)R_{mass}(\frac{i\pi}{2} + \theta_0 + \theta) = R(\frac{i\pi}{2} + \theta) \end{aligned}$$

where we used massive crossing-unitarity relation [1] above.

7.3.2 Sinh-Gordon form-factors

The form-facotrs for the massive Sinh-Gordon model were found in [93]. Let us list here some of them that we need. For the field ϕ itself, the form-factors between the ground state and n-particle states are:

$$\begin{aligned} F_{2n+1}(\beta_1, ..., \beta_{2n+1}) &= \langle 0|\phi(0)|\beta_1, ..., \beta_{2n+1}\rangle = \\ &= H_{2n+1}Q_{2n+1}(e^{\beta_1}, ..., e^{\beta_{2n+1}})\prod_{i<j}\frac{F_{min}(\beta_i - \beta_j)}{e^{\beta_i} + e^{\beta_j}} \end{aligned} \tag{7.55}$$

where H_n are normalization constants

$$H_{2n+1} = \frac{1}{\sqrt{2}}\left[\frac{4\sin\frac{\pi B}{2}}{F_{min}(i\pi, B)}\right]^n$$

Q_{2n+1} are symmetric polynomials in the variables $p_i = e^{\beta_i}$,

$$Q_1 = 1, \qquad Q_3 = \exp(\beta_1 + \beta_2 + \beta_3),$$

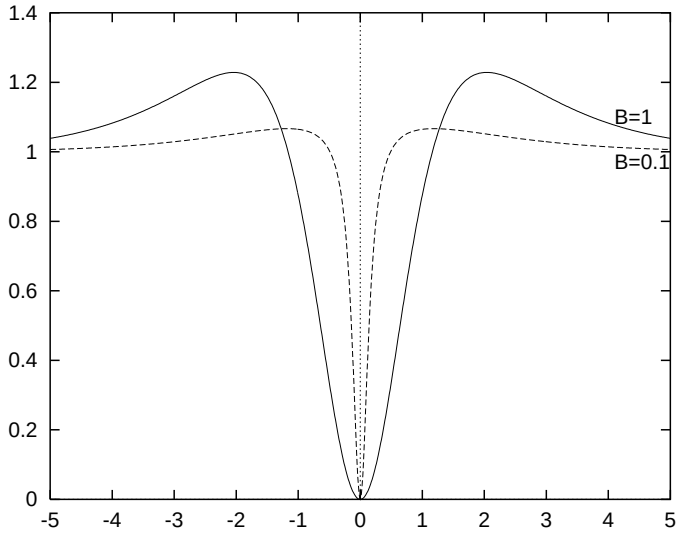

Figure 7.3: Plot of $|F_{min}(\beta, B)|^2$ for two different couplings.

$$Q_5 = \sigma_5^{(5)}(\sigma_2^{(5)}\sigma_3^{(5)} - c_1^2\sigma_5^{(5)}), \qquad c_1 = 2\cos\frac{\pi B}{2}$$

By parity, only form-factors with odd number of particles are allowed. We used the standard basis of elementary symmetric functions $\sigma_i^{(n)}$ in variables p_j in the formulas above, and

$$F_{min} = D\exp\left[8\int_0^\infty \frac{dx}{x}\frac{\sinh\frac{Bx}{4}\sinh(1-\frac{B}{2})\frac{x}{2}\sinh\frac{x}{2}}{\sinh^2 x}\sin^2\frac{x(i\pi-\beta)}{2\pi}\right]$$

$$D = \exp\left[-4\int_0^\infty \frac{dx}{x}\frac{\sinh\frac{Bx}{4}\sinh(1-\frac{B}{2})\frac{x}{2}\sinh\frac{x}{2}}{\sinh^2 x}\right]$$

The plot of F_{min} is given in Figure 7.3.

Since the sinh-Gordon form-factors (7.55) for the field operator ϕ are scalars with respect to the Lorentz transformations, they are invariant under the simultaneous shift of all the rapidities $\beta_i \to \beta_i + \beta_0$, where β_0 is some constant. Taking the massless limit implies making the substitution $\beta_i = \theta_i + \beta_0$ with $\beta_0 \to \infty$ for the right-moving particles, and making the substitution $\beta_i = -\theta_i - \beta_0$ for the left-moving particles. Here θ_i are the rapidities of massless particles. So, the massless form-factors derived by this procedure are:

$$\begin{aligned}
\langle 0|\phi_R(0)|\theta_1,...,\theta_{2n+1}\rangle_R &= N_0^{-1/2}H_{2n+1}Q_{2n+1}(e^{\theta_1},...,e^{\theta_{2n+1}})\prod_{i<j}\frac{F_{min}(\alpha_i-\alpha_j)}{e^{\theta_i}+e^{\theta_j}} \\
\langle 0|\phi_L(0)|\theta_1,...,\theta_{2n+1}\rangle_L &= N_0^{-1/2}H_{2n+1}Q_{2n+1}(e^{\theta_1},...,e^{\theta_{2n+1}})\prod_{i<j}\frac{\overline{F}_{min}(\theta_i-\theta_j)}{e^{\alpha_i}+e^{\alpha_j}}
\end{aligned}$$

where we used the fact that $F_{min}(-\theta) = \overline{F}_{min}(\theta)$. The normalization factor N_0 can be fixed by comparison with the massless free boson two-point correlation function (7.57). Inserting

into the vacuum two-point correlation function of free fields the full set of normalized intermediate states, and using the form-factors above, we obtain the contribution from each n-particle state in the form

$$\frac{1}{2N_0}\left(\frac{a_n}{z^2}+\frac{a_n}{\bar{z}^2}\right)$$

with some constant coefficients a_n,

$$a_n = \int \frac{d\theta_1 \dots d\theta_{2n+1}}{(2\pi)^n n!} \left(e^{\theta_1}+\dots+e^{\theta_n}\right)^2 e^{-(e^{\theta_1}+\dots+e^{\theta_n})} |F_n(\theta_1,\dots,\theta_n)|^2.$$

The normalization factor N_0 can then be obtained by summing the series $\sum a_n$ and requiring the result to be 1. One can compute a_n numerically and observe that they decrease very fast with n, and so can be truncated after a few terms. In particular, using one, three and five particle form-factors we found the approximate value of N_0:

$$N_0 = 1.005 \qquad B = 1.0$$

$$N_0 = 1.0002 \qquad B = 0.1$$

Note that the rate of convergence of the series $\sum a_n$ gives us a hint about the convergence of analogous series in the case with the interaction at the boundary (see below). The rapid convergence holds in the massive case as well, and has a physical explanation [94].

7.4 Calculation of correlation functions

In the massless limit the Green's function of current-current type on the half-line can be factorized as follows:

$$\begin{aligned} G(x_i,t_i,g,M_B) &= \langle 0|\partial_x\phi(x_1,t_1)\partial_x\phi(x_2,t_2)|0\rangle = \\ &= G_0(x_1-x_2,t_1-t_2,g)+G_1(x_1+x_2,t_1-t_2,g,M_B) \end{aligned} \qquad (7.56)$$

(this can be easily seen from the form-factor approach below). The first term G_0 does not depend on boundary coupling and is in fact equal to the current-current correlation function in the translationally invariant system on the line. It is the second term G_1 where the breakdown of translational invariance manifests itself explicitly and which carries all the dependence on the boundary coupling.

In general M_B is the only dimensional coupling that enters the Green's function. There are two values of M_B where the theory is scale-invariant. One of them, $M_B = 0$, corresponds to the free boundary condition $\partial_x\phi|_{x=0} = 0$, while another one, $M_B = \infty$, corresponds to the fixed boundary condition $\phi|_{x=0} = 0$. For these values of M_B the Green's functions are known exactly:

$$G|_{M_B=0} = G_0(x_1-x_2)+G_0(x_1+x_2)$$
$$G|_{M_B=\infty} = G_0(x_1-x_2)-G_0(x_1+x_2)$$

where

$$G_0(x,t) = \frac{1}{2\pi}\frac{x^2-t^2}{(x^2+t^2)^2} \tag{7.57}$$

Thus, the boundary mass M_B induces the boundary RG flow from short to large distances, which vary G_1 between $-G_0$ and $+G_0$.

We will work on the half-plane which geometry is shown in Figure 7.4. Based on the euclidean duality, there are two alternative ways to introduce the Hamiltonian picture [1]. First, one can take x to be euclidean time. In this case the equal time section is an infinite line x =const, $y \in (-\infty, \infty)$. Hence the associated space of states is the same as in the bulk theory. The boundary at $x = 0$ appears as the "time boundary," or initial condition at $x = 0$ which is described by the *boundary state* $|B\rangle$ (a particular state from the bulk Hilbert space). The correlators are expressed as

$$\langle O_1(x_1,y_1)...O_N(x_N,y_N)\rangle = \frac{\langle B|\mathcal{T}_x[O_1(x_1,y_1)...O_N(x_N,y_N)]|0\rangle}{\langle 0|B\rangle}, \tag{7.58}$$

where $O_i(x,y)$ are the Heisenberg local field operators

$$O_i(x,y) = e^{-xH}O_i(0,y)e^{xH}, \tag{7.59}$$

and $\mathcal{T}_x$ means x-ordering.

Alternatively, one can take the direction along the boundary to be the time. In this case boundary appears as a boundary in space, and the Hilbert space of states is associated with the semi-infinite line y =const, $x \in [0,\infty)$. The correlation functions of any local fields $O_i(x,y)$ can be computed in this picture as the matrix elements

$$\langle O_1(x_1,y_1)...O_N(x_N,y_N)\rangle = \frac{\langle 0||\mathcal{T}_y[O_1(x_1,y_1)...O_N(x_N,y_N)]||0\rangle}{\langle 0||0\rangle}, \tag{7.60}$$

where $||0\rangle$ is the ground state of the boundary Hamiltonian, $O_i(x,y)$ are understood as the corresponding Heisenberg operators

$$O_i(x,y) = e^{-yH_B}O_i(x,0)e^{yH_B}, \tag{7.61}$$

and $\mathcal{T}_y$ means y-ordering.

The equality of expressions (7.58) and (7.60) can be understood as a definition of the boundary state, which is chosen such as to provide the equivalence of correlators.

7.4.1 Boundary-in-time representation

First suppose that $x > 0$ is imaginary time coordinate and y is space coordinate, $z = x + iy$. It means that time translation is performed by the operator $T = \exp(xH)$, with H being the bulk Hamiltonian.

We wish to compute the following matrix element:

$$\begin{aligned}\langle B|\partial_x\phi(x_1,y_1)\partial_x\phi(x_2,y_2)|0\rangle &= \langle B|\partial_z\phi_R(z_1)\partial_{\bar{z}}\phi_L(\bar{z}_2)|0\rangle \\ &+ \langle B|\partial_{\bar{z}}\phi_L(\bar{z}_1)\partial_z\phi_R(z_2)|0\rangle\end{aligned} \tag{7.62}$$

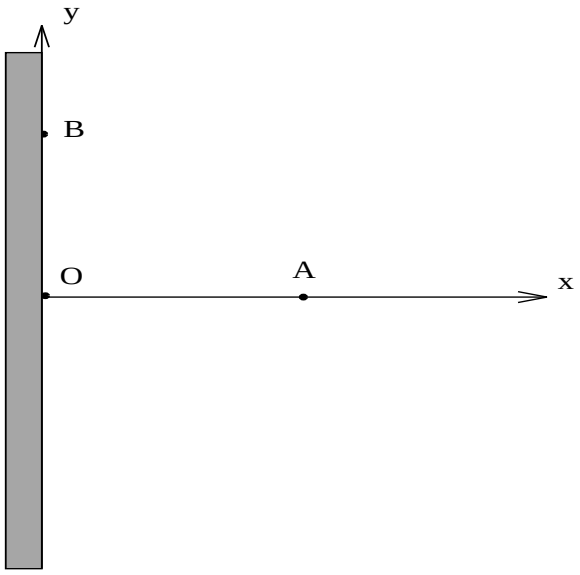

Figure 7.4: The geometry of space-time.

where ϕ is a massless free field $\phi = \phi_L(\bar{z}) + \phi_R(z)$ and $|B\rangle$ denotes the massless boundary state of the sinh-Gordon model [1]:

$$|B\rangle = |0\rangle + \sum_{N=1}^{\infty} \int_{-\infty<\theta_1<\ldots<\theta_N<\infty} \left[\prod_{i=1}^{N} \frac{d\theta_i}{2\pi} K(\theta_i)\right] A_L(\theta_N)...A_L(\theta_1)A_R(\theta_1)...A_R(\theta_N)|0\rangle \quad (7.63)$$

Because $|B\rangle$ has chirality zero, products of the fields of the same chirality do not contribute to the right hand side of eq. (7.62). Parameter θ is a massless rapidity in terms of which the energy and momentum of particles read: [5]

$$E_L = -P_L = \mu e^{\theta}, \qquad E_R = P_R = \mu e^{\theta}, \quad (7.64)$$

and $A_{L,R}(\theta)$ are the left and right moving particle creation operators, the particles in our case being the massless sinh-Gordon bosons. The fact that the sinh-Gordon particle bounces elastically off the boundary allows us to have a much simpler expression for the boundary state (7.63) than that for the plane waves. Substituting the boundary state (7.63) into (7.62) and using the fact that left (right) moving field acts only on left (right) moving particles, we obtain the following expansion in terms of the form-factors:

$$\begin{aligned} &\langle B|\partial_x\phi(x_1,y_1)\partial_x\phi(x_2,y_2)|0\rangle = \langle 0|\partial_x\phi(x_1,y_1)\partial_x\phi(x_2,y_2)|0\rangle + \\ + &\sum_{N=1}^{\infty} \mu^2 \int_{-\infty<\theta_1<\ldots<\theta_N<\infty} \left[\prod_{i=1}^{N} \frac{d\theta_i}{2\pi} K(\theta_i)\right] \langle 0|\phi_L(0)|\theta_1,...,\theta_N\rangle_L \langle 0|\phi_R(0)|\theta_1,...,\theta_N\rangle_R \\ \times &\left(\sum_{i=1}^{N} e^{\theta_i}\right)^2 \left(e^{-(x_1+x_2+iy_1-iy_2)\mu\left(\sum_{i=1}^{N} e_i^{\theta}\right)} + \text{c.c.}\right) \end{aligned}$$

[5] Here μ is an arbitrary mass scale.

$$\equiv \quad G_0(z_1 - z_2) - \sum_{n=0}^{\infty} I_{2n+1} \tag{7.65}$$

The product of two massless form-factors for the left-moving and the right-moving field above is in fact equal to $|F_N(\theta_1, ..., \theta_N)|^2$, the modulo square of the bulk massive form-factor (with the only difference that θ is now the *massless* rapidity).

The first term in (7.65) is G_0, the Green's function of the free massless fields on the plane:

$$G_0(z, \bar{z}) = \frac{1}{4\pi}\left(\frac{1}{z^2} + \frac{1}{\bar{z}^2}\right)$$

The explicit expressions for the first few terms I_{2n+1} are:

$$I_1 = \frac{\mu^2}{2N_0}\int_{-\infty}^{+\infty}\frac{d\theta}{2\pi}e^{2\theta}\left(e^{-(x_1+x_2-iy_1+iy_2)\mu e^{\theta}} + \text{c.c.}\right)\tanh\frac{\theta-\theta_B}{2} \tag{7.66}$$

Changing variables, $p = \exp(\theta)$, it can be rewritten as

$$I_1 = \frac{\mu^2}{4\pi N_0}\int_0^{\infty} pdp\frac{p-T_B}{p+T_B}\left(e^{-(z_2+\bar{z}_1)\mu p} + c.c\right), \qquad T_B \equiv e^{\theta_B} \tag{7.67}$$

and

$$I_3 = \frac{\mu^2 H_3^2}{3!N_0} \qquad \int_{-\infty}^{\infty}\prod_{i=1}^{3}\frac{d\theta_i}{2\pi}\tanh\frac{\theta_i-\theta_B}{2} \tag{7.68}$$
$$\times \quad \prod_{i<j}^{3}\frac{|F_{min}(\theta_i-\theta_j)|^2}{2(1+\cosh(\theta_i-\theta_j))}\left(\sum_{i=1}^{3}e^{\theta_i}\right)^2\left(e^{-(z_2+\bar{z}_1)\mu\left(\sum_{i=1}^{3}e^{\theta_i}\right)} + c.c\right)$$

Plot of these two contributions to the two-point correlation function for the points OA ($x_1 = y_1 = y_2 = 0$) is shown in figures 7.5 and 7.6, and few values of I_5 are given in Table 7.1. It turns out that the series $\sum I_n$ converge fast because each term I_n is by the factor of hundred smaller than I_{n-2}. We checked it up to $n = 5$. Each integral I_n converges for any finite value of $(x_1 + x_2)$, but is divergent for $x_1 = x_2 = 0$. Therefore, we need to do an additional work to find the correlation function between two points on the boundary, OB (Fig. 7.4).

Let us find equivalent expressions for the integrals I_n which would be finite for $x_1 = x_2 = 0$. For this, we note that the contour of integration can be rotated to go from 0 to $i\infty$ in the complex p-plane, eq. (7.67). This rotation is equivalent to the shift of countour of integration in θ-plane up by $i\pi/2$, with having the contour to pass below the poles of $K(\theta)$ (figure 7.7). For the complex conjugated term one has to rotate countour clockwise in p-plane (shift by $-i\pi/2$ in θ-plane). So, we obtain

$$I_n = -\mu^2\int_{-\infty}^{\infty}\left[\prod_{i=1}^{n}\frac{d\theta_i}{2\pi}R(\theta_i)\right]\left(\sum_{i=1}^{n}e^{\theta_i}\right)^2|F_n(\theta_1, ..., \theta_n)|^2 e^{-(y_1-y_2-ix_1-ix_2)\mu\left(\sum_{i=1}^{n}e^{\theta_i}\right)} + c.c \tag{7.69}$$

where we used eq. (7.54) and $y_1 - y_2 > 0$ is assumed.

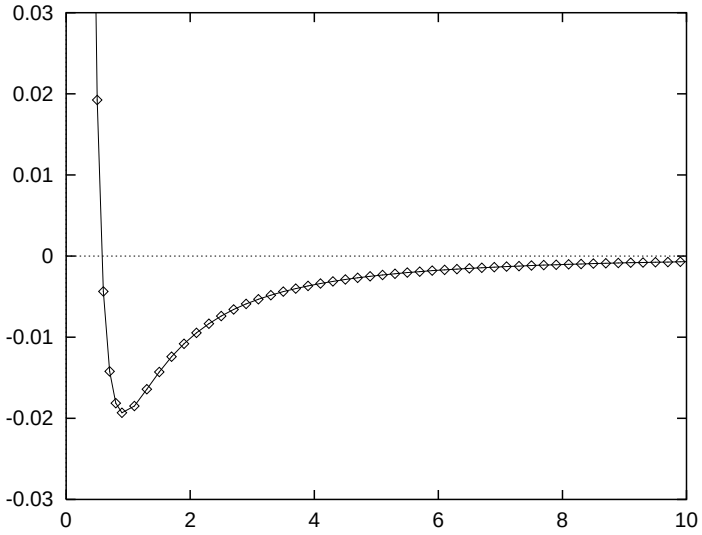

Figure 7.5: Plot of the one-particle contribution to correlator between two points $(0, 0)$ and $(x, 0)$ as a function of x.

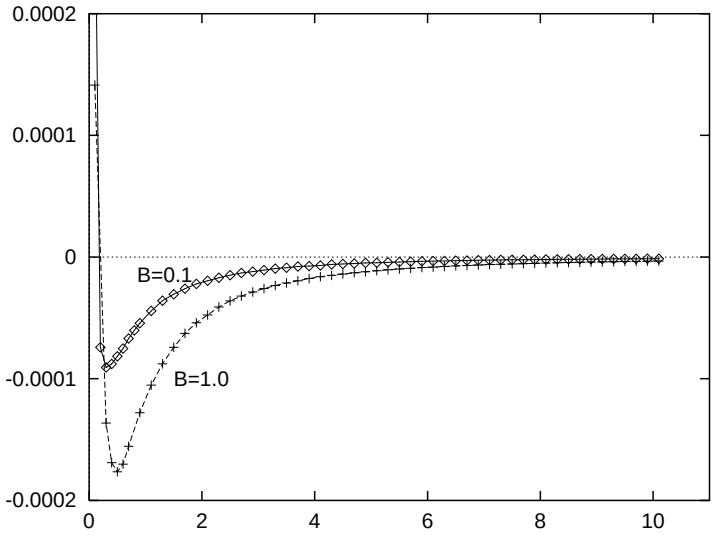

Figure 7.6: Plot of the three-particle contribution to correlator for two different couplings; the curve for B=0.1 is shown scaled by the overall factor 10 compared to the true curve.

x	I_5
1.1	$-4.65436256 \cdot 10^{-6}$
2.1	$-2.02534138 \cdot 10^{-6}$
3.1	$-1.11571005 \cdot 10^{-6}$
4.1	$-7.03902032 \cdot 10^{-7}$
5.1	$-4.81526684 \cdot 10^{-7}$

Table 7.1: Five-particle contribution for $B = 1$.

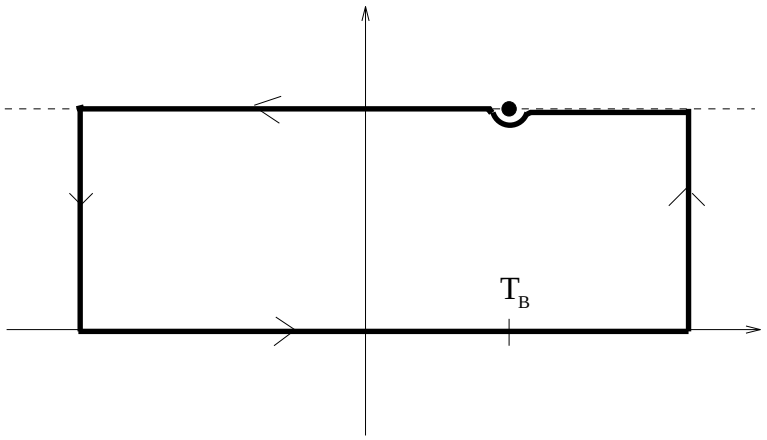

Figure 7.7: The contour of integration in the complex θ plane. The vertical intervals of the contour are assumed to be sent to infinity.

Notice that this expression could be also obtained if we had started from the dual picture where time goes along the boundary and space is a half-line and inserted a full basis of asymptotic states of the form $|\theta_1, ..., \theta_n\rangle_L + R(\theta_1)...R(\theta_n)|\theta_n, ..., \theta_1\rangle_R$ between the fields in the correlator. This dual picture is to be discussed in detail in the next section.

For the points OB in Fig. 7.4 ($x_1 = x_2 = 0, y_2 = 0$) expression (7.69) reads:

$$I_n = -\mu^2 \int_{-\infty}^{\infty} \frac{d\theta_1 ... d\theta_n}{(2\pi)^n} \left[\prod_{i=1}^{n} R(\theta_i) + \prod_{i=1}^{n} \bar{R}(\theta_i) \right] \cdot \left(\sum_{i=1}^{n} e^{\theta_i} \right)^2 |F_n(\theta_1, ..., \theta_n)|^2 e^{-y_1 \mu (\sum_{i=1}^{n} e^{\theta_i})} \tag{7.70}$$

E.g. for $n = 1$ we have

$$I_1 = -\frac{\mu^2}{2\pi N_0} \int_{-\infty}^{\infty} d\theta e^{2\theta - y_1 \mu e^{\theta}} \tanh(\theta - \theta_B).$$

7.4.2 Boundary-in-space representation

One can in principle compute the same correlation correlation functions adopting a different point of view on the space-time geometry (figure 7.4). In euclidean field theory the role of

space and time can be interchanged. Now, in the alternative representation, $x > 0$ is a space coordinate, and y is an imaginary time coordinate. The theory is invariant under the global time shift, which is performed by the operator $T = \exp(yH)$.

However, the theory, being defined on a semi-infinite line, has rather intricate structure of the ground state, and the form-factors are not known to us *a priori*. In particular, the ground state is not invariant under the space translations. One can speculate [1] that the ground state for a theory on a half-line $||0\rangle$ can be obtained from the bulk vacuum $|0\rangle$ by the action of a "boundary creation operator" $\hat{B}$: $||0\rangle = \hat{B}|0\rangle$. Speaking loosely, boundary is an infinitely heavy inpenetrable particle sitting at the origin. The asymptotic particle states are not pure L or R moving, but rather the superpositions of those. E.g., one-particle states are

$$||\theta\rangle = |\theta\rangle_L + R(\theta)|\theta\rangle_R, \qquad \theta > 0 \tag{7.71}$$

To find the correlation function $\langle 0||\partial_x\phi(x_1, y_1)\partial_x\phi(x_2, y_2)||0\rangle$ we conjecture that the following equality holds:

$$\langle 0||\partial_x\phi(x_1, y_1)\partial_x\phi(x_2, y_2)||0\rangle = \sum_n \frac{\langle 0|\partial_x\phi(x_1, y_1)||n\rangle\langle n||\partial_x\phi(x_2, y_2)|0\rangle}{\langle n||n\rangle}, \tag{7.72}$$

with the particular ansatz for the intermediate states $||n\rangle$:

$$||\theta_1, \ldots, \theta_n\rangle = |\theta_1, \ldots, \theta_n\rangle_L + R(\theta_1)\cdots R(\theta_n)|\theta_n, \ldots, \theta_1\rangle_R \tag{7.73}$$

(in the *bra* states, $\langle n||$, the factors $R(\theta)$ become complex conjugated). Substituting (7.73) into (7.72), combining the complex conjugated terms in the series and using the `bulk` form-factors, we indeed get the correct expression for the correlator (7.69). In the course of this calculation one has to use the unitarity of the reflection matrix, $\overline{R}(\theta)R(\theta) = 1$, as well as the property that the vacuum average of the quantum field ϕ vanishes, $\langle\phi\rangle = 0$.

Note that in principle it is possible to formulate the set of general equations for the form-factors of integrable models on a half-line, $\langle 0||\phi(0)|n\rangle$, in analogy with the equations of [72]. E.g., it is obvious that the following should hold:

$$\langle 0||\phi(0)|\theta\rangle = R(\theta)\langle 0||\phi(0)|-\theta\rangle.$$

7.4.3 The renormalization group analysis

Let us study the behavior of integrals I_n under the change of scale $z \to e^\lambda z$. Such a rescaling can be compensated by the change $\theta_B \to \theta_B + \lambda$ and by the overall normalization factor $Z(\lambda) = e^{2\lambda}$ to have the integrals (and hence the correlator) unchanged. Repeating this RG transformation, we will flow to the UV or IR fixed points $\theta_B = \pm\infty$ (depending whether $\lambda > 0$ or $\lambda < 0$). For such values of θ_B the hyperbolic tangent factors in the integrands are equal to ± 1, and the integrals are proportional to $\pm 1/z^2$. On the plots Figure 7.5 and Figure 7.6 one can see two regimes: $\mu z \ll 1$ and $\mu z \gg 1$ when the functions behave as $\pm 1/z^2$. The non-trivial behaviour at the intermediate scales is due to the presence of boundary, which introduces a scale μe^{θ_B} corresponding approximately to the position of the deep. Shifting θ_B corresponds to the motion of the deep to the right or left on Figures 7.5 and 7.6, untill it will go away completely and one of the regimes will dominate over all scales.

7.4.4 The use of Kubo's formula

To use the Kubo formula (7.3), we adopt the first point of view where the boundary is taken into account through the introduction of the boundary state $|B\rangle$. Write :

$$\langle \partial_{\bar{z}}\phi(x,y)\partial_{z'}\phi(x',0)\rangle = \int_0^\infty dE\mathcal{G}(E)\exp\left[-E(x+x')-iEy\right]. \tag{7.74}$$

One obtains $\mathcal{G}(E)$ simply by fixing the energy to a particular value in (7.65). When this is done, the remaining integrations occur on a finite domain for each of the individual particle energies since $\sum_{i=1}^{2n+1} e^{\theta_i} = E$, and there is no problem of convergence anymore. One then gets :

$$\begin{aligned}\mathcal{G}(E) &= \sum_{n=0}^{\infty}\int_{-\infty}^{\ln E}\frac{d\theta_1\ldots d\theta_{2n}}{(2\pi)^{2n+1}(2n+1)!}\frac{E^2}{E-e^{\theta_1}-\ldots-e^{\theta_{2n}}}\\ &\quad K(\theta_1)\ldots K(\theta_{2n})K\left(\ln\left(E-e^{\theta_1}-\ldots-e^{\theta_{2n}}\right)\right)\\ &\quad \left|F_{2n+1}\left(\theta_1\ldots\theta_{2n},\ln\left(E-e^{\theta_1}-\ldots-e^{\theta_{2n}}\right)\right)\right|^2,\end{aligned} \tag{7.75}$$

with the constraint $\sum_{i=1}^{2n} e^{\theta_i} \leq E$. The denominator might suggest some possible divergences; it is important however to realize that it vanishes if and only if the particle with rapidty θ_{2n+1} has vanishing energy, in which case the form factor vanishes too. By using the dual picture, one writes :

$$\langle \partial_{\bar{z}}\phi(x,y)\partial_{z'}\phi(x',y') >= \int_0^\infty dE\mathcal{F}(E)\exp\left[-iE(x+x')-E(y-y')\right], \tag{7.76}$$

The two expressions are in correspondence by the simple analytic continuation :

$$\mathcal{G}(E) = i\mathcal{F}(iE). \tag{7.77}$$

Eq. (7.74) is the only correlation contributing to ΔG for positive Matsubara frequencies, and

$$\Delta G(\omega_M) = \frac{\mathcal{G}(\omega_M)}{4\ \omega_M}. \tag{7.78}$$

Here we have used the fact that $\omega_M L \ll 1$, i.e. the system, although large, is much smaller than the wavelength associated with the (modulus of the) AC frequency. To go to real frequencies, we can simply substitute $\omega_M \to -i\omega$ in the K matrices in the integrals (7.65):

$$\Delta G(\omega) = \frac{1}{4\omega}\mathrm{Im}\mathcal{G}(-i\omega) = \frac{1}{4\omega}\mathrm{Re}\mathcal{F}(\omega). \tag{7.79}$$

7.4.5 The numerical work

We computed the integrals for 3 and 5 particle contributions to correlation functions numerically using Monte-Carlo simulations. The domain of integration was the hypercube with

the length of the side equal 40. Because of exponential decay of the integrand, the contribution of the region outside the box is small withing our accuracy. Since the integrals diverge as the imaginary time approaches zero, we found it technically more difficult to find the reliable results for $x < 0.1$. We took $5 \cdot 10^7$ points to evaluate the integrand inside the box. We checked that the Monte-Carlo result is stable by increasing the number of points and estimated the relative error in 3 and 5 dimensional integrals to be about 1%, while the 1-dimensional integrals were evaluated with 0.001% accuracy. The higher-particle contributions can be computed in the same manner, but require considerable amount of computer time. Because we expect them to be very small, we found their evaluation unnecessary for the purpose of the present research.

7.5 Boundary sine-Gordon correlators

We wish to apply now the formalism developed in the previous section to the massless boundary sine-Gordon model, with $\mathcal{B} = M \cos\phi(0)$. The basic procedures and formulas of the previous section apply directly to the present section, the difference appearing in a few technicalities.

7.5.1 Conductance at $g = 1/3$

We are interested in the value of coupling constant $\beta^2 = 8\pi/3$ in (7.49), which corresponds to the quantum Hall liquid regime $\nu = 1/3$. The particle spectrum in the sine-Gordon model depends on the coupling constant. At $g = 1/3$, we have three particles in the spectrum: a soliton, antisoliton and their bound state – breather. The breather is completely analogous to the scalar particle of the sinh-Gordon model, while the other two particles introduce technical differences.

Let us describe what these differences are. In the boundary state, (7.63), one has to introduce soliton and antisoliton creation operators $A^{(+)}$ and $A^{(-)}$, and their boundary reflection matrices:

$$|B\rangle = |0\rangle + \sum_{N=1}^{\infty} \int_{-\infty<\theta_1<\ldots<\theta_N<\infty} K^{a_1 b_1}(\theta_1)\ldots K^{a_N b_N}(\theta_N) \\ A_L^{a_N}(\theta_N)\ldots A_L^{a_1}(\theta_1) A_R^{b_1}(\theta_1)\ldots A_R^{b_N}(\theta_N)|0\rangle \tag{7.80}$$

(the summation over the particle indices a, b is assumed)

$$K^{ab}(\theta) = R_b^a\left(\frac{i\pi}{2} + \theta\right)$$

The breather reflection coefficient is still given by formula (7.53), while for the soliton and antisoliton massless reflection matrices are

$$\begin{aligned} R_{\mp}^{\pm}(\theta) &= e^{\sqrt{8\pi/3}} R(\theta), \\ R_{\pm}^{\pm}(\theta) &= e^{-\sqrt{8\pi/3}} R(\theta), \end{aligned} \tag{7.81}$$

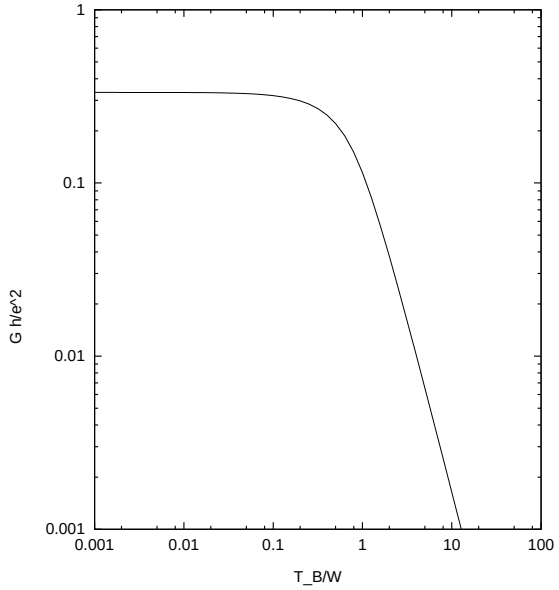

Figure 7.8: Frequency dependent conductance at $T = 0$.

$$R(\theta) = \frac{1}{2\cosh(\theta - \frac{i\pi}{4})} \frac{\Gamma(\frac{3}{8} - \frac{i\theta}{2\pi})\Gamma(\frac{5}{8} + \frac{i\theta}{2\pi})}{\Gamma(\frac{5}{8} - \frac{i\theta}{2\pi})\Gamma(\frac{3}{8} + \frac{i\theta}{2\pi})} \tag{7.82}$$

(for the arbitrary β expressions we refer to [31]). Correspondingly, there are more terms in the series expansion of the correlators since there are more intermediate particles. The leading contribution, I_1, is still the one-particle contribution of the breather. The next-after-leading contribution comes from two particles in the intermediate state, soliton and antisoliton. Its magnitude is approximately 20% of the value of I_1. Note that soliton and antisoliton can appear only in pairs since the total topological charge of the intermediate states should vanish in order for it to contribute to the correlator. The next terms come from the three-particle states of the breather with soliton and antisoliton, and the three breathers. Their magnitude is 1% of the value of the leading contribution. The form-factors for different particles in the sine-Gordon model have been originally obtained by Smirnov in the massive case [72], and their massless limit is given in [70]. These expressions are much more cumbersome than that of sinh-Gordon model.

The leading contribution to the conductance computed along the lines of the discussion above is given by

$$\Delta G(\omega)^{(1)} = -\mu^2 \frac{\pi d^2}{8} \mathrm{Re} \tanh \left[\frac{1}{2} \log \left(\frac{\omega}{\sqrt{2} T_B} \right) - \frac{i\pi}{4} \right] \tag{7.83}$$

where $\mu \approx 3.14$ and $d \approx 0.1414$. The contribution from the soliton-antisoliton state can be found in [70]. We plot the full function $G(\omega)$ in figure 7.8.

7.5.2 The free point, $g = 1/2$

In the free case $\beta^2 = 4\pi$ one has simply:

$$\begin{aligned} R^{\pm}_{\mp}(\theta) &= P(\theta) = \frac{e^{\theta}}{e^{\theta}+i}, \\ R^{\pm}_{\pm}(\theta) &= Q(\theta) = \frac{i}{e^{\theta}+i}. \end{aligned} \tag{7.84}$$

As for the form-factors, only the soliton-antisoliton form-factor is non-zero,

$$f(\theta_1, \theta_2) = 2\pi e^{(\theta_1+\theta_2)/2}.$$

Thus, we find for the conductance

$$G(\omega) = \frac{1}{2}\left[1 - \frac{T_B}{\omega}\tan^{-1}(\omega/T_B)\right] \tag{7.85}$$

This is in agreement with the solution of [76] and also [95].

Chapter 8

Conclusion

This review is concerned with the study of 2D integrable models with boundary. In chapters 1 through 6 the formalism is developed for dealing with such models and particular examples are discussed. It involves a construction of solutions to the classical equations of motion for a model on a half-line, solution of the quantum XXZ chain in a boundary magnetic field, investigation of the boundary bound states (a phenomenon caused by the presence of boundaries), generalization of the Destri-deVega technique, which allows to find the exact ground state scaling energy, to the theories with boundaries. All this work was carried out mostly for the quantum sine-Gordon/Thirring model, which provides a good basis for theoretical investigations withing the framework of quantum integrable models.

There is a room for the further development of the above formalism. For example, we often have chosen the boundary conditions to be a specific, Dirichlet boundary condition. Consideration of more general boundary conditions will most certainly be associated with the increased complexity, while it is not clear to us whether the outcome will prize us with a new interesting physics, or at least whether the most general boundary condition has any vital applications. An interesting direction of research is associated with the technique of the thermodynamic Bethe ansatz and the corresponding finite-difference equations [96, 97]. Another interesting direction has to deal with the non-integrable deformations of integrable models [98].

In chapter 7 we described some of the applications of boundary integrable models to condensed matter physics. In particular, we developed a technique to compute exactly time dependent properties of the Kondo problem and/or two-state problem of dissipative quantum mechanics, as well as the conductance of the one-dimesional wires with a tunneling through impurity. These problems have potential experimental applications and a room for further theoretical work. The latter includes the computation of the voltage and temperature dependent behavior of the conductance, quantum noise, as well as studying of the Coulomb blocade phenomenon.

Bibliography

[1] Ghoshal S. and Zamolodchikov A.B., Int. J. Mod. Phys. A9 (1994) 3841.

[2] Fendley P and Saleur H, cond-mat/9403095.

[3] Affleck I and Sagi J, Nucl. Phys. B417 (1994) 374.

[4] Ludwig A, in "Recent Progress in Statistical Mechanics and Quantum Field Theory" World Scientific 1995.

[5] Zamolodchikov A.B. and Zamolodchikov Al.B., Ann.Phys. 120 (1980) 253.

[6] Cardy J, Nucl. Phys. B240(1984) 514; *ibid* B324 (1989) 581.

[7] Cardy J and Lewellen D, Phys. lett. B259 (1991) 274.

[8] Zamolodchikov Al.B., Nucl. Phys. B342 (1990) 695.

[9] Thacker H.B., Rev. Mod. Phys. 53 (1981) 253.

[10] Andrei N., Furuya K. and Lowenstein J., Rev. Mod. Phys. 55 (1983) 331.

[11] Bergknoff H. and Thacker H.B., Phys. Rev. D19 (1979) 3666.

[12] Lüscher M., Nucl. Phys. B117 (1976) 475.

[13] Destri C. and deVega H.J., Nucl. Phys. B290 (1987) 363.

[14] Faddeev L.D. and Takhtajan, Phys. Lett. A85 (1981) 375.

[15] Yang C.N. and Yang C.P., J. Math. Phys. 10 (1969) 1115.

[16] Takahashi and Suzuki, Progr. Theor. Phys. 48 (1972) No 6B.

[17] Japaridze G.I., Nersesyan A.A. and Wiegmann P.B., Nucl. Phys. B230 (1984) 511.

[18] Korepin V.E., Theor. Math. Phys. 41 (1979) 953.

[19] Saleur H. and Skorik S., Phys. Lett. B336 (1994) 205.

[20] Gaudin M., "La Fonction d'Onde de Bethe", Paris:Masson.

[21] Kirillov A.N. and Liskova N.A., hep-th/9403107.

[22] Jackiw R. and Woo G., Phys. Rev. D12 (1975) 1643.

[23] Saleur H., Skorik S. and Warner N., Nucl. Phys. B441 (1995) 421.

[24] Sklyanin E.K., Func. Anal. Appl. 21 (1987) 164.

[25] Bikbaev R.F. and Tarasov V.O., Algebra and Analysis 3 (1991) 78.

[26] Habibullin I.T., Theor. Math. Phys. 86 (1991) 28.

[27] Tarasov V.O., Inverse Problems 7 (1991) 435.

[28] Ablowitz M. and Segur H., "Solitons and the inverse scattering transform", SIAM Studies in Appl. Math. 1981.

[29] Deleonardis R.M., Trullinger S.E. and Wallis R.F., J. Appl. Phys. 51 (1980) 1211-1226.

[30] Habibullin I.T., Matem. Zametki 49 (1991) 418.

[31] Fendley P, Saleur H. and Warner N.P., Nucl. Phys. B430 (1994) 577.

[32] Kapustin A. and Skorik S., Phys. Lett. A196 (1994) 47.

[33] Olshanetsky M.A. and Perelomov A.M., Phys. Rep. 71 (1981) 313; *ibid* 94 (1983) 313.

[34] Inozemtsev V.I. and Meshcheryakov D.V., Lett. Math. Phys. 9 (1985) 13.

[35] J.F. van Diejen, J. Math. Phys. 35 (1994) 2983.

[36] Korepin V., Theor. Math. Phys. 34 (1978) 1.

[37] Pöschl G. and Teller E., Z. Physik 83 (1933) 143.

[38] Kulish P., "Factorization of Scattering Characteristics and Integrals of Motion." In: Nonlinear Evolution Equations Solvable by the Spectral Transform, F.Calogero (ed.), Research Notes in Mathematics, Pitman Publishing, London, 1978.

[39] Fendley P. and Saleur H., Nucl. Phys. B428 (1994) 681.

[40] Skorik S. and Saleur H., J.Phys. A28 (1995) 6605.

[41] Ghoshal S., Int. J. Mod. Phys. A9 (1994) 4801.

[42] M. Grisaru, L. Mezincescu, R. Nepomechie, J. Phys. A28 (1995) 1027.

[43] R.Dashen, B.Hasslacher, A.Neveu, Phys.Rev.D11 (1975) 3424.

[44] Sklyanin E.K., J.Phys. A21 (1988) 2375.

[45] Alcaraz F, Barber M, Batchelor M, Baxter R and Quispel G, J. Phys. A20 (1987) 6397.

[46] Reshetikhin N and Saleur H, Nucl. Phys. B419 (1994) 507.

[47] Destri C and de Vega H, J.Phys. A22 (1989) 1329.

[48] Ameduri M, Konik R and LeClair A, Phys. Lett. B354 (1995) 376.

[49] Jimbo M, Kedem R, Tojima T, Konno H and Miwa T, Nucl. Phys. B441 (1995) 437.

[50] Babelon O, de Vega H and Viallet C, Nucl. Phys. B220 (1983) 13.

[51] Destri C and Lowenstein J, Nucl. Phys. B205 (1982) 369.

[52] Kirillov A. N. and Reshetikhin N, J.Phys. A20(1987) 1565, 1587.

[53] McCoy B and Wu T, "The two dimensional Ising model," Cambridge, MA: Harvard University Press, 1973.

[54] Destri C and de Vega H, Nucl. Phys. B438 (1995) 413.

[55] Pasquier V and Saleur H, Nucl. Phys. B330 (1990) 523.

[56] LeClair A, Mussardo G, Saleur H and Skorik S, Nucl.Phys. B453 (1995) 581.

[57] Blöte H, Cardy J and Nightingale M, Phys. Rev. Lett. 56 (1986) 742.

[58] Belavin A, Polyakov A and Zamolodchikov A, Nucl. Phys. B241 (1984) 333.

[59] Affleck I and Ludwig A, Phys. Rev. Lett. 67 (1991) 161.

[60] Bauer M and Saleur H, Nucl. Phys. B320 (1989) 591.

[61] A. LeClair and C. Vafa, Nucl. Phys. B401 (1993) 413.

[62] Reshetikhin N and Smirnov F, Comm. Math. Phys. 131 (1990) 157.

[63] LeClair A., Phys. Lett. 230B (1989) 103.

[64] Bernard D. and LeClair A., Nucl. Phys. B340 (1990) 409.

[65] Kapustin A. and Skorik S., to be published in J.Phys. A, hep-th/9506067.

[66] M. Gaudin, Phys. Rev. Lett. 26 (1971) 1301.

[67] M.T. Batchelor, C.J. Hamer, J. Phys. A23 (1990) 761.

[68] C.N. Yang, C.P. Yang, Phys.Rev. 150 (1966) 321, 327.

[69] Fendley P and Saleur S, Lectures given at Summer School in High Energy Physics and Cosmology, Trieste, Italy (1993). Published in Trieste HEP Cosmol. 1993:301-332; hep-th/9310058.

[70] Lesage F, Saleur H and Skorik S, cond-mat/9512087, 9603043.

[71] Mussardo G, Talk given at 2nd TIFR International Colloquium on Modern Quantum Field Theory, Bambay (India) 1994; hep-th/9405128.

[72] Smirnov F, "Form factors in completely integrable models of quantum field theory", World Scientific 1992.

[73] Delfino G, Mussardo G and Simonetti P, Phys. Rev. D51 (1995) 6620.

[74] Konik R, LeClair A and Mussardo G, hep-th/9508099.

[75] Kubo R, Canadian Journal of Physics 34 (1956) 1274.

[76] C.L. Kane, M.P.A. Fisher, Phys. Rev. B46 (1992) 15233.

[77] Fendley P, Ludwig A and Saleur H, Phys. Rev. Lett. 74 (1995) 3005; *ibid* 75 (1995) 2196; Phys. Rev. B52 (1995), in press.

[78] Milliken F, Umbach C and Webb R, Solid State Commun. 97 (1996) 309.

[79] Moon K, Yi H, Kane C, Girvin S and Fisher M.P.A., Phys. Rev. Lett. 71 (1993) 4381.

[80] Leung K, Egger R and Mak C, Phys. Rev. Lett., in press.

[81] Anderson P and Yuval G, Phys. Rev. Lett. 23 (1969) 89.

[82] Affleck I and Ludwig A, Nucl. Phys. B428 (1994) 545.

[83] Shiba H, Progr. Theor. Phys. 54 (1975) 967.

[84] Caldeira A and Leggett A, Ann. Phys. 149 (1983) 374.

[85] Leggett A, Chakravarty S, Dorsey A, Fisher M P A, Garg A and Zwerger W, Rev. Mod. Phys. 59 (1987) 1.

[86] Wiegmann P and Finkelstein A.M., JETP 48 (1978) 102.

[87] Guinea F, Hakim V and Muramatsu A, Phys. Rev. B32 (1985) 4410.

[88] Anderson P, Yuval G and Hamann D, Phys. Rev. B1 (1970) 4664.

[89] Costi T and Kieffer K, to appear in Phys. Rev. Lett. 95; cond-mat/9601107.

[90] Wen X.G., Int. J. Mod. Phys. B6 (1992) 1711.

[91] Mahan G, "Many-particle physics" Plenum Press 1981.

[92] Corrigan E, Dorey P and Rietdijk R, Progr. Theor. Phys. Suppl. 118 (1995) 143.

[93] Fring A, Mussardo G and Simonetti P, Nucl. Phys. B393 (1993) 413.

[94] Cardy J and Mussardo G, Nucl. Phys. B410 (1993) 451.

[95] Konik R, hep-th/9507053.

[96] Bazhanov V, Lukyanov S and Zamolodchokov A, hep-th/9412229.

[97] Zamolodchikov Al.B., preprint ENS-LPS-335 (1991).

[98] Delfino G, Mussardo G and Simonetti P, hep-th/9603011.